# Artificial membranes soaked with natural oils for *in vitro* drug permeability evaluations

**M Fensham**

orcid.org/0000-0003-1191-4986

Dissertation accepted in fulfilment of the requirements for the degree Master of Science in Pharmaceutics at the North-West University

| | |
|---|---|
| Supervisor: | Prof S Hamman |
| Co-supervisor: | Prof J Steenekamp |
| Co-supervisor: | Mr W Gerber |

Graduation: October 2019

Student number: 24086398

# DECLARATION BY RESEARCHER

I, Mark Fensham, hereby declare that this dissertation, titled “Artificial membranes soaked with natural oils for *in vitro* drug permeability evaluations” is my own work and has not previously been submitted for examination at any institution. I also declare that the sources utilised in this dissertation have been referenced and acknowledged. I further declare that this research study was submitted to the Turn-it-in software program and a satisfactory report was obtained regarding plagiarism.

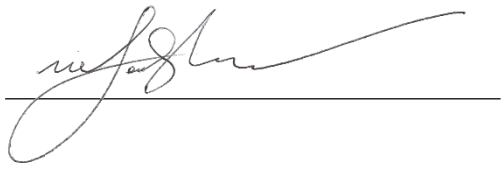

**M. Fensham**

# ACKNOWLEDGEMENTS

Herewith, I would like to express my deepest appreciation to the following individuals and establishments.

***Prof Sias Hamman:***

It has truly been a privilege to work under your guidance and supervision these past few months. You have been an exemplary mentor to me, learning from you has brought me great pleasure and it will continue to do so. I wholeheartedly thank you for your input, patience, dependability, generosity, kindness and understanding. I put the relationship of a fine teacher to a student just below the relation of a mother to a son.

***Prof Jan Steenekamp:***

I particularly enjoyed my undergraduate time spent with you in the classroom, you were the first lecturer I could not wait to see. It was during this time, that I came to realise my ambition to peruse a Master's Degree in Pharmaceutics. Thank you for your contributions in bringing my ambition to fruition.

***Dr De Wet Wolmarans:***

Thank you for the immense role you have played during my final year as an undergrad and also the time, effort and guidance you have given me during this journey. Not to mention, your willingness to listen for the sake of listening and not listening for the sake of replying.

***To my parents, Mark and San-Marie Fensham:***

Who are children if not mere reflections of a lineage of parents. Thank you for the values you have instilled in me, especially perseverance and integrity. I would not be who I am today without your commitment and support. Your love is an endless source that sows both inspiration and motivation within me and for that, I am forever thankful.

***To my grandparents, Pieter and Emma-Rentia Janse van Rensburg:***

I will never forget those who helped me up the ladder, you will always have a special place in my heart and never be forgotten. I want to become a successful person so I can share the joys and riches of life with family and friends like you. A great deal of inspiration and motivation has been sourced from your unconditional support and for that, I thank you.

***Dwayne Maritz:***

I do not know how to thank a friend who understands all the things I never say and never says anything I do not understand. The secret to lifelong friendship is to treat it not just as a gift, but

also as a responsibility. Thank you for playing your part to perfection. Our friendship has seen many years and will see plenty more.

***Dillan Usher:***

The time and experiences we shared as undergrads are invaluable to me, your friendship has been and will always, be appreciated.

***Wouter du Toit and the Arrie Nel Pharmacy Group:***

Thank you for your valuable support as I pursue my ambitions. I look forward to a fruitful journey together as it has been and will continue to be, a great pleasure to work alongside you.

***North-West University:***

I am proud to have studied at this prestigious institution. Thank you to all the personnel and other parties involved in making this research possible and even more so, enjoyable! It is a privilege to have the NWU as my alma mater.

# TABLE OF CONTENTS

# LIST OF TABLES

## Chapter 2:



## Chapter 3:

# LIST OF FIGURES

## Chapter 2:



## Chapter 3:

# LIST OF ABBREVIATIONS AND SYMBOLS

**Abbreviations:**

| | |
|---|---|
| 2/A/A1 | Rat fetal intestinal epithelial cells |
| ANOVA | Analysis of variance |
| API | Active pharmaceutical ingredient |
| ATP | Adenosine triphosphate |
| BCS | Biopharmaceutics Classification System |
| BP | British Pharmacopoeia |
| C | Celsius |
| CA | Cellulose acetate |
| Caco-2 | Human colorectal carcinoma cells |
| CANM | Cellulose acetate-nitrate mixture |
| $cm^3$ | Cubic centimetre |
| CN | Cellulose nitrate |
| CYP3A4 | Cytochrome P450 3A4 |
| e.g. | *Exempli gratia* (for example) |
| *et al.* | And others |
| FAME | Fatty acid methyl esters |
| g | Gram |
| GC-MS | Gas chromatography-mass spectrometry |
| GI-tract | Gastrointestinal tract |
| h | Hour |
| HCI | Hydrochloric acid |
| HPMC | Hydroxypropyl methylcellulose |
| HSD | Honestly significant difference |
| HT29 | Human colon cancer cell line |

| | |
|---|---|
| i.e. | *Id est (*in other words) |
| KRB | Krebs-Ringer bicarbonate buffer |
| LC-MS | Liquid chromatography-mass spectrometry |
| LLC-PK1 | Pig kidney epithelial cells |
| LOD | Limit of detection |
| Log | Logarithm |
| $P_{o/w}$ | Lipid/water partition coefficient |
| LOQ | Limit of quantification |
| ln | Natural logarithm |
| m | Metre |
| $m^2$ | Square metre |
| $m^2/s$ | Square metre per second |
| min | Minutes |
| MDCK | Madin-Darby canine kidney cells |
| mg | Milligram |
| ml | Millilitre |
| mm | Millimetre |
| MW | Molecular weight |
| N | Newton |
| nm | Nanometre |
| $P_{app}$ | Apparent permeability coefficient |
| PA | Polyamide |
| PAMPA | Parallel artificial membrane permeability assay |
| pH | Power of hydrogen |
| pKa | Acid dissociation constant |
| PSA | Polar surface area |
| $R^2$ | Correlation coefficient |

| | |
|---|---|
| R6G | Rhodamine 6G |
| RSA | Republic of South-Africa |
| RSD | Relative standard deviation |
| SD | Standard deviation |
| TC7 | Caco-2 subclone |
| USA | United States of America |
| w/w | Weight per weight |

**Symbols**:

| | |
|---|---|
| α | Alpha |
| ° | Degrees |
| δ | Delta |
| γ | Gamma |
| ≥ | Greater-than or equal to |
| > | Greater-than |
| ∞ | Infinity |
| ≤ | Less-than or equal to |
| < | Less-than |
| µ | Micro |
| ω | Omega |
| ± | Plus-minus |
| % | Percentage |
| ® | Registered |

# LIST OF EQUATIONS

## Chapter 2:



## Chapter 3:

# ABSTRACT

An essential step in the drug discovery and development process, is the swift assessment of membrane permeability properties of new chemical compounds. Considering the unavoidable limitations associated with cell cultures, excised tissues and animal models, non-biological based methods could provide an appealing alternative. Artificial membranes provide a cost-effective, high throughput alternative for drug permeation evaluation, especially for measurement of passive diffusion.

The purpose of this study was to develop an effective *in vitro* method/technique by utilising artificial membranes (i.e. cellulose acetate, cellulose nitrate, cellulose acetate-nitrate mixture and polyamide) in combination with natural oils (i.e. cognac, emu and olive oil), for the evaluation of drug passive diffusion that mimics epithelial cell membrane permeability. Therefore, transport studies with a model compound (i.e. Rhodamine 6G or R6G) were conducted across selected artificial membranes with different chemical compositions and characteristics on their own as well as in combination with the selected oils. The artificial membrane permeation results were compared to the permeation of R6G across excised pig intestinal tissues. All permeation studies were conducted in a Sweetana-Grass diffusion apparatus. The natural oils that were used in this study were chemically characterised by means of gas chromatography linked to mass spectrometry (GC-MS) analysis to determine their unique fatty acid compositions. The aim was to establish if any of the selected membranes alone or in combination with any of the selected oils could be used as a surrogate to biological tissues for assessing *in vitro* passive drug permeability.

The transport results indicated that the rate and extent of R6G permeation were in general dependent on the chemical composition of the artificial membrane as well as the type of oil used in combination with the artificial membrane. Some membranes showed permeation data close to that obtained with the excised pig intestinal tissues. For example, the apparent permeability coefficient ($P_{app}$) value for R6G across the membrane consisting of cellulose nitrate (i.e. 0.197 x $10^{-7}$ cm/s) was very similar to the $P_{app}$ value obtained for R6G across the excised pig intestinal tissues (i.e. 0.210 x $10^{-7}$ cm/s). The membrane consisting of cellulose acetate-nitrate mixture soaked with emu oil also produced a $P_{app}$ value (i.e. 0.191 x $10^{-7}$ cm/s) fairly close to that obtained for R6G across the excised pig intestinal tissue, indicating that emu oil has the ability to simulate to some extent the natural behaviour of the pig intestinal epithelial membrane.

Gastro-retentive matrix type tablets containing R6G were formulated and tested for R6G delivery across a selected artificial membrane (i.e. cellulose nitrate) alone and in combination with the selected oils. This membrane was specifically chosen for the R6G delivery from gastro-retentive tablets because it produced a $P_{app}$ value close to that obtained across excised pig intestinal

tissues. The release of R6G from the gastro-retentive tablets exhibited zero order kinetics as determined by applying different mathematical models to the dissolution data by means of the DDSolver software program. The permeation of R6G across the artificial membrane from the gastro-retentive matrix tablets showed a lag phase followed by an almost straight line, which was in correlation with the release profile. The results of this study confirmed that the use of certain artificial membranes alone and in combination with natural oils can provide permeation results close to that of excised pig intestinal tissues for the lipophilic compound, R6G.

**Keywords:** Artificial membranes, *in vitro* model, natural oils, kinetic drug modelling, gastro-retentive dosage forms, controlled drug release, Sweetana-Grass diffusion chambers, excised pig intestinal tissues.

# PREFACE

This dissertation is submitted in article format. The research article, as presented in Chapter 3, has been prepared according to the formatting requirements of the selected academic journal (i.e. Pharmaceutical Development and Technology) to which it will be submitted. The relevant contributions of the principal author and co-authors are stated below, including permission (i.e. Letter of agreement) from the co-authors for the inclusion of the research article in this dissertation for the purpose of examination.

M. Fensham; Planned and performed the experiments. Collection, analysis and interpretation of data. Compiled and wrote the original draft of the manuscript and designed the figures.

J. Hamman; Conceptualisation of the research and acquisition of funding. Review, intellectual input and editing of the manuscript. Supervised the research.

J. Steenekamp; Conceptualisation of the research. Review, intellectual input and editing of the manuscript.

A. Jacobs; Performed the chemical characterisation of the natural oils by means of GC-MS experiments. Wrote GC-MS methodology.

# LETTER OF AGREEMENT

NWU®
NORTH-WEST UNIVERSITY
NOORDWES-UNIVERSITEIT
YUNIBESITI YA BOKONE-BOPHIRIMA

Private Bag X6001, Potchefstroom
South Africa 2520

Tel: 018 299-1111/2222
Web: http://www.nwu.ac.za

April 2019

**To whom it may concern,**

Dear Sir/Madam

CO-AUTHORSHIP ON RESEARCH PAPER

As co-authors of the research article, we hereby give permission to M. Fensham to submit this article as part of the degree *Master of Science* in *Pharmaceutics* at the North-West University.

- Artificial membranes in combination with selected natural oils for *in vitro* drug passive diffusion screening in Ussing type chamber apparatus applied to gastro-retentive systems

Yours sincerely,

**Prof S. Hamman**

**Prof J. Steenekamp**

**Mr A. Jacobs**

# CHAPTER 1: INTRODUCTION

## 1.1 Dissertation layout

This is an introductory chapter that serves as a basic guide to the dissertation and gives a concise overview of the study with reference to the research problem as well as the aim and objectives.

A literature overview concerning intestinal drug absorption is provided in Chapter 2, containing essential details of pre-clinical pharmacokinetic models used to evaluate membrane permeation.

Chapter 3 is presented in the form of a research article to be submitted for publication in the journal of 'Pharmaceutical Development and Technology'. The research article contains the materials and methods that were utilised, results and discussion of the findings and a conclusion regarding the outcomes of the study.

Chapter 4 provides the final conclusion and future recommendations.

All supplementary data are provided in addendums A, B, C and D.

## 1.2 Background

### 1.2.1 Drug absorption after oral administration

By definition, 'oral drug absorption' is the movement of drug molecules from the lumen of the gastrointestinal tract (GI-tract) into the bloodstream surrounding the GI-tract after oral administration (Chillistone & Hardman, 2017). Biological membranes are present in all organisms and serve as the outer sheaths of their cells. These biological membranes are inherently amphipathic in nature (i.e. containing both hydrophilic and hydrophobic parts), giving them the ability to be selectively permeable (Piacentini *et al*., 2017). Passive diffusion is a term that describes a specific mechanism of drug absorption, which involves the movement of molecules across biological membranes without the assistance of any active transporters. Passive diffusion is the transport mechanism of the majority of drugs and nutrient molecules (Ashford, 2013c).

The oral route of drug administration is one of the most utilised routes of administering drugs to patients for many reasons. It is non-invasive, convenient for self-administration and cost-effective compared to sterile dosage forms such as injections. The majority of conventional oral dosage forms (i.e. capsules and tablets) are formulated to disintegrate and subsequently release the drug fairly quickly from the product after administration. These 'immediate-release'

dosage forms exhibit drug absorption directly after drug release and provide a relatively quick onset of action. Unfortunately, after the drug has been absorbed, the plasma-drug concentration declines relatively rapidly and therefore also the therapeutic effect. A multiple dose regimen must be followed if the desired effect is a sustained therapeutic effect over an extended period of time. Alternatively, fewer doses of a modified-release dosage form can be utilised to ensure that a constant plasma-drug concentration is maintained over a longer time interval. Such modified-release drug delivery systems include delayed-release, extended-release and gastro-retentive dosage forms (McConnell & Basit, 2013).

### 1.2.2 Gastro-retentive drug delivery systems

Although extended-release dosage forms pose the ability to maintain plasma-drug concentrations over longer periods than immediate-release dosage forms, the gastric emptying time directly influence this dosage forms' ability to do so. Furthermore, the upper small intestine serves as the foremost location where most drug molecules are optimally absorbed. After a solid oral dosage form has been administered, it can reach the colon in a relatively short period of time (approximately 4 – 5 hours) in the fasted state, which is insufficient time for complete drug release and absorption specifically from modified-release dosage forms (Davis, 2005). Therefore, by retaining a modified-release drug delivery system in the stomach, the window of drug absorption can be significantly extended. Gastro-retentive drug delivery systems are specifically designed to provide increased residence time in the stomach and therefore allows for constant drug absorption from the upper small intestine since the dosage form does not move so readily to the colon where limited drug release and absorption can take place (Lopes et al., 2016).

### 1.2.3 Tabletting techniques

There are various techniques available to manufacture tablets, which include dry granulation, wet granulation and direct compression. Although each of the mentioned tabletting techniques has its advantages and disadvantages, the latter is the most preferred amongst tabletting techniques due to its simplicity and cost-effectiveness. The direct compression method involves the simple blending of excipients with the active pharmaceutical ingredient(s) (API) in finely divided powder form, followed by the direct compaction of the uniformly mixed powder mass into tablets (Dokala & Pallavi, 2013).

### 1.2.4 Techniques or models to evaluate drug delivery

There are currently various techniques available to evaluate the rate of drug permeation across epithelial cell membranes to estimate drug absorption after oral administration. These methods are *sensu lato* categorised into biological, non-biological, computational and

physicochemical models (Ashford, 2013a). These can be sub-divided into the following categories:

- *In vivo* (i.e. experimentation on a living organism such as humans, rats, pigs, hamsters, monkeys, rabbits and fish).
- *Ex vivo* (i.e. experimentation on excised tissues that are removed from organisms and that are for example used in permeation techniques such as everted sacs or rings and pieces of tissue used in Ussing type chambers).
- *In vitro* (i.e. experimentation on things outside the living organism such as cell cultures or artificial membranes).
- *In situ* (i.e. experimentation on an organ as part of a living organism, which includes the single pass perfusion and Loc-I-Gut techniques).
- *In silico* (i.e. experimentation based on computational simulations to assess various drug-related properties).

The ultimate goal of research on models for drug delivery is to find cost-effective surrogates to predict human drug delivery accurately. Fundamentally, it is not consistently possible to carry out research investigations using humans and therefore scientists had to establish and develop alternative methods to study pharmacokinetic drug parameters (Benam *et al*., 2015).

Animal models have exhibited challenges such as species differences in terms of gene expression of metabolic enzymes and transport proteins and other essential properties that necessitated the development of alternative models. Therefore, many pharmaceutical companies and investigators have prioritised studies utilising cultured human cells and animal tissues and even substituting these with non-biological based models to evaluate drug permeation (Benam *et al*., 2015).

Most artificial membranes are far less complex than biological membranes and they are usually hydrophilic, which created the need for a lipophilic component to be included in order to simulate the composition of a biological membrane (Corti *et al*., 2006; Piacentini *et al*., 2017). The parallel artificial membrane permeation assay (PAMPA) is a non-cellular based *in vitro* model developed by Kansy *et al.* (1998) to predict passive diffusion of drugs across the epithelium of the GI-tract (Buckley *et al*., 2012; Volpe, 2010). The PAMPA technique is based on a filter-supported lipid membrane and allows parallel screening of multiple compounds for permeation through artificial membranes. This is a simple technique that can readily provide information on passive transport permeability (Buckley *et al*., 2012; Petit *et al*., 2016).

However, PAMPA is relatively expensive due to the membrane composition and manufacturing method.

## 1.3 Research problem

The prompt evaluation of the drug-like properties, especially pharmacokinetic characteristics, of compounds during the process of lead compound development is of cardinal importance. Furthermore, there may be a need to evaluate the drug delivery potential of dosage forms, especially modified-release dosage forms over extended periods of time. The PAMPA system was developed for high throughput screening of drug solutions and is relatively expensive, therefore, a need exists for the development of a simple artificial membrane system that mimics the intestinal epithelial membrane in terms of drug permeation, but is able to test the delivery of drugs from solid oral dosage forms over extended periods of time.

Sweetana-Grass diffusion chamber apparatuses can be utilised to investigate drug permeation across excised animal tissues. However, when the delivery of a drug from a dosage form is investigated across excised animal tissues in this diffusion apparatus, the system faces certain limitations. The most important limitation is the lack of viability of the excised tissue during permeation studies over extended periods of time. This is especially problematic during testing of modified-release dosage forms intended for slow drug release.

In order to accurately test drug delivery from modified-release dosage forms, artificial membranes with the correct properties could provide a solution to overcome the tissue viability problem. Furthermore, the ethical considerations associated with the use of animal tissues and the cost of biological waste removal can be overcome with the use of artificial membranes that mimic the drug permeation properties of the intestinal epithelial membrane. The research problem is the lack of an effective artificial membrane model capable of predicting intestinal drug absorption from modified-release dosage forms over extended periods of time.

## 1.4 Aims and objectives

### 1.4.1 Study aim

The aim of this study is to screen different artificial membranes alone and impregnated with different natural oils in order to identify the best membrane/oil combination that is capable of simulating the passive diffusion properties of the GI-tract's epithelial membrane. A secondary aim was to apply the membrane/oil combination for evaluation of the delivery of drugs from gastro-retentive dosage forms in the Sweetana-Grass diffusion apparatus.

### 1.4.2 Study objectives

To appropriately address the aim of the study as stated above, the objectives are to:

- Evaluate the permeability of a selected model compound (i.e. Rhodamine 6G) across excised pig intestinal tissues in the Sweetana-Grass diffusion apparatus.
- Evaluate the permeability of a selected model compound (i.e. Rhodamine 6G) across various artificial membranes including cellulose acetate, polyamide-nylon 6, cellulose nitrate and cellulose acetate-nitrate mixture in the Sweetana-Grass diffusion apparatus.
- Determine the chemical composition of selected natural oils, namely olive oil, emu oil and cognac oil by means of gas chromatography linked to mass spectrometry (GC-MS).
- Evaluate the permeability of a selected model compound (i.e. Rhodamine 6G) across various artificial membranes soaked with each of the selected natural oils in the Sweetana-Grass diffusion apparatus.
- Formulate and manufacture (12 mm diameter) matrix type floating gastro-retentive tablets by means of direct compression containing the selected model compound (i.e. Rhodamine 6G).
- Evaluate the manufactured dosage forms in terms of physical as well as dissolution properties.
- Evaluate the delivery of the selected model compound (i.e. Rhodamine 6G) released from these gastro-retentive tablets across the most suitable artificial membrane and oil combination in the Sweetana-Grass diffusion chamber apparatus.
- Conduct a kinetic analysis of the model compound release and permeation data across the different membranes and excised tissues.
- To validate a fluorometric method for analysis or Rhodamine 6G in terms of accuracy, linearity, limit of detection, limit of quantification, precision and specificity.

## 1.5 Ethical aspects relating to research

An ethics application for experimental procedures utilising excised porcine tissue was approved by the North-West University animal ethics committee (AnimCare) (certificate number: NWU-00025-15-A4) (Addendum A). The excised intestinal tissue samples were directly obtained from routinely slaughtered pigs at the local abattoir (Potchefstroom, South-Africa). Since these animals are routinely slaughtered for meat production purposes, there are no ethical considerations directly related to the animals.

# CHAPTER 2: LITERATURE OVERVIEW OF PRE-CLINICAL PHARMACOKINETIC MODELS TO EVALUATE MEMBRANE PERMEATION

## 2.1 Introduction

### 2.1.1 The drug absorption process after oral administration

Pharmacokinetic processes describe a number of events that occur after the oral administration of a drug product, namely absorption, distribution, metabolism and elimination also known as 'ADME' (Holford, 2010). Of these pharmacokinetic processes, absorption and metabolism will be discussed in more detail in this section.

According to Chillistone and Hardman (2017), drug absorption can be defined as the movement of drug molecules from the area of administration (e.g. GI-tract) into the blood circulation surrounding the GI-tract. The oral route of drug administration remains the most abundantly used way of administering drugs to patients for several obvious reasons. Some of the benefits that contribute to it being the preferred route of drug administration include the large range of dosage forms that are suitable to be taken orally, the ease of self-administration that leads to a high rate of patient compliance and cost-effectiveness (Musther *et al.*, 2014; Shekhawat & Pokharkar, 2017; York, 2013).

Prerequisites for orally administered drugs include drug solubility, dissolution rate and permeability across the intestinal epithelial membrane (Shekhawat & Pokharkar, 2017). Furthermore, the drug absorption process after oral administration is dependent on the following factors that may influence the rate and extent of drug absorption (Ashford, 2013b):

- Physiological factors such as stomach emptying rate, presence of disease states, pH of the fluids at the site of administration, buffer capacity, presence of food, the permeability of membranes, the viscosity of luminal contents, motility flow rate and patterns, co-administered fluids and gastrointestinal secretions.
- Physicochemical factors such as particle size, wettability, hydrophilicity, crystal structure, molecular size and solubility of the drug compound.
- Dosage form factors such as mechanical strength, disintegration and dissolution rate, rate of drug release, mechanism of drug release, site of drug release, muco-adhesive properties and type of excipients included.

Bioavailability of a drug can be defined as the fraction of the administered drug dose that reaches the systemic circulation unchanged (Holford, 2010). The bioavailability of a drug is

governed by the drug absorption process amongst many other complex factors (Yang & Yu, 2009). The bioavailability of a drug is also dependent on the ability of the drug molecules to penetrate the epithelium membrane, the extent to which the drug is metabolised by enzymes in the liver and/or in the gastrointestinal epithelium (Chillistone & Hardman, 2017). When a drug is taken orally (i.e. conventional tablet or capsule), the dosage form must first disintegrate followed by dissolution of the drug into the surrounding fluids in order for the drug molecules to be able to cross the epithelial membrane (Ashford, 2013b) and to move into the blood vessels surrounding the GI-tract.

### 2.1.2 Anatomy and physiology of the human gastrointestinal tract

The digestive system, also known as the GI-tract, is an intricate structure comprised of a muscular tube consisting of different regions. The oral cavity, pharynx, oesophagus, stomach, small intestine and the large intestine collectively form the GI-tract (Martini *et al.*, 2014).

#### 2.1.2.1 Stomach

The stomach begins at the lower end of the oesophagus and angles downward across the midline to the right ending in the pylorus sphincter (Amerongen, 2018). The stomach diverges from the shape of a tube, by inflating outward to the left. This inflation on the long convex outer edge forms the greater curvature. The stomach's right border forms a short concave edge known as the lesser curvature. The pylorus is the valve regulating the opening from the stomach to the duodenum (Amerongen, 2018). The approximate length of the stomach is 10 cm for the lesser curvature and 40 cm for the greater curvature (Martini *et al.*, 2014). The stomach consists of three functional parts i.e. fundus, corpus and antrum (Neumann *et al.*, 2017).

#### 2.1.2.2 Small and large intestines

The small intestine is divided into three segments namely the duodenum, jejunum and ileum. The length of the small intestine is approximately 6 m and has a diameter ranging from 4 cm (starting from the pylorus) to 2.5 cm (ending at the large intestine) (Martini *et al.*, 2014). The final chemical decomposition of food by means of digestive enzymes and the absorption of electrolytes, nutrients and water takes place in the small intestine (Amerongen, 2018). The large intestine is also divided into three segments namely the caecum, colon and rectum that collectively span the length of the large intestine (approximately 1.5 m) with a diameter of approximately 7.5 cm (Martini *et al.*, 2014). The large intestine concludes the absorption of electrolytes, nutrients and water and forms the faecal mass.

#### 2.1.2.3 Surface area

Relatively limited drug absorption occurs in the stomach, which has a comparatively small surface area (approximately 0.053 $m^2$) with respect to that of the small intestine (approximately 200 $m^2$ as a result of the presence of villi and microvilli) (Ashford, 2013c; Chillistone & Hardman, 2017; Shekhawat & Pokharkar, 2017). The latter is the foremost site of drug absorption with residence time being a controlling factor in the rate and extent of drug absorption (Ashford, 2013c; Shekhawat & Pokharkar, 2017; Vo *et al.*, 2017).

#### 2.1.2.4 pH of the gastrointestinal tract

The highly acidic pH of the stomach (1 – 3.5) is maintained by the parietal cells' secretion of hydrochloric acid (HCl) (Ashford, 2013c; Shekhawat & Pokharkar, 2017). The secretion of HCl in the stomach creates an optimal environment for digestive enzymes (e.g. pepsin), which breaks down proteins into peptides and helps to protect humans against the invasion of certain bacteria and viruses. This highly acidic stomach contents can be dramatically changed after the ingestion of a meal and the extent of pH adjustment is dependent on the meal composition. The pH values of the stomach fluids following the ingestion of a meal generally vary between 3 and 7. The modified gastric pH, however, reverts back to a more acidic environment after approximately 2 – 3 hours (Ashford, 2013c).

Bicarbonate ions secreted by the pancreas into the small intestine contribute to the neutralisation of gastric acid. Consequently, there is a systematic rise in pH along the length of the small intestine, increasing gradually from the duodenum (pH of 5) to the ileum (pH of 8). The pH of the colon is then decreased to approximately 6.5 by bacterial enzymes, which digest carbohydrates into fatty acids (Ashford, 2013c).

The absorption of the majority of drug molecules (weak acids and bases) is greatly influenced by the varying pH values of the GI-tract. It is a prerequisite for a drug to be in its un-ionised form in order to cross the cell membrane (see section 2.1.3 below), but the ionised form is more soluble. The molecular structure and the pH of the surrounding fluids dictate the degree of drug ionisation. The majority of drugs are weak acids or weak bases, which exist in an equilibrium between the ionised and un-ionised fractions (Shekhawat & Pokharkar, 2017).

### 2.1.3 The structure of biological membranes

According to Bánfalvi (2016), biological membranes form the outer sheaths of all living cells and are therefore also known as plasma membranes. A typical biological membrane is characterised by a phospholipid bilayer structure that is bridged partly or completely by glycoproteins (refer to Figure 2.1 for a schematic illustration). All biological membranes are comprised of lipids, carbohydrates and proteins with a thickness ranging from 6 to 10 nm

(Martini *et al.*, 2014). The phospholipids in biological membranes are amphipathic, which means they contain hydrophilic heads and hydrophobic tails. The amphipathic nature of these phospholipids contributes to the selective permeability of biological membranes (Piacentini *et al.*, 2017). Selective permeability is the essential characteristic of a membrane to protect the cell contents, by effectively separating the cytoplasm of a cell from its surrounding environment (Piacentini *et al.*, 2017).

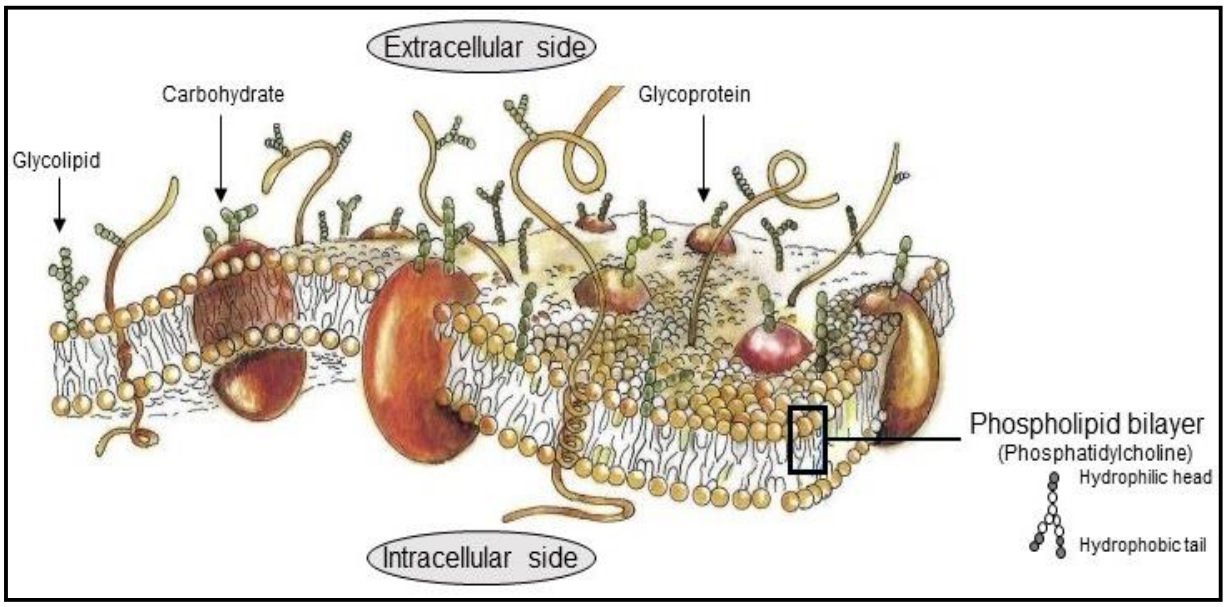


**Figure 2.1:** Schematic representation of the biological membrane (Giorno *et al.*, 2010; Singer & Nicolson, 1972).

## 2.2 Drug transport mechanisms

According to Ashford (2013c), there are two principal pathways of drug transport across the gastrointestinal epithelial cell wall, namely transport across the cells (i.e. the transcellular pathway) and transport between the cells (i.e. the paracellular pathway). The former can occur by means of transport mechanisms such as passive diffusion, carrier-mediated transport and endocytosis, while the latter only occurs by means of passive diffusion. Carrier-mediated transport takes place in the form of active transport and/or facilitated transport (Chillistone & Hardman, 2017).

### 2.2.1 Passive diffusion

Passive diffusion (refer to Figure 2.2 for a schematic illustration) is the mechanism of transport for most drugs across biological membranes. Molecules travel through the lipid membrane during transcellular passive diffusion and in between cells during paracellular passive diffusion. In both cases molecules move from a region with high concentration to a region with low concentration. The intestinal lumen represents the high concentration area, while the blood

represents the low concentration area (Ashford, 2013c). The concentration gradient between these areas of transport and the nature of the membrane dictate the rate and extent of drug permeation that occurs by means of passive diffusion (Ashford, 2013c; Chillistone & Hardman, 2017). This mechanism of transport requires no input of chemical energy and is induced by the difference in concentration of opposing sides of the membrane, which is known as the 'concentration gradient' (Bánfalvi, 2016).

### 2.2.2 Carrier-mediated transport

Some compounds (e.g. penicillins and angiotensin-converting enzyme inhibitors) and numerous nutrients (e.g. amino acids and sugars) are transported by means of active and or facilitated transport. The former is able to transport molecules against a concentration gradient and consequently requires cellular energy to do so (Ashford, 2013c). This transport process involves the binding of the drug molecule to an endogenous carrier protein in the membrane, after which the drug-carrier complex travels across the membrane (see Figure 2.2). Once on the other side of the membrane, the drug molecule is released and the carrier returns (Ashford, 2013c; Chillistone & Hardman, 2017). Compared to active transport, facilitated transport differs in that it cannot transport molecules against a concentration gradient of that molecule (Ashford, 2013c).

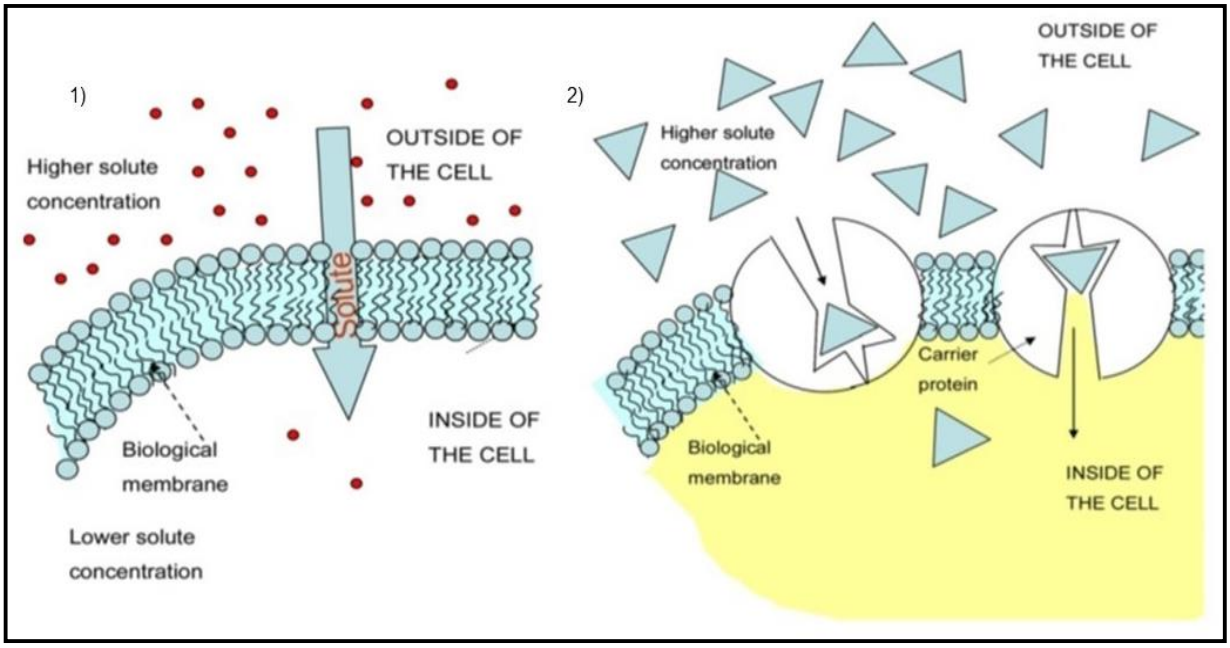


**Figure 2.2:** Schematic representation of 1) Passive diffusion with the concentration gradient and 2) Facilitated transport via carrier proteins (Piacentini *et al.*, 2017).

If adenosine triphosphate (ATP) is used directly in the carrier-mediated transport process, it is known as primary active transport. During primary active transport, ions or molecules bind to the carrier site, which stimulates ATP hydrolysis, causing conformation changes of the carrier

that ultimately moves molecules to the other side of the cell membrane. If the transport process includes the induction of an electrochemical gradient, it is known as secondary active transport (Piacentini *et al.*, 2017).

### 2.2.3 Vesicular transport

According to Ashford (2013c); Chillistone and Hardman (2017) this process involves the invagination of a molecule inside a part of the cell membrane, allowing intracellular integration of the molecule. Cells must sometimes transport particles i.e. food particles across their membranes and accomplish this process by means of endocytosis at the apical side of the membrane and exocytosis at the basolateral side (refer to Figure 2.3 for a schematic illustration). The substances that need to be transported, are encircled by an infolding of the cell membrane, resulting in the intracellular integration of the molecules (Piacentini et al., 2017).

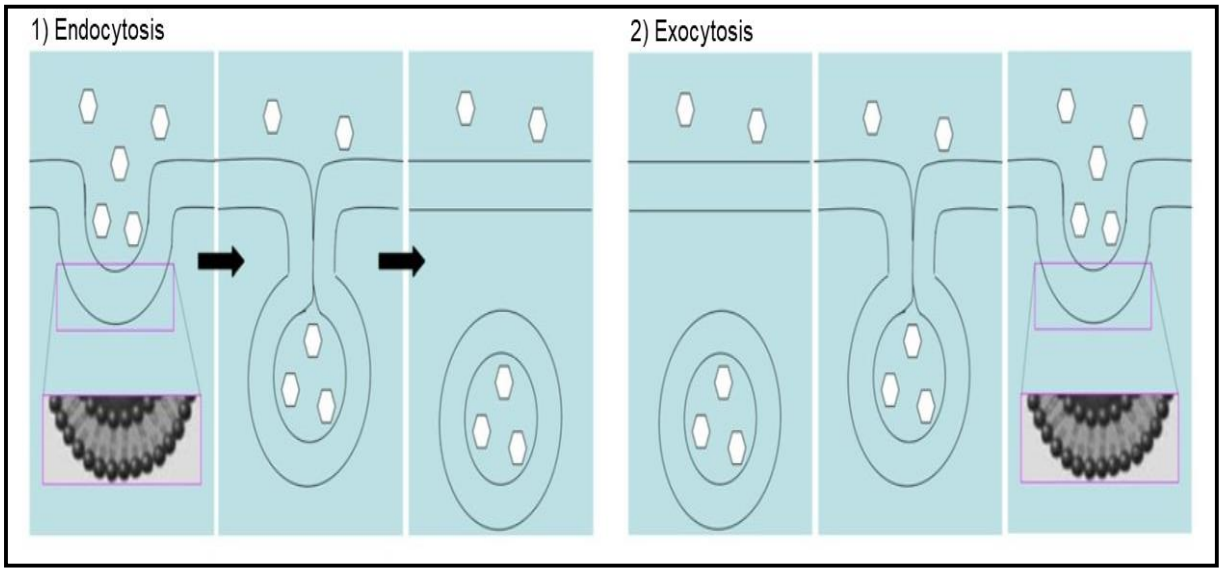


**Figure 2.3:** Schematic representation of 1) Endocytosis and 2) Exocytosis (Piacentini *et al.*, 2017).

## 2.3 Barriers to drug absorption

The entire GI-tract, stretching from the mouth to the anus is lined with a mucous membrane, also known as the mucosa, which serves as one of the primary barriers to the entry of materials into the body (DeSesso & Jacobson, 2001). The mucosa is comprised of a single layer of epithelial cells covering a thin sheet of connective tissue (i.e. the lamina propria) containing lymphatic capillaries and blood. A schematic illustration of the barriers to drug absorption is shown in Figure 2.4. It is a prerequisite for a drug to cross the epithelial cell membrane in order for it to be absorbed from the lumen of the GI-tract into the bloodstream. The mucosa of the GI-tract is comprised of non-uniform epithelial cell populations. However, there is a

predominant cell type (i.e. enterocytes) present in the absorbing regions, which are mainly responsible for the uptake of materials from the lumen. Enterocytes are comprised of columnar epithelial cells that are bound to adjacent cells at the luminal surface by means of tight junctions. Microvilli are present on the apical cell membrane surface of enterocytes, resulting in an increased surface area for absorption (Ashford, 2013c; Shekhawat & Pokharkar, 2017).

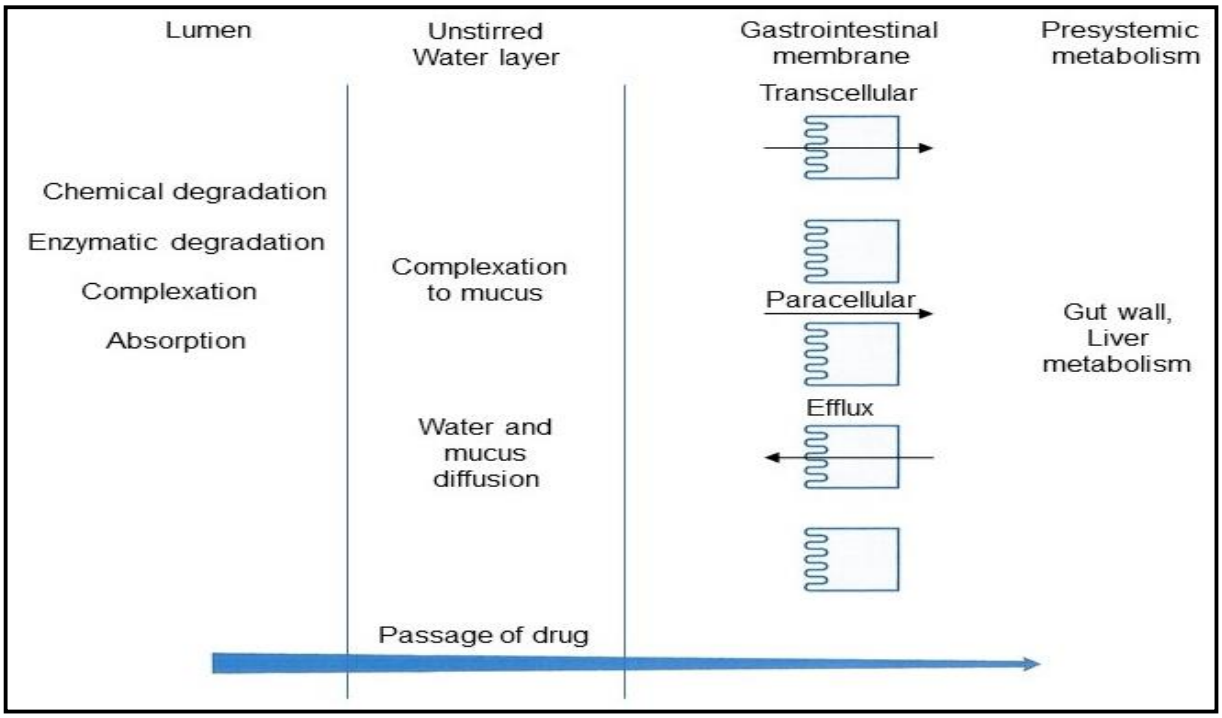


**Figure 2.4:** Schematic representation of barriers to drug absorption (Ashford, 2013b).

Considering, even if a significant amount of drug manages to pass through the intestinal barrier, the liver will further reduce the dose fraction that reaches the systemic circulation (Pereira *et al.*, 2016).

## 2.4 The Biopharmaceutics Classification System

The Biopharmaceutics Classification System (BCS), is based on drug solubility and membrane permeability (refer to Figure 2.5 for a schematic illustration) that are the two most important properties determining the bioavailability of a drug. The BCS classifies drugs into four distinctive groups namely; 1) Class I: drugs with high solubility and high permeability, 2) Class II: drugs with low solubility but high permeability, 3) Class III: drugs with high solubility but low permeability and 4) Class IV: drugs with low solubility and low permeability (Amidon *et al.*, 1995; Hosey & Benet, 2017; Yang & Yu, 2009).

According to the BCS, Class 1 drugs are highly soluble and dissolves rapidly and consequently the gastric emptying time, and not dissolution rate, is the rate-limiting step in the absorption process (Daousani & Macheras, 2016; Hosey & Benet, 2017). It is accepted that a drug is

highly soluble if the highest dose dissolves in 250 ml of water or less over a pH range of 1 – 8, then the drug can be classified into Class 1 in terms of solubility (Ashford, 2013a; Hosey & Benet, 2017). Additionally, the high rate of permeability of Class 1 drugs ensure that these substances are completely absorbed during the limited residence time in the GI-tract (Hosey & Benet, 2017).

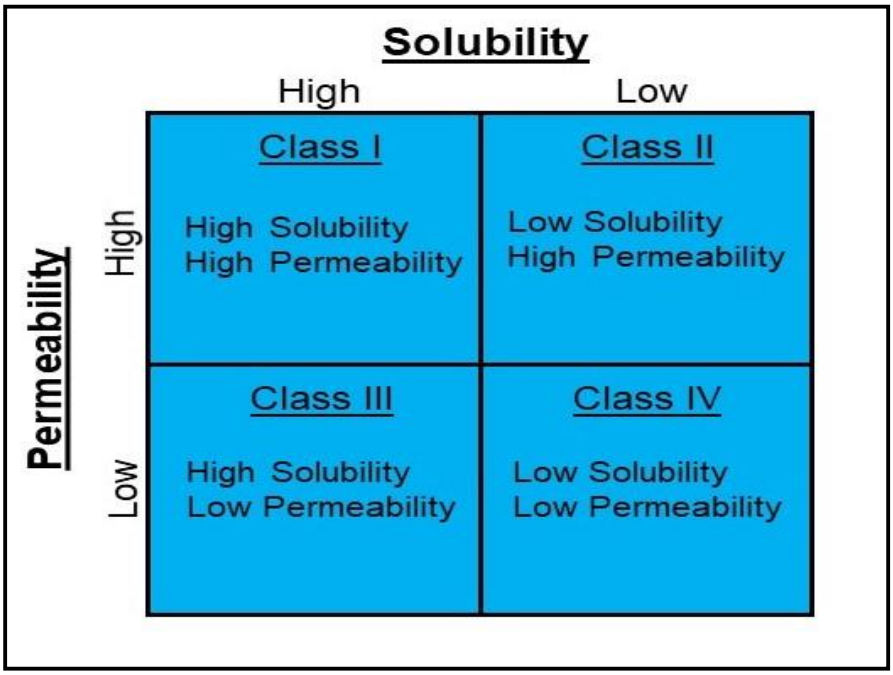


**Figure 2.5:** Schematic representation of the four classes of the Biopharmaceutics Classification System (BCS) (Hosey & Benet, 2017).

Class 2 drugs are well absorbed due to their high membrane permeability properties with dissolution being the rate-limiting step in the absorption process. Low solubility can seriously impact the bioavailability of a drug since only drug molecules in solution can be absorbed. The bioavailability of Class 3 and 4 drugs is limited by their inherently low permeability, which greatly influences the rate and extent of absorption. The absorption of these drugs can be site-specific, with gastrointestinal residence time being a limiting factor in the absorption process (Hosey & Benet, 2017). This leads to significant inter and intra-subject absorption variability and presents challenges with dosage form design for these drugs (Daousani & Macheras, 2016).

## 2.5 Pre-clinical pharmacokinetic models for membrane permeation evaluation

Pharmacokinetic models are of cardinal value as screening tools for predicting the biopharmaceutical properties of new compounds (Corti *et al.*, 2006; Zhang *et al.*, 2012). A variety of models, methods and techniques are used to estimate oral drug bioavailability, especially in terms of measuring the permeation rate of compounds across cell membranes. These models can broadly be categorised into computational (*in silico*), physicochemical (*in*

*vitro*), non-biological (*in vitro* such as artificial membranes) and biological (*in vivo* and *in situ* in animals, but also *in vitro* in cell cultures and *ex vivo* in excised tissues) (Ashford, 2013a; Joubert *et al.,* 2017).

### 2.5.1 *In vivo* models

*In vivo* studies are defined as experiments conducted in the living body of an organism (Merriam-Webster's Medical Dictionary, 2018). *In vivo* models measure the rate and extent of drug uptake into the systemic circulation in live animals or humans, amongst other uses. These models are also able to provide crucial information regarding all aspects of oral drug pharmacokinetics including permeability, metabolism, distribution and elimination. Various animal models exist, which have been developed to aid in the discovery of potential drug targets and to mimic certain human diseases. The animals utilised in these experiments include, but are not limited to i.e. rats, hamsters, guinea pigs, sheep, fish, birds, reptiles, monkeys, rabbits, cats, pigs and dogs. Rats are frequently utilised for *in vivo* studies because they are relatively inexpensive and require small doses of the test compound (Nef, 2001; Zhang *et al.*, 2012).

*In vivo* experimentation has hitherto, played a significant role in biomedical research, whilst being a controversial topic of scientific, philosophical and public discussion for centuries. A paradigm concerning the usefulness, needs and ethical treatment of animals in research has been developed, but the debate is ongoing. Animal experimentation is crucial for the central purposes of target estimation and validation of various parameters of new therapeutic drugs i.e. efficacy, safety and pharmacokinetics (Franco, 2013; Zhang *et al.*, 2012).

Even when the design and regulation of an animal study allow for the elimination of bias, the translational results to clinical practice may fail, due to discrepancies between the model and the clinical trials testing the treatment strategy. The reduced external validity of such findings are commonly caused by variations between animals and humans in the pathophysiology of diseases. However, animal models require improvement as the findings emerging from current pre-clinical animal models, often translate inadequately to human disease and clinical practice. Moreover, animal models are not the only origin of valuable data that supports new discoveries and therefore, alternative models need to be developed to reduce and/or replace the number of animals used in experiments while also increasing their welfare (Ashford, 2013a; Deferme *et al.*, 2008; Franco, 2013; Le Ferrec *et al.*, 2001; Nef, 2001; Patil *et al.*, 2014; Volpe, 2010; Zhang *et al.*, 2012).

During the past few decades, the use of animals for biomedical research has come under criticism by various animal protection and animal rights groups alike. Laws have been

implemented in several countries to make the practice of animal usage, more 'humane'. This has led to the 3R's movement, which supports the search for the 'replacement' of animals with non-living models, the 'reduction' in the use of animals and the 'refinement' of animal use practices. Notwithstanding, the total elimination of animal testing would significantly delay the development of essential medical devices, treatments and medicine. By implementing the three R's during the continual use of animals for scientific research, the scientific community can assert its moral conscience while upholding its obligation to humanity to promote the advancement of science for the betterment of civilisation and humanity itself (Franco, 2013; Hajar, 2011).

A summary of the advantages and disadvantages of *in vivo* models can be found in Table 1.

**Table 1:** Advantages and disadvantages of *in vivo* pharmacokinetic models (Ashford, 2013a; Deferme *et al.*, 2008; Le Ferrec *et al.*, 2001; Patil *et al.*, 2014; Volpe, 2010; Zhang *et al.*, 2012).

| Advantages | Disadvantages |
|---|---|
| • Most natural condition.<br>• Blood flow and the nervous system remains intact.<br>• Toxicity screening. | • Inability to identify individual rate-limiting factors.<br>• Limited subject availability and viability.<br>• Bioavailability influenced by first-pass hepatic metabolism.<br>• Time-consuming and arduous procedures.<br>• Variations among different species and differences with humans. |

### 2.5.2 *In situ* models

These models include intestinal perfusion in living subjects (e.g. Loc-I-Gut technique) where a region of the intestine is secluded by means of balloons in tubes that are inserted into the lumen of the GI-tract. The Loc-I-Gut perfusion technique isolates the luminal contents of the human small intestine from the proximal and distal ends, facilitating the investigation of permeation mechanisms and drug metabolism during drug absorption at specific areas in the GI-tract. *In situ* intestinal perfusion techniques can also be applied to animals. In this case, the animals are anaesthetised and the intestines exposed to allow for incisions to insert glass tubes, to ultimately isolate a part of the intestines. A drug solution is then slowly pumped through the isolated piece of the intestine. These models directly measure the decrease of a

drug in solution from the GI-tract and consequently its absorption (Ashford, 2013a; Volpe, 2010).

The most significant advantage of *in situ* techniques is the presence of an intact intestinal mucosa, blood flow and nervous system in the live animals. Even so, a major drawback of *in situ* techniques is the effect associated with the required surgical procedures and anaesthesia on pharmacokinetics (Ashford, 2013a; Deferme *et al.*, 2008; Harloff-Helleberg *et al.*, 2017; Le Ferrec *et al.*, 2001; Lozoya-Agullo *et al.*, 2015; Luo *et al.*, 2013; Volpe, 2010).

A summary of the advantages and disadvantages of *in situ* models can be found in Table 2.

**Table 2:** Advantages and disadvantages of *in situ* perfusion models (Ashford, 2013a; Deferme *et al.*, 2008; Harloff-Helleberg *et al.*, 2017; Le Ferrec *et al.*, 2001; Luo *et al.*, 2013; Volpe, 2010).

| Advantages | Disadvantages |
|---|---|
| • Closely resembles *in vivo* conditions.<br>• Intact intestinal mucosa, nervous system and blood flow.<br>• Transport mechanisms are present and viable.<br>• Regional absorption can be investigated. | • Need for anaesthesia and or surgery.<br>• Time-consuming and arduous.<br>• Low throughput screening tool.<br>• Complex analysis due to the biological medium (blood).<br>• Avoids the influence of first-pass hepatic metabolism when evaluating intestinal absorption.<br>• A physiologically complex system with intrinsic variability.<br>• No data of passage through the stomach. |

### 2.5.3 *In vitro* models

*In vitro* studies are defined as experiments conducted outside the living body of an organism in a scientific instrument (Merriam-Webster's Medical Dictionary, 2018). Several cellular-based models are available for drug permeation studies namely human Caucasian colon adenocarcinoma (Caco-2), dog kidney epithelial cells (MDCK), pig kidney epithelial cells (LLC-PK1), rat fetal intestinal epithelial cells (2/4/A1), Caco-2 sub-clone (TC7) and human colon cells (HT29). The Caco-2 cell line is an example of a frequently used *in vitro* cell culture model to measure drug transport across intestinal epithelial cell monolayers grown on membrane supports. The Caco-2 model is the most extensively characterised cellular-based model and

popular choice in examining drug permeability in both the academic and pharmaceutical industry (Deferme *et al.*, 2008; Le Ferrec *et al.*, 2001).

Caco-2 cells express most of the morphological and functional traits of absorptive intestinal cells, including enzymes (i.e. peptidase and disaccharidases) naturally expressed by enterocytes, despite being of colonic origin. The most essential metabolising enzyme in the human GI-tract (i.e. CYP3A4) is inconsequentially low or completely absent in Caco-2 cells, which may lead to overestimation of the absorbed fraction of CYP3A4 substrates. Despite the apparent correlation with *in vivo* drug absorption and Caco-2 cell permeability, the permeability of hydrophilic compounds that are predominantly transported by means of the paracellular pathway is low in the Caco-2 cell line. For example, several hydrophilic compounds of low molecular weight (i.e. atenolol, metformin and ranitidine) display low permeability in Caco-2 cells, despite showing absorption higher than 50% in humans (Deferme *et al.*, 2008; Walter & Kissel, 1995). This can be attributed to the relative tighter junctions (paracellular channels) compared to animal and human small intestine (Le Ferrec *et al.*, 2001; Pereira *et al.*, 2016).

The Caco-2 cell monolayer model grown on Transwell® membranes is static and consists of a single cell type, which is unable to produce mucus compared to the small intestine *in vivo* situation, which is a dynamic environment with changing pH values and muscular contractions catapulting intestinal contents along the length of the organ (Le Ferrec *et al.*, 2001; Pereira *et al.*, 2016).

The MDCK cell line is an alternative to Caco-2 cell monolayers that are frequently used for permeability measurements. The main advantage that MDCK cells pose over Caco-2 cells is a shorter culturing time to convergence (3 – 5 days vs 21 days). The non-intestinal and non-human origin of MDCK cells are regarded as disadvantages. Additionally, these cells have relatively low levels of metabolic activity and low expression of transporter proteins (Le Ferrec *et al.*, 2001; Pereira *et al.*, 2016).

*In vitro* models offer a sophisticated and highly accurate approach in the prediction of API bioavailability, mechanism of absorption and the impact of biological parameters. *In vitro* models contribute to a significant reduction in the use of *in vivo* models, facilitating the prompt identification of lead drug candidates with unsatisfactory pharmacokinetic properties (Ashford, 2013a; Billat *et al.*, 2017; Deferme *et al.*, 2008; Le Ferrec *et al.*, 2001; Pereira *et al.*, 2016; Volpe, 2010).

A summary of the advantages and disadvantages of *in vitro* models can be found in Table 3.

**Table 3:** Advantages and disadvantages of *in vitro* cellular based drug permeation models (Ashford, 2013a; Deferme *et al.*, 2008; Le Ferrec *et al.*, 2001; Volpe, 2010).

| Advantages | Disadvantages |
|---|---|
| • Human origin (similarity in cell morphology and biochemistry).<br>• Good screening model.<br>• Number of laboratory animals reduced.<br>• Transport mechanism evaluation.<br>• Evaluation of compound toxicity. | • Lack of certain cytochrome P450 enzymes.<br>• Absence of mucus layer.<br>• Long cell growth cycles.<br>• Risk of microbial contamination.<br>• High cost of implementation.<br>• More compact monolayer compared to the human small intestine.<br>• Inter-laboratory variability. |

### 2.5.4 *Ex vivo* models

*Ex vivo* models are based on the use of excised animal/human tissues to predict human intestinal drug absorption. Isolated sheets of the intestinal mucosa are obtained by cutting the subject intestine into segments and using them in different techniques. These techniques include everted sac or ring and Ussing type chamber apparatuses. For the latter, the excised tissue sheet with its serosa removed is mounted in between half cells of diffusion chambers filled with a suitable biological buffer. The chamber is divided into donor and receiving chambers and a drug solution can then be added to the donor side. The consequent accumulation of the drug into the receiving chamber is measured and plotted as a function of time. This technique allows assessment of permeability across different areas of the intestine, providing insight into the applicability of a drug to be used in an oral dosage form such as controlled-release dosage forms (Ashford, 2013a; Deferme *et al.*, 2008).

Everted intestinal sacs use whole, intact intestinal segments rather than being cut open to form sheets. These segments are excised from an animal's intestine and everted after placing it over a glass rod. The segment is tied at both ends and filled with a biological buffer. These sacs are incubated at 37°C in an oxygenated buffer containing the drug to be evaluated. The amount of drug accumulated inside the sac is then calculated per gram of wet tissue, over a specific interval of time (Ashford, 2013a). Everted intestinal rings also use whole intestinal segments that are excised and everted after placing the segment over a glass rod. However, the segment is then tied at one end and subsequently cut into small rings or sections and incubated in an oxygenated drug containing buffer solution at 37°C. Following a set period of time, drug uptake is terminated by rinsing the segment with ice-cold buffer solution and

allowing it to dry. Afterwards, the amount of drug accumulated is calculated per gram of wet tissue over a specific interval of time. However, before the tissue can be assayed for drug content, the tissue needs to be digested and the drug extracted. Since this is an uptake method, the polarity of absorption cannot be assessed (Ashford, 2013a).

*Ex vivo* models possess unique features that differentiate them from the *in vitro* cell culture models (e.g. the Caco-2 model) namely the presence of a mucus layer and the excised intestinal epithelium provides realistic paracellular permeability. Moreover, transporter proteins and drug metabolism enzymes are present. Nonetheless, results obtained from *ex vivo* models occasionally improperly estimate the degree of oral absorption due to the lack of an intact nervous system and the absence of normal blood flow (Luo *et al.*, 2013).

Undeterred by these shortcomings, *ex vivo* methods are extensively utilised in the design and testing of potential new drugs. *Ex vivo* models offer a highly accurate and sophisticated approach in the prediction of drug bioavailability, mechanism of absorption and the impact of biological factors on drug pharmacokinetics (Ashford, 2013a; Billat *et al.*, 2017; Deferme *et al.*, 2008; Le Ferrec *et al.*, 2001; Luo *et al.*, 2013; Ussing & Zerahn, 1951; Volpe, 2010).

A summary of the advantages and disadvantages of *ex vivo* models can be found in Table 4.

**Table 4:** Advantages and disadvantages of *ex vivo* models (Ashford, 2013a; Deferme *et al.*, 2008; Le Ferrec *et al.*, 2001; Luo *et al.*, 2013; Ussing & Zerahn, 1951; Volpe, 2010).

| Advantages | Disadvantages |
|---|---|
| • Relatively inexpensive.<br>• Simplicity (no bio-analysis).<br>• High reproducibility of results.<br>• Assessment of permeability across different areas of the intestine.<br>• Directional and mechanistic transport. | • Limited tissue availability and viability.<br>• Normal blood flow is absent.<br>• Lacks intact nervous system. |

### 2.5.5 *In silico* models

These models are purely based on computational simulations to assess certain drug-related physicochemical properties, which are used to predict their oral absorption potential. These simulations calculate, for example, the lipid/water partition coefficient based on fragment analysis (i.e. Log $P_{o/w}$ values). The modelling of membrane permeability and compound solubility contributes greatly to drug discovery, as these simulations can be used as tools for

prompt parameterisation of physiology or mechanistic-based pharmacokinetic models (Harloff-Helleberg *et al.*, 2017).

*In silico* models have also shown to be a useful tool in screening for new permeation enhancers and the optimisation of physicochemical features of surfactant enhancing systems for the oral delivery of proteins. Various commercial software programs for advanced *in silico* modelling are available, of which the three most commonly utilised programs (i.e. GastroPlus 8.0, Simcyp 13.3 and GI-Sim 4.1) were recently compared with regards to their ability to predict human intestinal drug absorption. The study concluded, that all three types of software provide useful information in formulation development. However, due to the non-transparent nature of the internal workings of *in silico* software, it is usually recommended to integrate a plethora of different models to assess the same compound (Harloff-Helleberg *et al.*, 2017).

Moreover, due to the complex degradation kinetics in the lumen and complex processes involved during permeation, the software is less applicable to biopharmaceuticals. It is also worth mentioning that the current *in silico* models lacks the ability to simulate the complex nature of *in vivo* environments that determine dissolution behaviour. All things considered, *in silico* models offer a simple, high-throughput approach that can screen drug candidates during the early stages of drug development (Ashford, 2013a; Billat *et al.*, 2017; Corti *et al.*, 2006; Deferme *et al.*, 2008; Harloff-Helleberg *et al.*, 2017; Le Ferrec *et al.*, 2001; Norris *et al.*, 2000; Volpe, 2010; Welling *et al.*, 2015).

A summary of the advantages and disadvantages of *in situ* models can be found in Table 5.

**Table 5:** Advantages and disadvantages of *in silico* pharmacokinetic models (Ashford, 2013a; Corti *et al.*, 2006; Deferme *et al.*, 2008; Le Ferrec *et al.*, 2001; Norris *et al.*, 2000; Volpe, 2010).

| Advantages | Disadvantages |
|---|---|
| • Animal/human subject not required.<br>• Prediction of absorption before compound synthesis. | • Inability to incorporate multitude of complex variables.<br>• Inability to model active transport processes. |

## 2.6 Artificial membranes

Since most drugs favour passive diffusion as a means of membrane transport during absorption, artificial membranes offer a potentially effective high throughput approach for the assessment of a drug candidate's passive diffusion properties (Corti *et al.*, 2006). Fundamentally, biological membranes are far more complex than artificial membranes. The

latter being purely hydrophilic, creates the need for a lipophilic component to be incorporated in order to mimic the composition of the biological membrane (Corti *et al.*, 2006; Deferme *et al.*, 2008; Piacentini *et al.*, 2017)

The non-cellular based *in vitro* model called parallel artificial membrane permeation assay (PAMPA) has been developed to predict transcellular, passive diffusion of drugs across the GI-tract epithelium (Buckley *et al.*, 2012; Deferme *et al.*, 2008; Volpe, 2010). The PAMPA technique was developed by Kansy *et al.* (1998) and is based on a filter-supported lipoid membrane to study the passive absorption process. It allows parallel screening of many compounds for permeation across artificial membranes and is therefore considered a high throughput screening assay for drug permeation properties. It consists of 96-well microtiter plates containing hydrophobic filters, saturated with organic solvent mixtures (Buckley *et al.*, 2012). This technique measures the ability of a test compound to diffuse into an acceptor compartment (containing an appropriate buffer solution), from a donor compartment (containing the test compound in a buffer solution) (Petit *et al.*, 2016).

PAMPA is increasingly used in pharmaceutical research within major pharmaceutical companies and contract research organisations. This procedure can swiftly provide information on passive-transport permeability that is not influenced by other mechanisms such as active transport, metabolism and paracellular transport. PAMPA is a simple, robust and the most regularly used *in vitro* method of predicting transcellular passive absorption of compounds. The prevalence for the use of PAMPA has exponentially risen in the industry as a cost-effective and versatile assay compared to cellular-based models such as Caco-2 (Petit *et al.*, 2016). It should be noted that the use of PAMPA varies across laboratories, e.g. different membrane constituents, permeation times and sink conditions can be applied. Therefore, methods of standardisation and validation should be introduced for this technique (Deferme *et al.*, 2008). The transport of a drug across an artificial membrane is dependent on the lipid constituent composition of the membrane and on the membrane's ability to retain the lipid constituent during the transport study (Volpe, 2010).

A summary of the advantages and disadvantages of artificial membranes can be found in Table 6.

**Table 6:** Advantages and disadvantages of artificial membranes (Deferme *et al.*, 2008; Volpe, 2010).

| Advantages | Disadvantages |
|---|---|
| • Animal/human subjects not required.<br>• High throughput and relatively simple.<br>• Possibility of automation.<br>• Tolerates wider pH ranges and higher solubilisation concentrations.<br>• Cost-effectiveness.<br>• Good predictability. | • Transport is dependent upon lipid composition and pH of the membrane.<br>• Membrane retention of lipophilic compounds can be difficult.<br>• Inability to model active transport. |

## 2.7 Natural Oils

### 2.7.1 Olive oil

The olive fruit (*Olea europaea)* grows on a small tree belonging to the family *Oleaceae.* Olive oil is obtained by means of cold pressing or other suitable mechanical methods from the drupes of *Olea europaea.* The cold-pressing method is an oil extraction technique that involves no heat or chemical treatment as opposed to alternative methods of extraction (Cicero *et al.*, 2018). Olive oil is primarily comprised of triglycerides (≥ 99%) and secondarily of free fatty acids, mono- and diglycerides, and a variety of lipids which include hydrocarbons, aliphatic alcohols, tocopherols, sterols and pigments. A multitude of phenolic and volatile compounds are also naturally present, contributing to the unique nature of the oil (Boskou *et al.*, 2006; Lopez *et al.*, 2014).

A plethora of fatty acids are present in olive oil namely ≤ 1.0% linolenic acid (ω-3), 0.5 to 5% stearic acid, 0.3 to 3.5% palmitoleic acid (ω-7), 3.5 to 21.0% linoleic acid (ω-6), 7.5 to 20.0% palmitic acid and 55.0 to 83.0% oleic acid (ω-9). Fatty acids present in trace amounts include arachidic, behenic, eicosenoic, heptadecanoic, heptadecenoic, lignoceric and myristic acid. The fatty acid composition of the oil may differ from sample to sample and is greatly dependent on the altitude, cultivar, time of harvest, climate, variety, stage of fruit maturity and extraction process (Boskou *et al.*, 2006). The hydrocarbon, squalene, has been thoroughly researched and is regarded as partially responsible for various health benefits and chemoprotective action against certain cancers (Rao *et al.*, 1998; Smith *et al.*, 1998).

Alter and Gutfinger (1982) revealed that phospholipids (i.e. phosphatidylcholine, phosphatidylethanolamine, phosphatidylinositol and phosphatidylserine) are indeed present in

olive oil. In a more recent publication, Boukhchina *et al.* (2004) quantified the presence of glycerophospholipids in olive oil by means of liquid chromatography linked to mass spectrometry (LC-MS). The phospholipids that were discovered and quantified included, phosphatidylethanolamine, phosphatidylcholine, phosphatidylglycerol, phosphatidic acid and phosphatidylinositol. Although, this study was based on a single sample of olive oil from the retail market.

Ultimately, several types of olive oils exist in the market place, with varying fatty acid contents. It is also worth mentioning that some classes of minor constituents (i.e. phospholipids) are only present in the unrefined oil as the filtration process reduces the levels present and refinement removes the constituents all together (Boskou *et al.*, 2006; Covas *et al.*, 2015).

### 2.7.2 Emu oil

The emu (*Dromaius novaehallandiae*) is a flightless bird indigenous to Australia. The bright yellow oil is obtained from the bird's adipose tissue deposits, i.e. retroperitoneal and subcutaneous fat. The collected tissue samples are then subjected to centrifugation or maceration, followed by the filtration of the liquified fat to obtain pure emu oil (Abimosleh *et al.*, 2012; Jeengar *et al.*, 2015; Miyashita *et al.*, 2018).

The fatty acids, in ascending order of approximate concentrations present in emu oil, include 1.1% linolenic acid (ω-3), 4.3% palmitoleic acid (ω-7), 8.5% stearic acid, 9.5% linoleic acid (ω-6), 24.0% palmitic acid and 49.1% oleic acid (ω-9). The fatty acid composition of emu oil can vary, depending on the method of extraction, adipose tissue type and the diet of the bird. Average oil lipid content from retroperitoneal adipose tissue is 98.0 % and subcutaneous adipose tissue is 98.8%, respectively (Abimosleh *et al.*, 2012; Jeengar *et al.*, 2015).

Beckerbauer *et al.* (2001) failed to identify any phospholipids in their test sample, they attributed the absence of phospholipids to the extraction of the oil from adipose tissue by means of rendering (i.e. process of liquifying fat into oil). This supports the idea that oil refinement processes are directly responsible for eliminating various minor oil constituents such as phospholipids.

### 2.7.3 Grape seed and Cognac oil

The common grapevine (*Vitis vinifera*) is a deciduous flowering plant belonging to the family *Vitaceae* that produces berries (known as 'grapes') of varying colours. Grapeseed oil contains a plethora of phenolic compounds (i.e. carotenoids, flavonoids, phenolic acids, stilbenes and tannins), fatty acids and vitamins with great economic importance to the cosmetic, food and pharmaceutical industry. Grapeseed oil is mainly comprised of triglycerides, which contain

high amounts of unsaturated fatty acids compared to alternative oil-rich seeds (Garavaglia *et al.*, 2016; Hanganu *et al.*, 2012; Lachman *et al.*, 2015).

The ever increasing interest in grapeseed oil as a functional food can be attributed to its high contents of hydrophilic constituents such as phenolic compounds, and lipophilic constituents such as unsaturated fatty acids, phytosterols and vitamin E. Grape seeds contain approximately 8 to 20% oil in dry basis and the oil yield is dependent on various factors including the extraction technique, solvent type, operating conditions, variety of cultivars and environmental factors during harvesting (Garavaglia *et al.*, 2016).

Grapeseed oil is mainly characterised by its high content of unsaturated fatty acids namely linoleic acid (ω-6) and oleic acid (ω-9) with a distinctly lower content of linolenic acid (ω-3) compared to that of olive and emu oil. Palmitoleic acid (ω-7) and linolenic acid (ω-3) can be found in grapeseed oil, but only in trace amounts (Martinello *et al.*, 2007; Passos *et al.*, 2010; Yalcin *et al.*, 2017).

The fatty acid composition of cold-pressed grapeseed oil consists mainly of linoleic acid (ω-6), contributing to 66.0 – 75.3% of the total fatty acid content. Various grape varieties exist, each of which has different fatty acid compositions. The grapeseed oil composition is greatly dependent on the grapevine variety, degree of seed maturation and environmental factors (Garavaglia *et al.*, 2016).

Experimental work done by Sabir *et al.* (2012) on the quantification of fatty acids in several grape seed varieties, produced the following results:

- Linoleic acid (ω-6), 53.3 – 70.4% with a mean of 64.79%.
- Oleic acid (ω-9), 16.2 – 31.2% with a mean of 22.64%.
- Palmitic acid, 6.9 – 12.9% with a mean of 9.30%.
- Stearic acid, 1.44 – 4.69% with a mean of 2.24%.
- Linolenic acid (ω-3), 0.20 – 0.91% with a mean of 0.48%.
- Arachidic acid, 0.03 – 0.18% with a mean of 0.096%.

Essential oils are defined as aromatic products which have complex composition profiles and are sourced from botanical raw plant material, either by means of distillation or any suitable mechanical method that does not utilise heat during the process of extraction. Cognac essential oil is also sourced from the common grapevine (*Vitis vinifera*) and is obtained by means of steam distillation. This method of extraction takes advantage of a compounds' volatility to evaporate when heated with steam and the hydrophobicity of the compound to

segregate into an oil phase during condensation. Hitherto, experimental work relating to the exact chemical composition of cognac oil is especially limited (El Asbahani *et al.*, 2015; Luminescents, 2019).

## 2.8 Modified-release drug delivery systems

'Modified-release' drug delivery refers to the regulation of drug release from a dosage form (i.e. capsule, pellet and tablet) through dosage form design with the objective of delivering a drug at a specific site in the GI-tract, at a desired rate and/or at pre-determined time points. The concept of modified-release dosage forms has been around since the late 19$^{th}$ century, but as knowledge and understanding of the GI-tract increased, so did the design of dosage forms improve to provide very specific drug release according to pre-determined requirements. The pharmaceutical industry has shown great interest in utilising these technologies to increase product performance (McConnell & Basit, 2013). Modified-release drug delivery is, therefore, a broad-ranging concept that describes a multitude of different approaches (i.e. delayed-release, extended-release and gastro-retentive dosage forms) that can be used to control the time, site or rate of drug release after administration (McConnell & Basit, 2013).

Conventional drug delivery systems or dosage forms that are administered by means of the oral route, produce an immediate drug release where the whole dose is released all at once as soon as possible after administration. However, there are certain situations that require modifications to this conventional drug release pattern of immediate-release dosage forms. These situations include prolonging the effects of a drug after a single dose, reducing side effects, reducing the number of doses given over a specific period of time (i.e. reduced dose frequency) and thereby improving patient compliance.

Polymers (e.g. hydroxypropyl methylcellulose (HPMC) and polyethene oxide) are commonly utilised in the development of solid oral modified-release matrix-type drug delivery systems. These polymers are incorporated in matrix type tablets that form highly viscous gel layers after administration and exposure to gastrointestinal fluids creating a diffusion-based drug release platform. Dosage forms with this mechanism of drug release usually approach zero-order drug release kinetics, but gastrointestinal hydrodynamics and motility contribute to additional erosion of the matrix system, which can complicate the true *in vivo* rate of drug release. The desired rate of drug release can be tailored to specific requirements by changing formulation variables such as the type of polymer utilised in the matrix system and by varying the concentrations of these polymers in the dosage form amongst other techniques (McConnell & Basit, 2013).

### 2.8.1 Delayed-release dosage forms

Delayed-release dosage forms are designed to release a drug only after a certain amount of time has elapsed after oral administration, which generates a lag time between the point of administration of the dosage form and when the drug is detectable in the blood plasma. This type of drug release is mostly utilised in site-specific targeting, i.e. drug is released at a specific gastrointestinal region (e.g. the colon or small intestine) (McConnell & Basit, 2013).

Gastro-resistant drug delivery systems are a type of delayed-release dosage form designed to initiate drug release only after a certain environmental pH is met. This is achieved by coating the dosage form with a certain polymer that is insoluble at a low pH and soluble at a higher pH. These drug delivery systems are also known as enteric coated dosage forms (McConnell & Basit, 2013). The rate of drug release from such systems is controlled by the exposure to a desired pH, allowing for the coating to dissolve. Gastro-resistant coatings are utilised in formulation design to protect the stomach from the drug or to protect pH sensitive drugs from the acidic environment of the stomach (McConnell & Basit, 2013).

### 2.8.2 Extended-release dosage forms

'Extended-release' is a term generally used interchangeably with 'sustained-release' and 'prolonged-release' dosage forms. These dosage forms are designed to release a drug over an extended period of time (e.g. 12 hours) at a pre-determined rate. Thus, resulting in 'sustained' drug plasma levels for longer periods than conventional immediate-release dosage forms provide (McConnell & Basit, 2013). Extended-release dosage forms that are designed to remain in the stomach, are known as gastro-retentive dosage forms (see section 2.10) (McConnell & Basit, 2013).

## 2.9 Matrix-type drug delivery systems

In these dosage forms, the drug is dispersed as solid particles within a matrix core formed by a water-insoluble polymer (e.g. polyvinyl chloride) or in a gel-forming polymer (e.g. HPMC) when the system comes into contact with water. Drug particles that are located at the surface of the dosage form dissolve relatively quickly after administration when exposed to gastrointestinal fluids and these drug molecules are released first. Drug particles at further distances from the exterior of the dosage form will be dissolved later when the fluid reaches them. These drug molecules are released by means of diffusion through liquid-filled pores of the matrix system or through the gel front to the surrounding environment of the dosage form.

Consequently, as the drug release process proceeds, the diffusion distance of the dissolved drug particles increases as illustrated in Figure 2.6 (Alderborn, 2013). The formulation design factors that control the rate of drug release from a matrix system include the porosity of the dosage form, the drug concentration within the matrix, the solubility of the drug and the diameter of the pores in the dosage form. The concentration gradient is regulated by the solubility of the drug contained in the core matrix. The attributes of the pore system can be influenced by the compacting pressure during tabletting and the inclusion of soluble excipients within the matrix system (Alderborn, 2013).

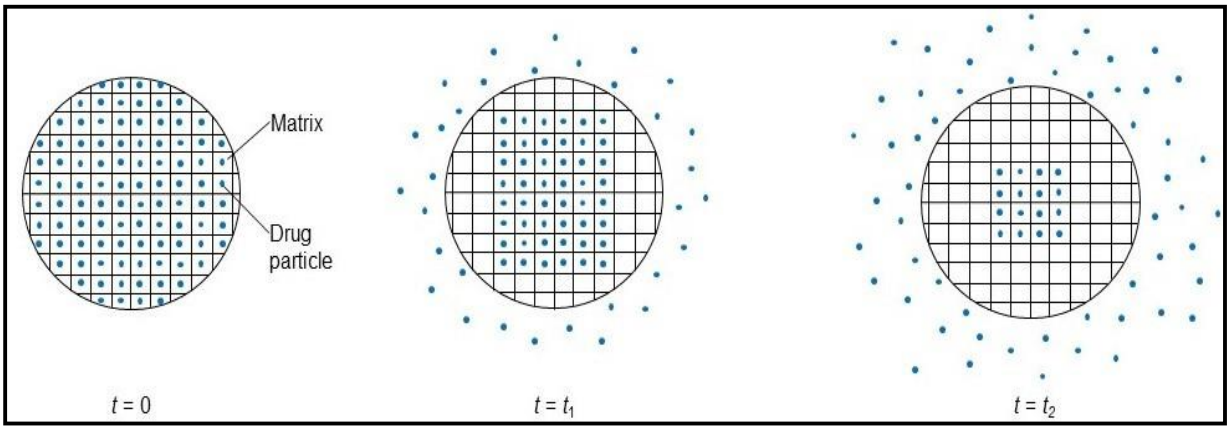


**Figure 2.6:** Schematic representation of the drug release mechanism from a diffusion-based matrix tablet (Alderborn, 2013).

A summary of the advantages and disadvantages of matrix tablets can be found in Table 7.

**Table 7:** Advantages and disadvantages of matrix tablets (Dash & Verma, 2013; Jaimini & Kothari, 2012).

| Advantages | Disadvantages |
|---|---|
| • Relatively inexpensive to produce.<br>• Simple to manufacture.<br>• Versatile and effective.<br>• Able to release compounds of high molecular weight.<br>• Suitable for degradable and non-degradable systems.<br>• Can be manufactured in a wide range of shapes and sizes.<br>• Maintains therapeutic concentrations over extended periods.<br>• No possibility of dose dumping in case of rupture.<br>• Reduction in drug toxicity owing to slow drug absorption.<br>• Minimises local and systemic side effects.<br>• Increased drug utilisation and treatment efficacy.<br>• Improved patient compliance.<br>• Reduction in healthcare cost.<br>• Usage of less total drug. | • The residual matrix must be removed after the drug has been released.<br>• Release rates are affected by food and GI-tract transit time.<br>• Engineering of zero-order release is difficult.<br>• Poor *in vitro – in vivo* correlation.<br>• Stability problems, not all drugs can be blended with the polymeric matrix.<br>• Requires additional patient education and counselling.<br>• Delayed onset of drug action.<br>• Release rate continuously decreases as a function of time owing to increased diffusional resistance. |

### 2.9.1 Biodegradable matrices

These matrix-type drug delivery systems are biologically degraded or eroded after administration by various enzymes produced by the surrounding living cells in order to release the drug. These matrices are comprised of polymers with the monomers linked to each other through functional groups that are unstable linkages. Examples of materials utilised in such matrices are polysaccharides, proteins, modified natural polymers and synthetic polymers (Jaimini & Kothari, 2012; Pundir *et al.*, 2013).

### 2.9.2 Hydrophobic matrices

In this matrix type oral dosage form, a hydrophobic or inert polymer is mixed with a drug and compressed into a tablet. Sustained drug release is generated by the dissolving drug's

diffusion through a network of channels that exist in between the compressed polymer particles. The following materials have been utilised to produce these matrices: polyvinyl chloride, polyethene, ethyl cellulose and acrylic polymers. Liquid penetration into the matrix is the rate-limiting step in these formulations. The drug contained in hydrophobic matrices is released by a diffusion-based mechanism (Jaimini & Kothari, 2012).

Factors controlling the rate of drug release from such matrices are the pore size, the number of pores present and the tortuosity of the matrix system. The drug release from such systems usually does not follow zero-order kinetics owing to the increasing distances that the drug particles have to travel to reach the exterior of the matrix. Consequently, the rate of drug release decreases with time (McConnell & Basit, 2013).

### 2.9.3 Hydrophilic matrices

Hydrophilic drug delivery systems can be utilised when sustained drug release is required. These matrix systems are specifically used in controlled drug delivery, due to their inherent versatility to obtain a desired drug release profile. However, these matrices are susceptible to effects by the varying environment of the GI-tract with regards to food, fluid and transit time. These can be challenging determinants for repeatable drug release from hydrophilic matrix systems as different drug blood profiles are achieved from the fed and fasted states (McConnell & Basit, 2013).

Hydrophilic matrix drug delivery systems are also known as swellable controlled-release dosage forms (refer to Figure 2.7 for a schematic illustration). Examples of materials used to produce such systems are polymers which include HPMC, hydroxyethylcellulose, methylcellulose, sodium carboxymethylcellulose, carob gum, agar-agar, chitosan, modified starches, alginates, molasses and acrylic acid polymers (Alderborn, 2013; Jaimini & Kothari, 2012: McConnell & Basit, 2013).

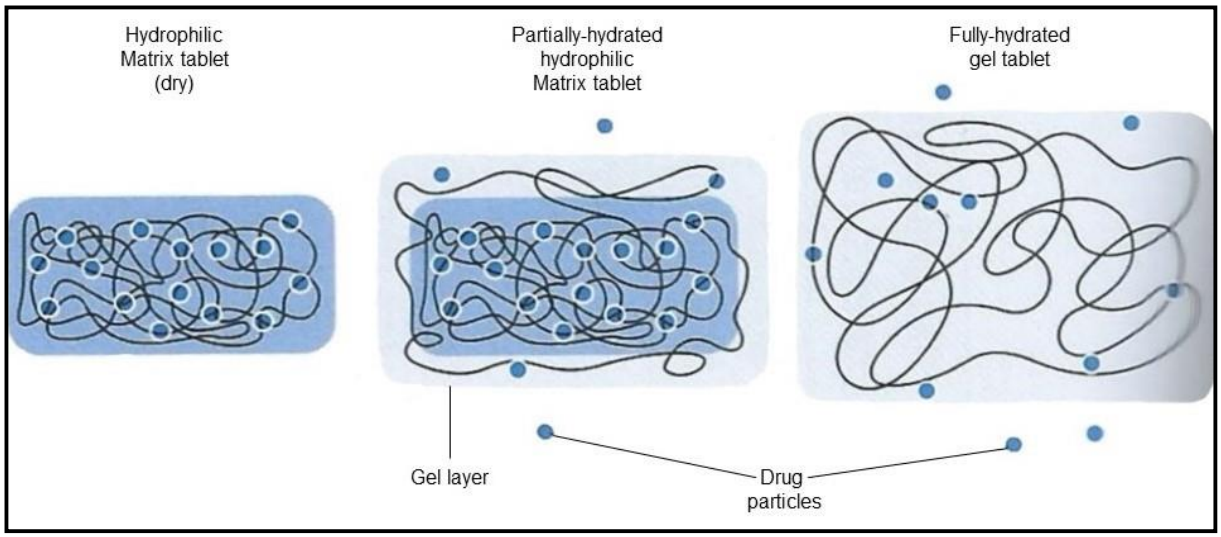


**Figure 2.7:** Schematic representation of the drug release process from a hydrophilic matrix tablet (McConnell & Basit, 2013).

Polymers are extensively utilised by the pharmaceutical industry in dosage form design. These polymers should have certain characteristics that act to control and maintain the rigidity of the matrix system over an extended period of time. HPMC is an inert, semi-synthetic polymer derived from cellulose ether that provides a dependable and robust mechanism for controlled drug release. The inherent non-ionic nature of the polymer minimises possible interaction issues when utilised in acidic and basic systems and delivers reproducible release profiles (Nokhodchi *et al.*, 2012).

Hydrophilic matrices swell on contact with water and exhibit a gradual increase in size as the water molecules enter the matrix. As the polymer swells, a gel layer is formed from the surface of the matrix system that acts as a platform for drug release. Drug particles would then move from within the gel layer by means of diffusion and/or erosion of the gel to the surrounding external environment of the dosage form. The mechanism of drug release from such systems can be diffusion from areas where polymer relaxation occurs, erosion or a combination of the two. Soluble drugs are primarily released by means of diffusion through the gel layer and insoluble drugs are primarily released by means of matrix erosion (Nokhodchi *et al.*, 2012).

### 2.9.4 Lipid matrices

These drug delivery matrices are produced by the utilisation of lipid waxes and related materials. Drug release from these matrices is generated by pore diffusion and erosion. Carnauba wax, together with stearic acid or stearyl alcohol have been utilised as a retardant base for various sustained-release formulations (Jaimini & Kothari, 2012).

## 2.10 Gastro-retentive drug delivery systems

An orally administered dosage form can reach the colon 4 – 5 hours after administration in the fasted state and that does not provide sufficient time for drug release and optimum absorption from a sustained-release dosage form. A potential simple way to improve drug absorption in the GI-tract is to hold a drug delivery system above the absorption window of that specific drug. Because most drugs' absorption windows are located in the small intestine, the obvious strategy is to keep the delivery system in the stomach (i.e. gastro-retention) (Davis, 2005).

Gastro-retentive systems are primarily designed to provide increased residence time in the stomach. They are intended to provide sustained drug release compared to the immediate drug release that conventional oral dosage forms (i.e. capsules and tablets) provide. Gastro-retentive delivery systems can significantly increase the bioavailability of drugs with a small window of absorption at a specific site (Chen *et al.*, 2013). A short gastric residence time results in the partial release of a drug from a sustained-release delivery system, leading to a sub-therapeutic dose available for absorption and consequently decreased efficacy (Ayre *et al.*, 2016; Zhang *et al.*, 2016).

Several formulation approaches have been used to increase the gastric residence time of oral dosage forms, which include bio-adhesive, floating, density-controlled and rapidly expanding delivery systems (Ayre *et al.*, 2016; Lopes *et al.*, 2016).

### 2.10.1 Bio-adhesive systems

Gastro-retentive drug delivery systems (refer to Figure 2.8 for a schematic illustration) based on the concept of bio-adhesion have been thoroughly utilised in order to create efficient and controlled drug delivery. During the last few decades, polymers (e.g. polyethylene glycol, HPMC, polyethylene oxide, sodium alginate) have generated great interest in the field of pharmaceutical technology to increase the gastric residence time of drug delivery systems by means of bio-adhesion (Ayre *et al.*, 2016; Shahid *et al.*, 2016; Singh *et al.*, 2017).

Bio-adhesive polymers are generally hydrophilic (water-inclination) macromolecular substances with a plethora of hydrogen bond forming groups such as amide, carboxyl, hydroxyl and sulphate groups (Khan *et al.*, 2014). Bio-adhesive drug delivery systems increase the affinity and duration of drug contact with biological membranes and are defined by their capacity to adhere to biological tissues (Lopes *et al.*, 2016). This capacity for adhesion to the gastrointestinal wall presents some valuable advantages such as longer residence time, and a closer and more enduring association between the local drug molecules and the epithelial membrane.

The inability to resist stomach secretions, constant mucus layer renewal and the high stomach hydration that decreases bio-adhesion of polymers are the main drawbacks of these systems (Ayre *et al.*, 2016; Lopes *et al.*, 2016).

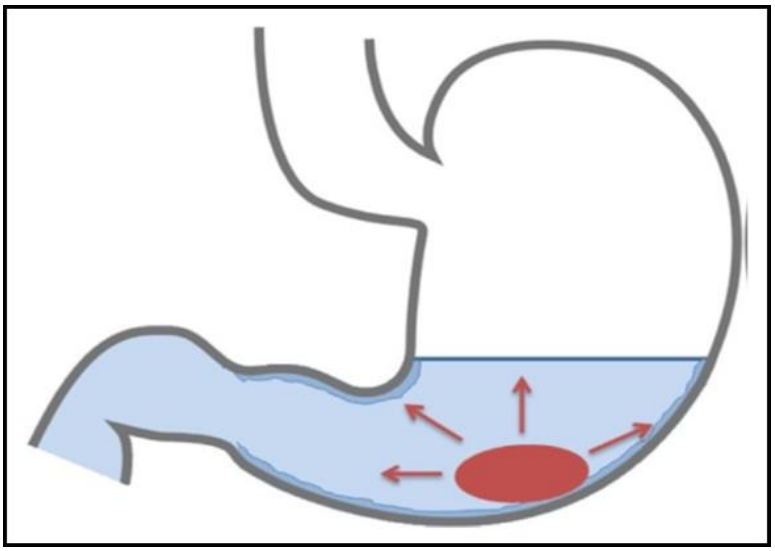

**Figure 2.8:** Schematic representation of drug release from a bio-adhesive gastro-retentive system (Lopes *et al*., 2016).

### 2.10.2 Floating systems

These gastro-retentive drug delivery systems (refer to Figure 2.9 for a schematic illustration) are the most favoured to provide successful gastro-retention of all the types of gastro-retentive systems described in the literature. These systems are characterised by their capacity to float on top of the gastric contents due to low density or gas production. The ability to float on the stomach contents allows the system to remain buoyant in the stomach for prolonged periods of time, while the drug is being released at a desired rate (Ayre *et al.*, 2016). The residuary system is eventually emptied from the stomach, depending on gastric contents and the floating force (Lopes *et al.*, 2016; Mayavanshi & Gajjar, 2008). Two distinct mechanisms allow these systems to remain buoyant in the stomach namely effervescent and non-effervescent mechanisms. The latter relies on a combination of swelling and gelling. For this purpose, different polymers can be used such as cellulose type hydrocolloid, polysaccharides and matrix forming polymers, such as HPMC, polyacrylate, polycarbonate, polymethacrylate, agar polystyrene, sodium alginate.

Upon contact with gastric fluid, effervescent gastro-retentive systems swell via hydration and form a gel layer with entrapped gas (e.g. carbon dioxide produced by effervescent action) around the core of the system, which ultimately controls the release of the drug. The entrapped gas provides the floating capacity of the system (Mayavanshi & Gajjar, 2008). Swellable polymers (e.g. methocel and chitosan) have been used in combination with effervescent

components (e.g. citric acid, sodium bicarbonate and tartaric acid) to keep matrix type systems buoyant (Ayre *et al.*, 2016). Hydrophilic polymers such as alginate and various types of HPMC are often used as matrices in non-effervescent systems, which also provide a sustained-release action (Lopes *et al.*, 2016).

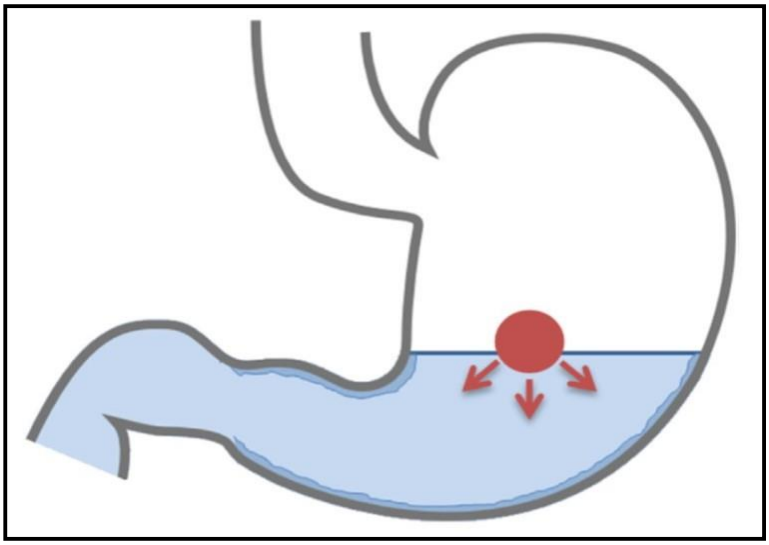

**Figure 2.9:** Schematic representation of drug release from a floating gastro-retentive system (Lopes *et al.*, 2016).

The controlled drug release of a floating system is attributed to the formation of a hydrated viscous gel layer around the tablet which acts as a platform to the diffusion of solute molecules to the outside of the matrix and to the intake of water. The degree of erosion, swelling and drug diffusion is determined by the nature of the matrix and polymer characteristics. Various floating gastro-retentive systems have been designed that combine several variables such as the area to volume ratio, coating, effervescence, geometric shape, size and production techniques (Lopes *et al.*, 2016; Mistry & Yadav, 2016).

### 2.10.3 Density-controlled systems

High-density gastro-retentive systems are designed to descend to the bottom of the stomach, where they remain situated for a prolonged period of time. This is achieved by increasing the system's density so that it is higher than that of the gastric fluids (approximately 1.004 g/cm$^3$). Data obtained from a study conducted by Clarke *et al.* (1995) pointed toward a somewhat proportional relationship between gastrointestinal residence time and density, the denser materials resulted in an increased stomach residence time. It has been reported that high-density pellets are capable of resisting gastric peristaltic movements. This ability has been attributed to their retention within the antrum of the stomach, which significantly increases gastric residence time. Furthermore, the extension of gastric residence time greatly depends on pellet density and to a lesser extent on the pellet size (Garg & Gupta, 2008; Lopes *et al.*,

2016). It is worth mentioning that data on these systems lack both animal and clinical studies. Additionally, it is technically difficult to produce high-density pellets that contain significant amounts of a drug (Lopes *et al.*, 2016; Moes, 2003).

### 2.10.4 Expanding systems

Expandable gastro-retentive systems (refer to Figure 2.10 for a schematic illustration) achieve increased gastric residence time by means of increasing their shape and volume by means of swelling (Lopes *et al.*, 2016). The incorporation of hydrophilic polymers, which are capable of absorbing large amounts of water upon contact with gastric fluids, are commonly utilised to produce these types of dosage forms. The flotation properties of these systems in addition to their expansion abilities are greatly influenced by the amount of gastric fluid present in the stomach (Lopes *et al.*, 2016).

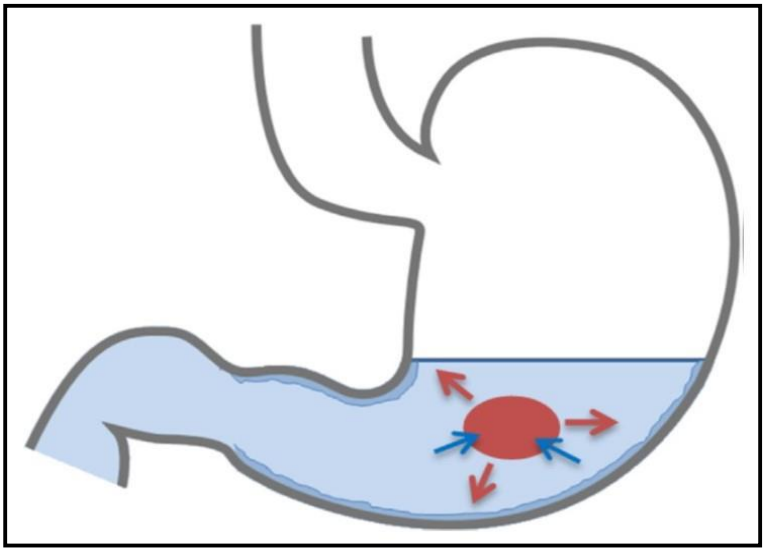

**Figure 2.10:** Schematic representation of drug release from an expanding gastro-retentive system (Lopes *et al.*, 2016).

## 2.11 Kinetic modelling of drug release

The development of modified-release dosage forms can be regarded as a significant medical advance in the area of drug delivery. The drug release profiles of these modified-release drug delivery systems can be divided into the following two general categories: slow drug release at a zero-order or first-order rate and an initial rapid-release followed by slow-release that is characterised by zero-order or first-order kinetics. The purpose of these systems is to maintain drug concentration in the blood or target tissues at a desired level for an extended period of time (Dash *et al.*, 2010).

The utilisation of mathematical modelling provides a useful tool in predicting and assessing the drug release kinetics of a dosage form. The complexities and phenomena associated with

drug release kinetics must be understood in order to develop mathematical models to best describe such processes. The model can also be described as a mathematical equation in which the ruling factors contributing to that specific release pattern are included (Dash *et al.*, 2010; Gouda *et al.*, 2017; Ramteke *et al.*, 2014).

Dissolution tests provide quantification of drug release profiles from dosage forms. The results obtained from these tests can be quantitatively analysed by means of various mathematical formulae. The development and refinement of tools that facilitate product evaluation during development by means of reducing bio-studies (i.e. clinical *in vivo* studies) are very advantageous in terms of cost and time. In order to compare the dissolution profiles of two drug delivery systems, model dependent (curve fitting), model independent and statistical analysis methods can be utilised (Dash *et al.*, 2010; Gouda *et al.*, 2017; Ramteke *et al.*, 2014).

### 2.11.1 Fundamentals of drug release kinetics

The elementary basis for evaluating the kinetics of drug release was provided by Noyes and Whitney in 1897. They expressed this fundamental principle in the form of an equation to define the dissolution from a single spherical particle:

$$dx/dt = C(S - x) \quad (1)$$

With dx/dt: The rate at which a solid substance dissolves in its own solution. S is the solubility of the substance, x is the concentration at time t and C is a constant.

Equation (1) can also be expressed as:

$$dC/dt = K(C_s - C) \quad (2)$$

With dC/dt: The rate of dissolution. $C_s$ is the saturation solubility of the substance, C is the definite concentration of the substance at time t and K is a constant.

The mathematical equation as initially provided by Noyes and Whitney has since been modified, with the first development coming from Eric Brunner and Stanislaus von Tolloczko in 1900, which concluded that the rate of dissolution also depends on the exposed surface area, surface structure, temperature, the rate of stirring and the arrangement of the apparatus (Dokoumetzidis & Macheras, 2006). The equation they proposed, was derived from Eq. 2 by making $K = K_1S$:

$$dC/dt = K_1S(C_s - C) \quad (3)$$

Where S is the surface area of the undissolved solid.

Additionally, Eric Brunner and Walter Nernst proposed a modified equation in 1904, derived from Eq. 3 by making $K_1 = D/Vh$:

$$dC/dt = DS/Vh(C_s - C) \quad (4)$$

Where D is the diffusion coefficient, V is the volume of the dissolution medium and h is the thickness of the diffusion layer.

Equation 4 can be simplified and expressed as:

$$dM/dt = KA(C_s - C_t) / h \quad (5)$$

With dM/dt: The rate of dissolution (mass transferred/time) which is directly proportional to the surface area of the undissolved solid, A, and the concentration difference, $(C_s - C_t)$, across the boundary layer and is inversely proportional to the boundary layer thickness, h. The diffusion coefficient is expressed by K in $m^2/s$. $C_t$ is the concentration of solute in solution at time t and $C_s$, is the saturated solubility of solid in the diffusion layer (Aulton, 2013; Dash *et al.*, 2010; Dokoumetzidis & Macheras, 2006; Gouda *et al.*, 2017; Ramteke *et al.*, 2014).

According to the Noyes and Whitney equation, drug molecules diffuse from a region of high concentration to a region of low concentration until systemic equilibrium is achieved. The rate of particle dissolution is directly proportional to the concentration gradient between the diffusion layer and the surrounding medium.

Hitherto, the contributions made by the above-mentioned scientists have resulted in considerable advancements in our understanding and evaluation of drug release kinetics. These fundamental contributions have enabled several scientists to develop drug release kinetic models throughout the 20$^{th}$ century, these models will be discussed in more detail below.

### 2.11.2 Zero-order kinetics

According to the elementary basis of pharmacokinetics, zero-order drug release from a dosage form can be expressed by the following equation:

$$C = C_o + K_o t \quad (6)$$

Where C is the amount of drug dissolved at time t, $C_o$ is the initial drug concentration in the solution (usually $C_o = 0$), and $K_o$ is the zero-order rate constant (concentration/time).

When the data obtained from drug release studies that follow zero-order kinetics are plotted as cumulative percentage of drug released as a function of time, it provides a linear graph with

a slope equal to $K_o$. These release kinetics represent a typical release profile to attain prolonged blood plasma levels and consequently also prolonged pharmacological action with oral administration (Dash *et al.*, 2010; Gouda *et al.*, 2017; Ramteke *et al.*, 2014).

### 2.11.3 First-order kinetics

The release of a drug which follows first-order kinetics can be expressed by the following equation:

$$\text{Log } C = \text{Log } C_o - K_1 t / 2.303 \quad (7)$$

Where $K_1$ is the first-order rate constant (per unit of time) and $C_o$ is the initial drug concentration.

When the data obtained from drug release studies that follow first-order kinetics are plotted as the logarithmic cumulative percentage of drug released versus time, it yields a straight line with a slope of $– K_1/2.303$ (Dash *et al.*, 2010; Gouda *et al.*, 2017; Ramteke *et al.*, 2014).

### 2.11.4 Hixson-Crowell model

The Hixon and Crowell cube root law describes the release from drug delivery systems where there is a change in diameter and surface area of the system during the dissolution process. Consequently, particles of regular area are directly proportional to the cube root of its volume. This concept was expressed in the form of an equation by Hixon and Crowell in 1931:

$$W_o^{⅓} – W_t^{⅓} = K_{HC} \times t \quad (8)$$

Where $W_o$ is the initial amount of drug in the dosage form, $W_t$ is the remaining amount of drug in the dosage form at time t and $K_{HC}$ is the Hixson-Crowell constant that describes the surface to volume relation.

When the data obtained from drug release studies are plotted as the cube root of drug percentage remaining in the matrix versus time, a straight line will be produced. This equation is utilised for interpretation of dissolution data of conventional, immediate-release or dispersible dosage forms (Dash *et al.*, 2010; Gouda *et al.*, 2017; Ramteke *et al.*, 2014).

### 2.11.5 Higuchi model

The first attempt to describe drug release from a matrix system was proposed by Higuchi in 1961 by means of the following equation:

$$Q = A\sqrt{D\delta/\tau\ (2C_o - \delta C_s)C_s t} \quad (9)$$

Where Q is the amount of drug released in time t per unit area A, D is the diffusion coefficient of the drug molecules in the matrix, $C_o$ is the initial drug concentration, $C_s$ is the drug's solubility in the matrix media, δ is the porosity of matrix and τ is the tortuosity.

Equation 9 can be simplified and expressed as:

$$Q = K_H \times t^{½} \quad (10)$$

Where $K_H$ is the Higuchi dissolution constant.

When dissolution data produce a linear Q versus $t^{½}$ plot with a slope equal to $K_H$, it indicates that the drug was released by means of a diffusion mechanism.

### 2.11.6 Korsmeyer-Peppas model

In 1983, Korsmeyer *et al.* proposed an equation that describes drug release from a polymeric matrix-type drug delivery system, which is described as follows:

$$M_t/M_\infty = Kt^n \quad (11)$$

Where $M_t/M_\infty$ is the fraction of drug released at time t, K is the release rate constant and $t^n$ is the release exponent.

The exponent, n, is used to characterise different release mechanisms (see Table 8) from cylindrical shaped matrices (in other words matrix type tablets). To ascertain the exponent of n, the portion of the release curve at $M_t/M_\infty < 0.6$ should be used. When the dissolution data obtained from drug release studies fit the Korsmeyer-Peppas model, the data plotted as logarithmic cumulative percentage of drug release versus log time will produce a straight line (Dash *et al.*, 2010; Gouda *et al.*, 2017; Ramteke *et al.*, 2014).

**Table 8:** Diffusional release mechanisms from polymeric films (Dash *et al.*, 2010; Ramteke *et al.*, 2014).

| Release exponent (n) | Drug transport mechanism | Rate (function of time) |
|---|---|---|
| 0.5 | Fickian transport | $t^{-0.5}$ |
| 0.45 < n < 0.89 | Non-Fickian transport | $t^{n-1}$ |
| 0.89 | Case II transport | Zero-order release |
| n > 0.89 | Super case II transport | $t^{n-1}$ |

### 2.11.7 Weibull model

The Weibull equation can be utilised for different dissolution processes. When applied to the dissolution of pharmaceutical dosage forms, the equation expresses the accumulation of drug fraction in solution:

$$M = M_o \left[1 - e^{-\frac{(t - T)^b}{a}}\right] \quad (12)$$

Where M is the amount of drug dissolved as a function of time t, $M_o$ is the total amount of drug being released, T accounts for the lag time measured due to the dissolution process, a is the scale parameter that describes the time dependence and b describes the shape of the dissolution curve progression.

If b = 1, the curve corresponds to the exact shape of an exponential profile with constant k = 1/a, expressed by the following equation:

$$M = M_o (1 - e^{-k(t - T)}) \quad (13)$$

If b > 1, the shape of the curve becomes sigmoidal with a turning point. If b < 1, the shape of the curve will show an abrupt increase compared to the curve of b = 1.

Equation 13 can be rearranged and expressed as:

$$\text{Log } [-\ln (1 - m)] = b \log (t - T_i) - \log a \quad (14)$$

A linear relation can be obtained from equation 11, for a log-log plot of -ln (1 - m) as a function of time, t. The slope of the line is used to obtain the shape parameter, b, and the scale parameter, a, is estimated from the ordinate value (1/a) at time = 1. However, a can be

replaced by dissolution time $T_d$, meaning a = $T_d$. The value of $T_d$ is read from the graph as the time value corresponding to the ordinate value -ln (1 - m) = 1 and thus m = 0.632. $T_d$ represents the time interval required to dissolve/release 63.2% of the total amount of drug present in the dosage form.

Drug delivery systems following this model will produce a linear plot when the data obtained from drug release studies are plotted as the logarithmic amount of drug dissolved as a function of log time. The Weibull model is more functional for comparing release profiles of matrix type drug delivery systems (Dash *et al.*, 2010; Ramteke *et al.*, 2014).

## 2.12 Conclusion

During the last century, there have been extensive advancements and discoveries in the field of pharmaceutical sciences. This branch of health science forms an integral part of the ever-expanding field of medicinal science. Considering the escalating interest of pharmaceutical companies for cell and tissue-free models to implement drug permeation testing during drug development and the unavoidable restrictions associated with animal models, artificial type models are needed in pre-clinical drug discovery research (Berben *et al.*, 2018; Nef, 2001). Therefore, during this study, natural oils (i.e. olive, emu and cognac oil) have been selected together with various artificial membranes (i.e. cellulose acetate, cellulose nitrate, cellulose acetate-nitrate mixture and polyamide) to study the permeation properties and equivalence of these membranes to biological membranes and ultimately, to identify and predict their applicability in permeation research.

Artificial membranes constitute an appealing alternative to the use of animal tissues or cells due to the simplicity, cost-effectiveness, time-sparing and reproducibility of results. The identification of a suitable artificial membrane simulating the behaviour of the epithelium of the natural GI-tract represents the critical step in the fulfilment of this research study.

# CHAPTER 3: AUTHOR GUIDELINES AND ARTICLE FOR PUBLICATION

The article to be published in 'Pharmaceutical Development and Technology' has been formatted according to the guidelines and template as provided by the academic journal. The Tables and Figures have been included in text as they would appear in the published article.

# AUTHOR GUIDELINES

The following guidelines have been compiled by the Taylor and Francis group and are available online at:

https://www.tandfonline.com/action/authorSubmission?show=instructions&journalCode=iphd20

**Preparing Your Paper**

All authors submitting to medicine, biomedicine, health sciences, allied and public health journals should conform to the Uniform Requirements for Manuscripts Submitted to Biomedical Journals, prepared by the International Committee of Medical Journal Editors (ICMJE).

**Structure**

Your paper should be compiled in the following order: title page; abstract; keywords; main text introduction, materials and methods, results, discussion; acknowledgments; declaration of interest statement; references; appendices (as appropriate); table(s) with caption(s) (on individual pages); figures; figure captions (as a list).

**Word Limits**

Please include a word count for your paper.

A typical paper for this journal should be no more than 12000 words, inclusive of tables, references, figure captions.

**Style Guidelines**

Please refer to these quick style guidelines when preparing your paper, rather than any published articles or a sample copy.

Any spelling style is acceptable so long as it is consistent within the manuscript.

Please use single quotation marks, except where ‘a quotation is “within” a quotation’. Please note that long quotations should be indented without quotation marks.

**Formatting and Templates**

Papers may be submitted in Word or LaTeX formats. Figures should be saved separately from the text. To assist you in preparing your paper, we provide formatting template(s).

Word templates are available for this journal. Please save the template to your hard drive, ready for use.

A LaTeX template is available for this journal. Please save the LaTeX template to your hard drive and open it, ready for use, by clicking on the icon in Windows Explorer.

If you are not able to use the template via the links (or if you have any other template queries) please contact us here.

**References**

Please use this reference guide when preparing your paper.

https://www.tandf.co.uk//journals/authors/style/reference/tf_CSE.pdf

**Checklist: What to Include**

*Author details.* Please ensure everyone meeting the International Committee of Medical Journal Editors (ICMJE) requirements for authorship is included as an author of your paper. All authors of a manuscript should include their full name and affiliation on the cover page of the manuscript. Where available, please also include ORCiDs and social media handles (Facebook, Twitter or LinkedIn). One author will need to be identified as the corresponding author, with their email address normally displayed in the article PDF (depending on the journal) and the online article. Authors' affiliations are the affiliations where the research was conducted. If any of the named co-authors moves affiliation during the peer-review process, the new affiliation can be given as a footnote. Please note that no changes to affiliation can be made after your paper is accepted. Read more on authorship.

*A structured or unstructured abstract of no more than 200 words.*

*Graphical abstract (optional).* This is an image to give readers a clear idea of the content of your article. It should be a maximum width of 525 pixels. If your image is narrower than 525 pixels, please place it on a white background 525 pixels wide to ensure the dimensions are maintained. Save the graphical abstract as a .jpg, .png, or .tiff. Please do not embed it in the manuscript file but save it as a separate file, labelled GraphicalAbstract1.

You can opt to include a video abstract with your article. Find out how these can help your work reach a wider audience, and what to think about when filming.

*Between 5 and 10 keywords.* Read making your article more discoverable, including information on choosing a title and search engine optimization.

*Funding details.* Please supply all details required by your funding and grant-awarding bodies as follows:

*For single agency grants*

This work was supported by the [Funding Agency] under Grant [number xxxx].

*For multiple agency grants*

This work was supported by the [Funding Agency #1] under Grant [number xxxx]; [Funding Agency #2] under Grant [number xxxx]; and [Funding Agency #3] under Grant [number xxxx].

*Disclosure statement.* This is to acknowledge any financial interest or benefit that has arisen from the direct applications of your research. Further guidance on what is a conflict of interest and how to disclose it.

*Data availability statement.* If there is a data set associated with the paper, please provide information about where the data supporting the results or analyses presented in the paper can be found. Where applicable, this should include the hyperlink, DOI or other persistent identifier associated with the data set(s). Templates are also available to support authors.

*Data deposition.* If you choose to share or make the data underlying the study open, please deposit your data in a recognized data repository prior to or at the time of submission. You will be asked to provide the DOI, pre-reserved DOI, or other persistent identifiers for the data set.

*Geolocation information.* Submitting a geolocation information section, as a separate paragraph before your acknowledgements, means we can index your paper's study area accurately in JournalMap's geographic literature database and make your article more discoverable to others.

*Supplemental online material.* Supplemental material can be a video, dataset, fileset, sound file or anything which supports (and is pertinent to) your paper. We publish supplemental material online via Figshare. Find out more about supplemental material and how to submit it with your article.

*Figures.* Figures should be high quality (1200 dpi for line art, 600 dpi for grayscale and 300 dpi for colour, at the correct size). Figures should be supplied in one of our preferred file formats: EPS, PS, JPEG, TIFF, or Microsoft Word (DOC or DOCX) files are acceptable for figures that have been drawn in Word. For information relating to other file types, please consult our Submission of electronic artwork document.

*Tables.* Tables should present new information rather than duplicating what is in the text. Readers should be able to interpret the table without reference to the text. Please supply editable files.

*Equations.* If you are submitting your manuscript as a Word document, please ensure that equations are editable. More information about mathematical symbols and equations.

*Units.* Please use SI units (non-italicized).

*Using Third-Party Material in your Paper*

You must obtain the necessary permission to reuse third-party material in your article. The use of short extracts of text and some other types of material is usually permitted, on a limited basis, for the purposes of criticism and review without securing formal permission. If you wish to include any material in your paper for which you do not hold copyright, and which is not covered by this informal agreement, you will need to obtain written permission from the copyright owner prior to submission. More information on requesting permission to reproduce work(s) under copyright.

*Disclosure Statement*

Please include a disclosure statement, using the subheading "Disclosure of interest." If you have no interests to declare, please state this (suggested wording: The authors report no conflict of interest). For all NIH/Wellcome-funded papers, the grant number(s) must be included in the declaration of interest statement. Read more on declaring conflicts of interest.

*Clinical Trials Registry*

In order to be published in a Taylor & Francis journal, all clinical trials must have been registered in a public repository at the beginning of the research process (prior to patient enrolment). Trial registration numbers should be included in the abstract, with full details in the methods section. The registry should be publicly accessible (at no charge), open to all prospective registrants, and managed by a not-for-profit organization. For a list of registries that meet these requirements, please visit the WHO International Clinical Trials Registry Platform (ICTRP). The registration of all clinical trials facilitates the sharing of information among clinicians, researchers, and patients, enhances public confidence in research, and is in accordance with the ICMJE guidelines.

*Complying With Ethics of Experimentation*

Please ensure that all research reported in submitted papers has been conducted in an ethical and responsible manner, and is in full compliance with all relevant codes of experimentation and legislation. All papers which report in vivo experiments or clinical trials on humans or animals must include a written statement in the Methods section. This should explain that all work was conducted with the formal approval of the local human subject or animal care committees (institutional and national), and that clinical trials have been registered as legislation requires. Authors who do not have formal ethics review committees should include a statement that their study follows the principles of the Declaration of Helsinki.

*Consent*

All authors are required to follow the ICMJE requirements on privacy and informed consent from patients and study participants. Please confirm that any patient, service user, or

participant (or that person's parent or legal guardian) in any research, experiment, or clinical trial described in your paper has given written consent to the inclusion of material pertaining to themselves, that they acknowledge that they cannot be identified via the paper; and that you have fully anonymized them. Where someone is deceased, please ensure you have written consent from the family or estate. Authors may use this Patient Consent Form, which should be completed, saved, and sent to the journal if requested.

*Health and Safety*

Please confirm that all mandatory laboratory health and safety procedures have been complied with in the course of conducting any experimental work reported in your paper. Please ensure your paper contains all appropriate warnings on any hazards that may be involved in carrying out the experiments or procedures you have described, or that may be involved in instructions, materials, or formulae.

Please include all relevant safety precautions; and cite any accepted standard or code of practice. Authors working in animal science may find it useful to consult the International Association of Veterinary Editors' Consensus Author Guidelines on Animal Ethics and Welfare and Guidelines for the Treatment of Animals in Behavioural Research and Teaching. When a product has not yet been approved by an appropriate regulatory body for the use described in your paper, please specify this, or that the product is still investigational.

# ARTICLE FOR PUBLICATION

## Artificial membranes in combination with selected natural oils for *in vitro* drug passive diffusion screening in Ussing type chamber apparatus applied to gastro-retentive systems

Mark Fensham[a], Jan Steenekamp,[a] Adriaan Jacobs[b] and Josias Hamman*[a]

[a]*Centre of Excellence for Pharmaceutical Sciences, North-West University, Private Bag X6001, Potchefstroom, 2520, South Africa;*
[b]*Centre of Excellence for Nutrition, North-West University, Private Bag X6001, Potchefstroom, 2520, South Africa.*

*Corresponding author: Josias Hamman (PhD), Centre of Excellence for Pharmaceutical Sciences, North-West University, Private Bag X6001, Potchefstroom, 2520, South Africa; E-mail: Sias.Hamman@nwu.ac.za; Tel.: +27 18 299 4035; Fax: +27 18 299 2248.

# Artificial membranes in combination with selected natural oils for *in vitro* drug passive diffusion screening in Ussing type chamber apparatus applied to gastro-retentive systems

This study aimed to develop an effective *in vitro* technique for the screening of passive drug diffusion utilising artificial membranes in combination with three selected oils (i.e. cognac, emu and olive oil). Artificial membranes of varying chemical composition and characteristics have been investigated individually and in combination with the selected oils in terms of the passive diffusion of a fluorescent probe (i.e. Rhodamine 6G or R6G), in a diffusion apparatus as compared to excised pig intestinal tissues. In general, the permeation results showed that the rate and extent of R6G permeation were dependent on the membrane composition as well as the type of oil used. The apparent permeability coefficient ($P_{app}$) value for R6G across the cellulose nitrate membrane ($0.197 \times 10^{-7} \pm 0.069$ cm/s) was the closest to the $P_{app}$ of R6G across the excised pig intestinal tissue ($0.210 \times 10^{-7} \pm 0.080$ cm/s). The cellulose acetate-nitrate mixture membrane impregnated with emu oil also produced a $P_{app}$ value ($0.191 \times 10^{-7} \pm 0.010$ cm/s) that was relatively close to that of R6G across the excised pig intestinal tissue. The delivery of R6G from gastro-retentive matrix type tablets correlated with the release of R6G from the gastro-retentive tablets.

Keywords: Artificial membrane, cognac oil, controlled drug release, emu oil, *in vitro* permeation, gastro-retentive dosage form, kinetic drug modelling, olive oil.

## 1. Introduction

There is a need for more cost-effective, high throughput *in vitro* models to study the pharmacokinetic parameters of drugs, especially for the screening of new chemical entities to evaluate their drug-like properties (Benam et al. 2015). The therapeutic efficacy of orally administered drugs is dependent on the absorption and bioavailability of the drug. The rate of drug dissolution in the gastrointestinal fluid and permeation across the lipid bilayer of the epithelial membrane are some of the important factors that influence oral drug absorption and ultimately also its bioavailability (Corti et al. 2006; Shekhawat and Pokharkar 2017). The oral route of drug administration remains the most prominent and preferred route of medicine administration, owing to its numerous intrinsic advantages (McConnell and Basit 2018). On the other hand, the oral route of administration can also be an unpredictable and highly fluctuating route of treatment, predominantly pertaining to drugs that have poor solubility, slow rate of dissolution, poor intestinal permeability and a narrow window of absorption (Lopes et al. 2016; Vo et al. 2017). Furthermore, an increasing number of novel chemical entities are generated by combinational chemistry and parallel synthesis, which creates the need for accurate high throughput *in vitro* screening methods for rapid evaluation of drug absorption potential (Corti et al. 2006; Deferme et al. 2008).

*In vitro* models offer a cost-effective, accurate and high throughput approach for the prediction of drug-membrane permeability. *In vitro* models significantly contribute towards reducing the use of animals as *in vivo* models, facilitating the rapid identification of novel drug candidates with desirable pharmacokinetic properties (Pereira et al. 2016). Several methods exist for *in vitro* prediction and evaluation of drug permeability. These techniques include epithelial cell monolayers (e.g. Caco-2 cell line), parallel artificial membrane permeability assays (PAMPA) and excised tissues mounted in Ussing type chambers. The Caco-2 cell line is one of the most frequently implemented *in vitro* methods, owing to its ability in mimicking most transport pathways in the gastrointestinal tract and showing

functional properties of the human intestinal epithelium (Ashford 2018; Corti et al. 2006). However, the limitations of this cell culture method include relatively long cell growth cycles, absence of a mucus layer, high cost of implementation, risk of microbial contamination and intra- and inter-laboratory variability (Volpe 2010).

*In silico* methods are founded on computational simulations to assess physicochemical properties of drug molecules such as lipophilicity (Log $P_{o/w}$), molecular weight (MW), polar surface area (PSA), acid dissociation constant (pKa) and hydrogen bonding potential. However, these models lack the ability to simulate the complex nature of the *in vivo* environment that influences dissolution behaviour as well as active transport, bowel movement, fluid composition and volume. Although *in silico* models offer a simple, high throughput approach capable of screening novel drug candidates during the early stages of development, certain challenges remain that needs to be overcome in order to be more effective (Ashford 2018; Berben et al. 2018; Harloff-Helleberg et al. 2017).

*Ex vivo* models are based on the use of excised tissues sourced from humans or animals mounted in a diffusion apparatus to evaluate and predict intestinal absorption. These models possess unique qualities that differentiate them from cellular based *in vitro* models such as the presence of a mucous layer, metabolism enzymes and transporter proteins. Pig intestinal tissue has demonstrated a high similarity with that of human intestinal tissue (Westerhout et al. 2014). Therefore, excised intestinal tissues mounted on Ussing type chambers have demonstrated to be an effective biological method for drug permeation experiments. However, limited availability of human intestinal tissues and the genetic differences between different animal species to humans are some of the challenges associated with this method of screening for drug permeability (Joubert et al. 2017; Westerhout et al. 2014). Furthermore, results obtained from these models often improperly estimate the degree of drug absorption due to limitations such as the lack of an intact nervous system, limited tissue viability and the absence of normal blood flow (Luo et al. 2013). Limited tissue

viability is especially important when evaluating the drug delivery potential of sustained-release dosage forms over extended periods of time.

Since many drugs favour passive diffusion as means of crossing the epithelial membrane during absorption, artificial membranes offer a potentially useful high throughput approach for assessing drug candidate absorption potential (Berben et al. 2018; Corti et al. 2006). The PAMPA technique is based on a filter-supported lipid membrane and is one of the most frequently utilised *in vitro* methods for predicting absorption (Petit et al. 2016; Buckley et al. 2012; Volpe 2010). However, this technique presents some limitations owing to the presence of solvent, absence of stirring conditions and the difficulty to reach and maintain sink conditions during permeation experiments (Buckley et al. 2012; Petit et al. 2016).

Several characteristics that differ and shift throughout the gastrointestinal tract (i.e. commensal flora, pH, gastrointestinal transit time, surface area and enzymatic activity) can significantly influence drug absorption. Conventional drug delivery systems fail to overcome these intricate attributes imposed by the gastrointestinal tract and are especially inappropriate for drugs that are preferentially absorbed in the stomach and duodenum, since conventional systems lack the capacity to resist gastric emptying (Lopes et al. 2016). Therefore, the partial release and concomitant reduction of drug dose efficacy are consequences of the inability of conventional formulations to be retained in the stomach. Currently, the majority of drug candidates being developed are poorly soluble and their primary site of absorption is limited to the small intestine, resulting in sub-optimal and varying systemic drug exposure (Berben et al. 2018). A gastro-retentive drug delivery system can facilitate a predictable drug release profile that allows for more complete absorption and increased therapeutic efficacy, owing to the ability of the formulation to facilitate and maximise drug absorption throughout the entire gastrointestinal tract. With this strategy, *in vivo* drug dissolution is limited to the stomach, which enables perpetual drug release and absorption (Lopes et al. 2016; Streubel et al. 2006; Vo et al. 2017). Gastro-retentive drug delivery systems, therefore, provide a solution to

problems such as a narrow absorption window as well as the delivery of poorly soluble and permeable drug compounds (Streubel et al. 2006; Vo et al. 2017).

This study investigated the suitability of artificial membranes in combination with oils as an *in vitro* method for the evaluation of drug permeation by passive diffusion. This model was then applied to measure the delivery of a compound from modified release gastro-retentive drug delivery systems over extended periods of time while overcoming the limitation of tissue degradation as experienced with *ex vivo* models. This study investigated the permeation of a fluorescent probe (R6G) across different artificial membranes alone and in combination with selected natural oils, which were compared to the permeation of R6G across excised pig intestinal tissue. R6G is a lipophilic (Log $P_{o/w}$ = 6.35) xanthene-based organic fluorescent dye that is extensively used as a fluorescent probe in experiments including permeation studies (Nair et al. 2005). R6G has a molecular weight of 479.01 g/mol and can be dissolved in water, ethanol, methanol and various other organic solvents (CHEMBL 2018; Sigma-Aldrich 2019). The artificial membrane that exhibited fluorescent probe permeation closest to that obtained across excised pig intestinal tissue was then used alone and in combination with the selected oils for the evaluation of drug delivery from a gastro-retentive drug delivery system. The natural oils that were chosen for this study included olive oil (*Olea europaea*), emu oil (*Dromaius novaehallandiae*) and cognac oil (*Vitis vinifera*), each having unique fatty acid profiles (Garavaglia et al. 2016; Lopez et al. 2014; Miyashita et al. 2018).

## 2. Materials and methods

### *2.1 Materials*

R6G, Krebs-Ringer bicarbonate buffer (KRB), hydrochloric acid (HCl), sodium bicarbonate, magnesium stearate, Styrene-DVB (Styrene-divinylbenzene copolymer), olive oil and cognac oil were purchased from Sigma-Aldrich (Johannesburg, RSA). Pharmacoat® (Hydroxypropyl methylcellulose) was purchased from Shin-Etsu Chemical Co (Tokyo, Japan). Pharmacel® 101 (Microcrystalline cellulose) was purchased from Warren Chem Specialities (Pretoria, RSA). Kollidon® VA64 (Vinylpyrrolidone-vinyl acetate copolymer) was purchased from BASF (Ludwigshafen, Germany). Cellulose acetate (CA) and polyamide (PA) membrane filters were purchased from Sartorius (Midrand, RSA). Cellulose acetate-nitrate mixture (CANM) and cellulose nitrate (CN) membrane filters were purchased from Merck (Sandton, RSA). Emu oil (Ziva Emuphoria, batch number TEO0940) was purchased from a local pharmacy (Potchefstroom, RSA). Costar® 96-well plates were purchased from The Scientific Group (Randburg, RSA). Pig intestinal tissue was collected from the local abattoir (Potchefstroom, RSA).

### *2.2 Fluorescence spectrophotometric analysis*

A fluorescence spectrophotometric analytical method was utilised to measure the R6G concentration in the samples obtained from the assay, dissolution and permeation studies using a SpectraMax Paradigm® multi-mode detection platform plate reader equipped with SoftMax® Pro Data analysis software. The excitation and emission wavelengths were set to 510 nm and 560 nm, respectively (Sigma-Aldrich 2019).

The fluorescence spectrophotometric analytical method was validated in terms of linearity, precision, accuracy, limit of detection (LOD), limit of quantification (LOQ) and

specificity according to previously published methods (Ramadan et al. 2012; Shabir 2003; Singh 2013; USP 2017).

### *2.3 Preparation of pig intestinal tissue for ex vivo transport studies*

A piece of approximately 40 cm of pig jejunum tissue was collected from a local abattoir (Potchefstroom, RSA) immediately after slaughtering of a domestic pig (*Sus scrofa domesticus*). After excision of the pig jejunal segment, it was rinsed and submerged in freshly prepared ice-cold KRB.

Upon arrival at the laboratory, the intestinal segment was transferred onto a glass rod and kept moist by continuously rinsing the tissue with KRB. The serosal layer was removed by means of blunt dissection and the tissue was cut alongside its mesenteric border using a scalpel blade and the resulting sheet of intestinal tissue was transferred onto a piece of filter paper. It was cut into smaller segments and mounted between the half-cells of six Sweetana-Grass diffusion chambers. Peyer's patches (i.e. epithelial adaptations), that can affect drug permeability, were avoided when selecting jejunal tissue pieces suitable for mounting between the half-cells of the diffusion apparatus.

### *2.4 Artificial membranes for in vitro transport studies*

The characteristics of four selected artificial membranes (i.e. chemical composition, pore size, thickness and porosity percentage) are presented in Table 1. Artificial membranes refer to synthetically produced filters from different materials (i.e. cellulose acetate, cellulose nitrate, cellulose acetate-nitrate mixture, polyamide, polyvinylidene-fluoride and polytrifluoro-ethylene).

Table 1. Characteristics of selected artificial membranes.

| Artificial membrane chemical composition | Manufacturer | Pore size (µm) | Thickness (µm) | Porosity (%) |
|---|---|---|---|---|
| Cellulose acetate (CA) | Sartorius | 0.2 | 120 | 90 |
| Polyamide (PA) | Sartorius | 0.2 | 115 | 85 |
| Cellulose nitrate (CN) | Whatman | 0.1 | 130 | 90 |
| Cellulose acetate-nitrate mixture (CANM) | Millipore | 0.025 | 100 | 72 |

Each artificial membrane was cut to size and then mounted between the half-cells of Sweetana-Grass diffusion chambers as previously described for a similar *in vitro* diffusion chamber setup (Corti et al. 2006). For the membrane in combination with oil permeation experiments, each selected artificial membrane was impregnated with each of the selected oils (i.e. cognac oil, olive oil and emu oil) by submersion of the membrane in each oil for 10 min as described previously (Corti et al. 2006). Thereafter, the excess oil was removed by placing the membrane between two absorbing pieces of filter paper for 4 min.

### *2.5 Permeation media*

KRB (pH 7.4) was used during the *ex vivo* permeation studies across excised pig intestinal tissues and during the permeation studies across the selected artificial membranes. In addition, 0.1 N HCl (pH 1.2) was used as a medium during the *in vitro* permeation studies across the selected artificial membranes. This acidic medium was included to evaluate the permeation of a fluorescent probe in solution across the selected artificial membranes at conditions in which the gastro-retentive systems were evaluated during the application part of the study.

### *2.6 Preparation of Rhodamine 6G solutions for permeation studies*

R6G was used as a model compound in this study at a concentration of 5 µg/ml throughout all the permeation experiments by completely dissolving the compound in KRB or 0.1 N HCl. For the *ex vivo* permeation experiments across excised pig intestinal tissues and the *in vitro* permeation experiments across the selected artificial membranes, a clear solution of R6G in KRB was placed in the donor chamber (7 ml), while KRB without additives was placed in the acceptor chamber (7 ml). The *in vitro* experiments in 0.1 N HCl were carried out using a clear solution of R6G in 0.1 N HCl placed in the donor chamber (7 ml), while 0.1 N HCl without additives was placed in the acceptor chamber (7 ml).

### *2.7 Chemical characterisation of the selected natural oils*

The selected oils of natural origin used in this study to impregnate the artificial membranes, namely cognac oil, emu oil and olive oil, were chemically characterised in terms of their fatty acid composition.

#### *2.7.1 Fatty acid extraction from olive, emu and cognac oil samples*

Olive, emu and cognac oil samples (20.0 mg) were dissolved in 10 ml chloroform:methanol (2:1, volume:volume). Aliquots were dried using nitrogen gas and trans-methylated with methanol:sulphuric acid (95:5, volume:volume) at 70°C for 2 h. The resulting fatty acid methyl esters (FAMEs) were extracted using hexane and water. The top hexane phase containing the FAMEs was aspirated, evaporated to dryness using nitrogen gas, re-dissolved in a small volume of hexane, and analysed by gas chromatography-electron ionisation mass spectrometry. All solvents used during the extraction procedure contained 0.01% butylated hydroxytoluene.

*2.7.2 Analysis by gas chromatography-mass spectrometry*

Samples were analysed on a 7890A gas chromatograph system equipped with a 5975C mass spectrometer (Agilent Technologies, California, USA). The gas chromatography separation of FAMEs was carried out on a BPX70 capillary column (60 m × 0.25 mm × 0.25 μm; SGE Analytical Science) by using helium as the carrier gas at a flow rate of 1.3 ml/min. A sample volume of 1 μl was injected with a split ratio of 1:1 and an inlet temperature of 250°C. The oven temperature was ramped from 130°C to 200°C at 2°C/min, held for 4 min, then from 200°C to 220°C at 5°C/min, held for 5 min, after which it was ramped to 240°C at 10°C/min and held for 5 min. The total analysis time was 55 min. Electron ionisation mass spectrometry was carried out in scan mode with the mass spectrometer source temperature maintained at 230°C. The FAMEs were quantified using MassHunter quantitative analysis software (Version B.05.02, Agilent Technologies, California, USA). FAME peaks were identified and calibrated against a standard reference mixture of 33 FAMEs (Nu-Check-Prep) and two single FAME standards (Larodan Fine Chemicals AB). Relative percentages of fatty acids were calculated by expressing the concentration of a given FAME as a percentage of the total concentration of all FAMEs identified in the sample (Baumgartner et al. 2012).

### *2.8 Development of floating gastro-retentive matrix tablets*

Powder mixtures (50.0 g) were prepared containing HPMC (54.3% w/w), microcrystalline cellulose (25.0% w/w), vinylpyrrolidone-vinyl acetate copolymer (10.0% w/w), styrene-divinylbenzene copolymer (10.0% w/w) and R6G (0.2% w/w). The powders were mixed with a Turbula® mixer (Willy. A. Bachofen, Switzerland) for 10 min at 69 rpm. Thereafter, magnesium stearate (0.5% w/w) was added and the powder batches mixed for an additional 2 min. Directly after mixing, matrix tablets (500.0 mg) were manufactured by means of direct compression with a Korsch® XP1 single station tablet press (Frankfurt, Germany) fitted with 12 mm round and flat-faced punches.

### *2.9 Evaluation of floating gastro-retentive matrix tablets*

#### *2.9.1 Friability*

In accordance with BP specifications, ten tablets were selected at random, brushed to eliminate any adhering dust, weighed and placed in the drum of a friability test apparatus (ERWEKA TAR, Heusenstamm, Germany). The apparatus was operated at 25 rpm for 4 min to produce a total of 100 rotations. Subsequently, the tablets were brushed and weighed again. Any loss in sample weight due to abrasion or fracture were recorded. The percentage friability was calculated with Equation 1 (BP 2019).

$$\% \text{ Friability} = (W_o - W / W_o) \times 100 \quad (1)$$

Where $W_o$ is the initial sample mass before the friability test commenced, and W is the final sample mass obtained after completing the friability test. A loss of sample mass $\leq 1.0\%$ is considered acceptable.

#### *2.9.2 Mass variation*

This was determined in accordance with BP specifications by weighing twenty randomly selected tablets and calculating the average mass of the sample. The % deviation in the mass of each individually weighed tablet was recorded. The required range of mass variation for tablets $\geq 250$ mg is not more than 5% (BP 2019).

#### *2.9.3 Hardness, thickness and diameter*

These physical parameters were determined with a semi-automated combination apparatus (ERWEKA TBH 425, Heusenstamm, Germany) assessing a quantity of ten tablets that were selected at random.

#### *2.9.4 Disintegration*

In accordance with BP specifications, six randomly selected tablets were tested with a

disintegration test apparatus (ERWEKA ZT 320, Heusenstamm, Germany). The disintegration medium (i.e. water) was maintained at 37±0.5°C for the duration of the experiment (15 min) (BP 2019).

*2.9.5 Assay*

R6G content was determined by selecting one tablet at random and crushing it in a mortar using a pestle. The powdered mass was rinsed out with an adequate volume of 0.1 N HCl into a 200 ml volumetric flask. The flask was placed on a magnetic stirrer for 15 min and made up to volume. Thereafter, the flask was placed in an ultrasonic bath (Integral systems, Randburg, RSA) for 5 min to ensure the R6G was completely dissolved. Samples were filtered through a 0.45 µm membrane filter and R6G content in the collected samples was determined with fluorescence spectrometry. Tests were performed in triplicate.

*2.9.6 Buoyancy*

The *in vitro* buoyancy experiments were executed in accordance with a previously published method (Basak et al. 2007). A single tablet was placed in a beaker containing 100 ml 0.1 N HCl to mimic the gastric environment (pH 1.2). The buoyancy or floating ability of the tablets was determined by means of visual observation as a function of time. The experiments were conducted in triplicate.

*2.9.7 In vitro dissolution experiments*

Dissolution experiments were executed by utilising the paddle method in a six-station dissolution apparatus (Distek model 2500, New Jersey, USA) with an automated sampling system to determine the release characteristics of the matrix tablets and uncompressed powder mixture in 0.1 N HCl (pH 1.2) at 37 ± 0.5°C.

*In vitro* dissolution experiments were performed with 500.0 mg uncompressed powder mixture and with the matrix type tablets. Each dissolution vessel was filled with 600 ml of

pre-heated media, with paddle set at 50 rpm for the duration of the experiments. During the dissolution experiment with the fabricated tablets, samples of 4 ml were collected with the automated sampling system and replaced with equal amounts of pre-heated media at 7-time intervals i.e. 15, 30, 60, 120, 180, 300 and 480 min. As for the dissolution experiment with the uncompressed powder, samples of 4 ml were collected with the automated sampling system and replaced with equal amounts of pre-heated media at 6-time intervals i.e. 20, 40, 60, 80, 100 and 120 min.

Each withdrawn sample was filtered through a 10 µm membrane by the automated sampling system of the dissolution apparatus to produce particulate free samples. R6G content in the collected samples was determined with fluorescence spectrometry. At each time interval of withdrawal, the cumulative percentage R6G released was calculated (Equation 8).

### *2.10 Permeation studies*

#### *2.10.1 Permeation across artificial membranes*

All the *in vitro* permeation studies were conducted in a Sweetana-Grass diffusion chamber apparatus (Harvard NaviCyte apparatus, Warner Instruments, USA). The permeation of R6G (5 µg/ml) from the donor chamber into the acceptor chamber was determined. Each artificial membrane with and without oil impregnation was mounted between the half-cells of 3 diffusion chambers and tested individually. Carbogen (5% $CO_2$ / 95% $O_2$) gas was bubbled through the permeation medium continuously at both sides of the mounted artificial membrane. The temperature was maintained at 37±0.5°C by placing the assembled half-cells onto a heating block. Samples of 180 µl were collected from the acceptor chamber and replaced with equal amounts of pre-heated medium (i.e. KRB or 0.1 N HCl) every 20 min for the duration of the experiment (120 min).

The *in vitro* transport experiments were also conducted with the gastro-retentive matrix tablets by placing a single 500.0 mg tablet in the donor chamber containing 7 ml of

KRB or 0.1 N HCl, while 7 ml of KRB or 0.1 N HCl without additives was placed in the acceptor chamber. Samples of 180 µl were collected from the acceptor chamber and replaced with equal amounts of pre-heated medium every 60 min for the duration of the experiment (480 min). R6G concentration in the collected samples was determined with fluorescence spectrometry. Accumulation of R6G into the acceptor chamber was plotted as a function of time and the apparent permeability coefficient values ($P_{app}$, Equation 9) were calculated. All permeation studies were conducted in triplicate.

*2.10.2 Permeation across excised pig intestinal tissue*

The *ex vivo* permeation studies were conducted in a Sweetana-Grass diffusion chamber apparatus (Harvard NaviCyte apparatus, Warner Instruments, USA). The permeation of R6G (5 µg/ml) was determined from the donor to the acceptor chamber in the same way as described for the artificial membranes, and as previously published (Westerhout *et al.*, 2014).

### *2.11 Data processing and statistical analysis*

*2.11.1 Kinetic modelling of in vitro R6G release*

The *in vitro* release (dissolution) data of the gastro-retentive matrix tablets were applied to various kinetic models with DDSolver (Microsoft Excel add-in software program, which is used for non-linear fitting of data to conduct kinetic analysis), which included First-order, Zero-order, Higuchi, Korsmeyer-Peppas, Weibull and Hixson-Crowell expressions (Dash et al. 2010; Gouda et al. 2017; Hadi et al. 2013; Papadopoulou et al. 2006; Ramteke et al. 2014; Shoaib et al. 2006).

Zero-order equation:

$$F = K_o \times t \quad (2)$$

Where F is the amount of drug dissolved at time t and $K_o$ is the zero-order rate constant (concentration/time).

First-order equation:

$$LogC = LogC_o - k_1 t / 2.203 \quad (3)$$

Where $C_o$ is the initial drug concentration and $K_1$ is the first-order rate constant (per unit of time).

Higuchi equation:

$$Q = K_{hg} \times t^{½} \quad (4)$$

Where Q is the amount of drug released at time t and $K_{hg}$ is the Higuchi dissolution constant.

Korsmeyer-Peppas equation:

$$Mt/M_\infty = K_{pe} \times t^n \quad (5)$$

Where $Mt/M_\infty$ is the fraction of drug released at time t, $K_{pe}$ is the release rate constant and $t^n$ is the release exponent. The exponent of (n) is used to characterise the drug release mechanism from matrix type tablets.

Values of $n = 0.5$ depicts Fickian transport, while $0.45 < n < 0.89$ indicates non-Fickian transport. $n = 0.89$ depicts case II transport, while $n > 0.89$ indicates super case II transport.

Weibull equation:

$$Mt/M_{\infty} = 1 - \exp(-at^{b}) \quad (6)$$

Where $Mt/M_{\infty}$ is the amount of drug released as a function of time t, a and b are constants. Values of $b > 1$, indicates that a complex mechanism governs the rate of drug release.

Hixson-Crowell equation:

$$W_o^{1/3} - W_t^{1/3} = K_{hc} \times t \quad (7)$$

Where $W_o$ is the initial amount of drug in the dosage form, $W_t$ is the amount of drug released at time t and $K_{hc}$ is the Hixson-Crowell rate constant.

*2.11.2 Percentage transport*

The concentration of R6G in the permeation samples was corrected for dilution and the transport was expressed as a percentage of the initial R6G concentration applied to the donor chamber (Equation 8). The percentage transport was then plotted as a function of time to produce percentage transport curves.

$$\% \text{ Transport} = (C_t / C_d) \times 100 \quad (8)$$

Where $C_t$ is the R6G concentration at a specific time interval and $C_d$ is the initial R6G concentration applied to the donor chamber.

The apparent permeability coefficient ($P_{app}$) values for R6G were calculated from the percentage transport curves according to a previously described equation (Corti et al. 2006; Zhao et al. 2016).

$$P_{app} = dQ/dt\ (1/A.60.100) \quad (9)$$

Where $P_{app}$ is the apparent permeability coefficient (cm/s), dQ/dt is the permeability rate

(amount/minute) and A is the diffusion area of the membrane in the Sweetana-Grass diffusion chamber (1.78 $cm^2$).

A one-way analysis of variance (ANOVA) was executed on all experimental data to establish if there were any statistically significant differences between the $P_{app}$ values of the artificial membrane groups and that of the pig intestinal group. Non-parametric analysis was executed by means of the Tukey HSD and Kruskal-Wallis post-hoc tests. Statistically significant differences were accepted when $p < 0.05$.

## 3. Results and discussion

### *3.1 Fluorescence spectrophotometric analysis*

#### *3.1.1 Linearity*

The standard curve obtained when the fluorescence values of R6G were plotted as a function of concentration (0.0098 µg/ml - 5.0000 µg/ml) is shown in Figure 1. A correlation coefficient ($R^2$) value of 0.999 was obtained through linear regression of the standard curve line.

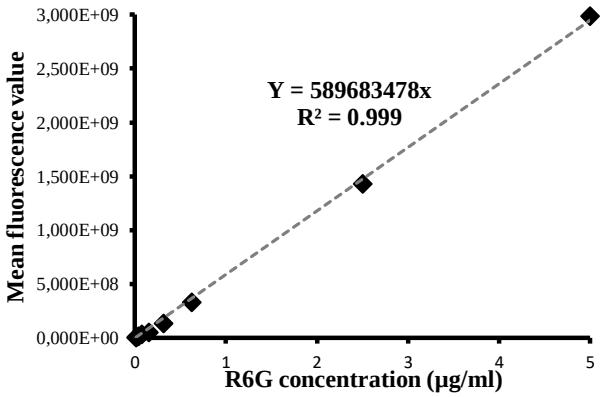


Figure 1. Standard curve for Rhodamine 6G (R6G) where fluorescence was plotted as a function of concentration with the straight-line equation and correlation coefficient ($R^2$) indicated on the graph.

The fluorescence spectrophotometric analytical method used for R6G analysis in this study, therefore, met the proposed criteria for linearity, namely a $R^2$ value of $\geq 0.995$ (USP 2017).

*3.1.2 Precision*

The calculated % RSD values obtained from the intra-day precision measurements for each of three R6G concentrations (1.5, 3 and 5 µg/ml) were 1.8, 1.1 and 1.3%, respectively. The calculated % RSD values obtained from the inter-day precision measurements for each of the same three R6G concentrations were 1.7, 1.1 and 1.4%, respectively. The intra-day and inter-day precision of the fluorescence spectrophotometric analytical method for R6G complied with the recommended % RSD value of ≤ 2% (USP 2017).

*3.1.3 Accuracy*

The calculated percentage recovery for each of three R6G concentrations (1.5, 3 and 5 µg/ml) was 98.7, 99.6 and 99.1%, respectively. The % recovery values obtained for the fluorescence spectrophotometric analytical method for R6G complied with the specification of 100 ± 2% for accuracy (USP 2017).

*3.1.4 Limit of detection (LOD) and limit of quantification (LOQ)*

The LOD and LOQ values for R6G with the fluorescence spectrophotometric analytical method were calculated to be 0.012 ng/ml and 0.036 ng/ml, respectively. The concentration of R6G in all the permeation experiment samples were higher than the LOD and LOQ, demonstrating the analytical method's ability to detect and quantify the R6G accurately in the samples obtained.

*3.1.5 Specificity*

Specificity of the analytical method used for R6G analyses in the presence of all formulation components (i.e. excipients contained in matrix tablet formulation) was determined and the required percentage recovery of 98.5% was within the limits of 100 ± 2% (USP 2017).

### *3.2 Chemical characterisation of the selected natural oils*

Table 2 depicts the fatty acid composition of the selected oils (i.e. olive oil, cognac oil and emu oil) as determined by GC-MS analysis.

Table 2. The fatty acid composition (relative fatty acid percentages) of the selected natural oils (means of analyses performed in triplicate).

| Fatty acid | | Olive oil (%) | Cognac oil (%) | Emu oil (%) |
|---|---|---|---|---|
| Myristic acid | $C_{14:0}$ | 0.04 | 8.97 | 0.36 |
| Palmitic acid | $C_{16:0}$ | 13.23 | 59.26 | 25.88 |
| Palmitoleic acid | $C_{16:1}$ *cis*-ω7 | 1.08 | 2.39 | 4.03 |
| Stearic acid | $C_{18:0}$ | 3.60 | 5.17 | 12.00 |
| Elaidic acid | $C_{18:1}$ *trans*-ω9 | 0.17 | 0.97 | 0.73 |
| Oleic acid | $C_{18:1}$ *cis*-ω9 | 71.15 | 8.30 | 46.44 |
| Vaccenic acid | $C_{18:1}$ *trans*-ω7 | 1.87 | 0.62 | 1.96 |
| Linoleic acid | $C_{18:2}$ *cis*-ω6 | 7.19 | 11.92 | 7.63 |
| γ-Linolenic acid | $C_{18:3}$ *cis*-ω6 | Null | 0.03 | 0.02 |
| α-Linolenic acid | $C_{18:3}$ *cis*-ω3 | 0.79 | 1.99 | 0.44 |
| Arachidic acid | $C_{20:0}$ | 0.43 | 0.19 | 0.11 |
| Eicosenoic acid | $C_{20:1}$ *cis*-ω9 | 0.27 | 0.04 | 0.25 |
| Eicosadienoic acid | $C_{20:2}$ ω6 | Null | 0.01 | 0.06 |
| Arachidonic acid | $C_{20:4}$ *cis*-ω6 | Null | Null | 0.06 |
| Behenic acid | $C_{22:0}$ | 0.13 | 0.10 | 0.02 |
| Lignoceric acid | $C_{24:0}$ | 0.05 | 0.03 | 0.01 |

### *3.3 Evaluation of floating gastro-retentive matrix tablets*

#### *3.3.1 Physical and chemical parameters*

The mean values ± SD of all the evaluated parameters of the matrix type gastro-retentive tablets are shown in Table 3. The tablets did not disintegrate in a time period of < 15 min as a result of formulation design (i.e. modified release matrix tablets and not immediate release tablets). The % friability of the gastro-retentive tablets was slightly above 1.0%, which can be attributed to the presence of Styrene-DVB (a low-density polymer to ensure adequate floating

properties) in the tablets, which also reduced the hardness of the tablets.

Table 3. Physical and chemical characteristics of the gastro-retentive matrix type tablets.

| Gastro-retentive drug delivery systems | |
|---|---|
| Weight (mg) | 500.35 ± 4.52 |
| Diameter (mm) | 11.99 ± 0.01 |
| Thickness (mm) | 4.98 ± 0.02 |
| Hardness (N) | 53.10 ± 3.41 |
| Friability (%) | 1.92 |
| Disintegration (min) | > 15 |
| Mass variation (%) | < 5 |
| Assay (%) | 97.97 ± 0.199 |
| Buoyancy (h) | > 12 |

*3.3.2 In vitro dissolution and drug release kinetics*

The dissolution results for the powder mixture as well as gastro-retentive matrix type tablets are shown in Figure 2.

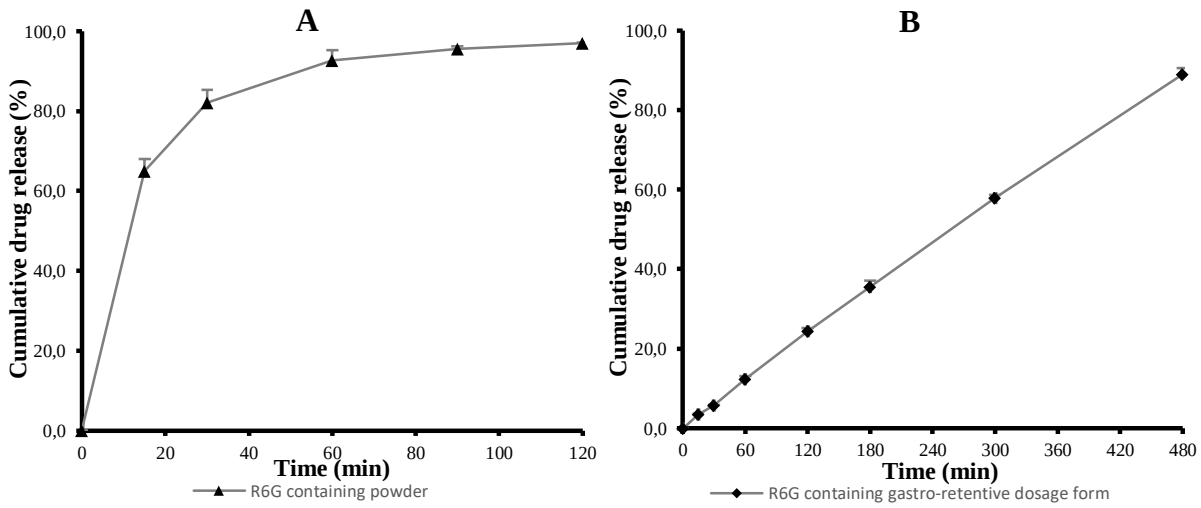


Figure 2. Dissolution profiles of R6G from A) the powder mixture and B) gastro-retentive drug delivery system.

The R6G released from the powder mixture demonstrated a typical immediate release dissolution curve with 97% release after 120 min. On the other hand, continuous release of

R6G independent of concentration can be observed from the gastro-retentive dosage form as demonstrated by a dissolution curve that is nearly a straight line. The results obtained from the kinetic analysis are given in Table 4.

Table 4. Release kinetics of R6G from the gastro-retentive matrix type tablets.

| Zero-order | First-order | Weibull | Higuchi | Hixson-Crowell | Korsmeyer-Peppas | |
|---|---|---|---|---|---|---|
| $K_o$ | $K_1$ | b | $K_{hg}$ | $K_{hc}$ | $K_{pe}$ | n |
| 0.189 | 0.003 | 1.813 | 3.236 | 0.001 | 0.272 | 0.942 |
| $R^2$ | $R^2$ | $R^2$ | $R^2$ | $R^2$ | $R^2$ | |
| 0.997 | 0.961 | 0.994 | 0.867 | 0.981 | 0.999 | |

When the dissolution data were fitted to different mathematical models, the gastro-retentive dosage form's drug release profile showed very good correlation coefficient values for the zero-order and Korsmeyer-Peppas models. This confirmed that the R6G release approached zero-order kinetics from the gastro-retentive dosage form. Furthermore, the b value above 1 and n value close to 1 indicated that the dissolution process from the matrix type tablet was most probably governed by a complex mixture of mechanisms including erosion, diffusion and swelling (Papadopoulou et al. 2006; Shoaib et al. 2006).

### *3.4 Permeation across excised pig intestinal tissue and artificial membranes*

The results obtained from the R6G permeation in KRB across the excised pig intestinal tissue as well as the selected artificial membranes with and without oil impregnation are shown in Figure 3. From the permeation curves in Figure 3, it is clear that the chemical composition and other characteristics (e.g. pore density) of the artificial membranes affected the permeability of R6G. However, membranes with the largest pore size (i.e. CA and PA) did not produce higher rates of permeability compared to the membranes with smaller pore sizes (i.e. CN and CANM). The chemical composition of the membranes, therefore, played a larger role in R6G permeation than the pore size. Figure 3 shows that in KRB, the R6G permeation across two of the selected artificial membranes (i.e. PA and CANM) exhibited a higher rate

and extent of permeation compared to that across the excised pig intestinal tissue, while it was marginally higher for the membrane consisting of CA. The membrane consisting of CN exhibited a slightly lower permeation curve for R6G as compared to that obtained for the excised pig intestinal tissue.

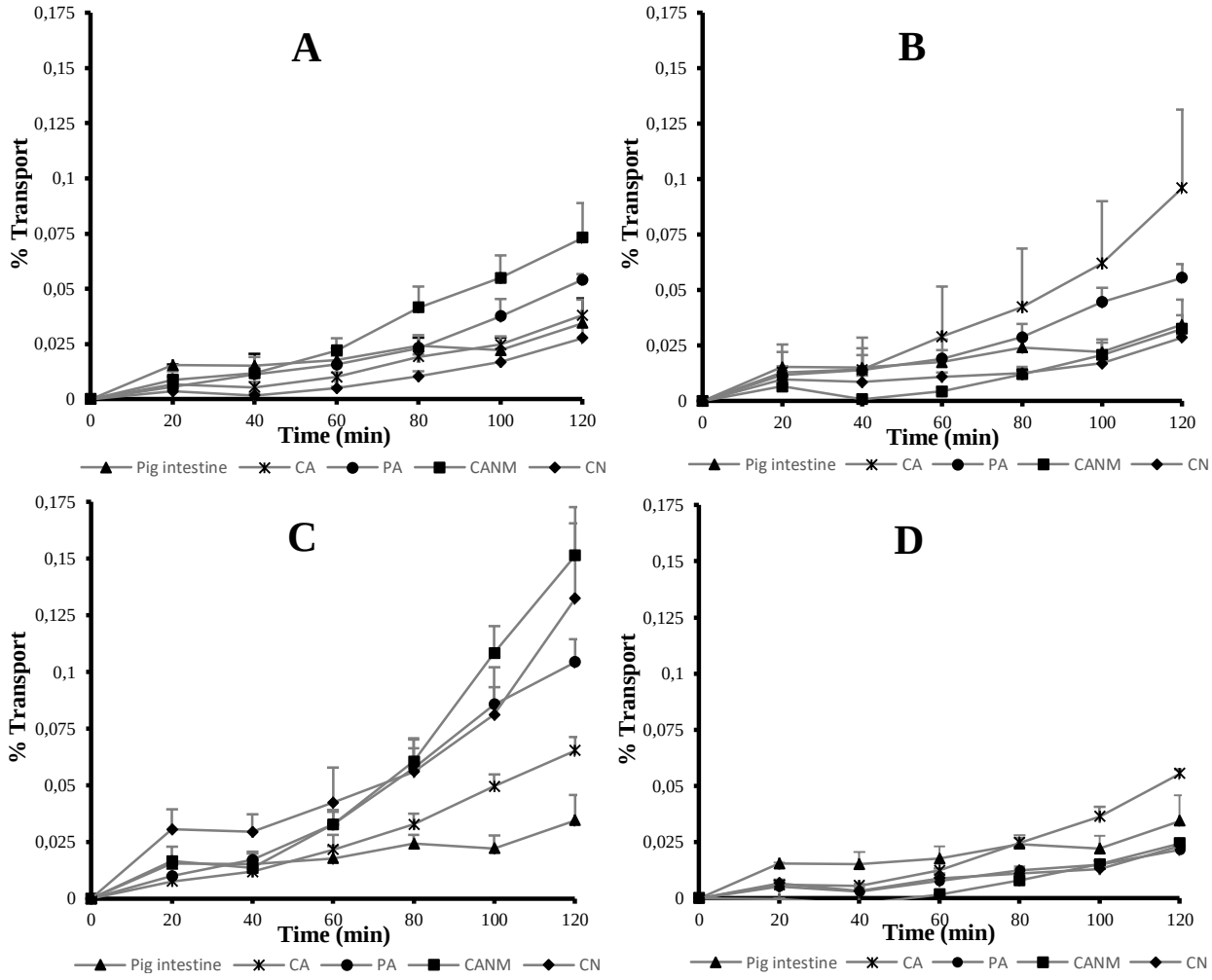


Figure 3. Percentage R6G permeation plotted as a function of time across excised pig intestinal tissue as well as artificial membranes with and without oil impregnation in KRB. A) R6G permeation across membranes without oil impregnation, B) R6G permeation across membranes with olive oil impregnation, C) R6G permeation across membranes with cognac oil impregnation and D) R6G permeation across membranes with emu oil impregnation.

Impregnation of the membranes with the selected oils changed the permeation of R6G. For example, impregnation with cognac oil (Figure 3C) led to a general increase in the permeation of R6G across all the membranes, which was higher than the permeation across the excised pig intestinal tissue. Impregnation with olive oil (Figure 3B) increased the rate and extent of R6G permeation across the CA membrane, but decreased it across the CANM membrane. The permeation curve of R6G across the CANM and CN membranes impregnated with olive oil produced a relatively similar permeation curve to that across pig intestinal tissue. Impregnation of the membranes with emu oil changed the R6G permeation closer to that of R6G across the pig intestinal tissue in general for all the membranes. This indicated that emu oil was able to imitate the biological membrane of the excised pig intestinal tissues the best of the selected oils investigated in this study in the neutral environment of KRB.

The results obtained from the R6G permeation across the selected artificial membranes with and without oil impregnation in 0.1 N HCl, are shown in Figure 4. In this medium, the membranes with the largest pore sizes (i.e. CA and PA) produced in general lower rates of R6G permeability and membranes with smaller pore sizes (i.e. CN and CANM) produced higher permeation rates. Figure 4 shows that in HCl, the R6G permeation across each of the selected artificial membranes exhibited a higher rate and extent compared to that across the excised pig intestinal tissue in KRB. Furthermore, impregnation of the membranes with the selected oils changed the permeation of R6G. As similarly observed in Figure 3, impregnation with cognac oil led to an increase in the permeation of R6G across all the membranes, which was higher than across excised pig intestinal tissue. Conversely, olive oil impregnation decreased the rate and extent of R6G permeation across all the membranes compared to those without oil impregnation. Membrane impregnation with emu oil also changed the R6G permeation closer to that across the pig intestinal tissue in general for all the membranes. In accordance with the permeation studies in KRB, this further indicates that emu oil was able to imitate the biological membrane of the excised pig intestinal tissues the best of

the selected oils investigated in this study in the acidic environment of HCl. The $P_{app}$ values for R6G calculated from the permeation curves for KRB and HCl are shown in Table 5.

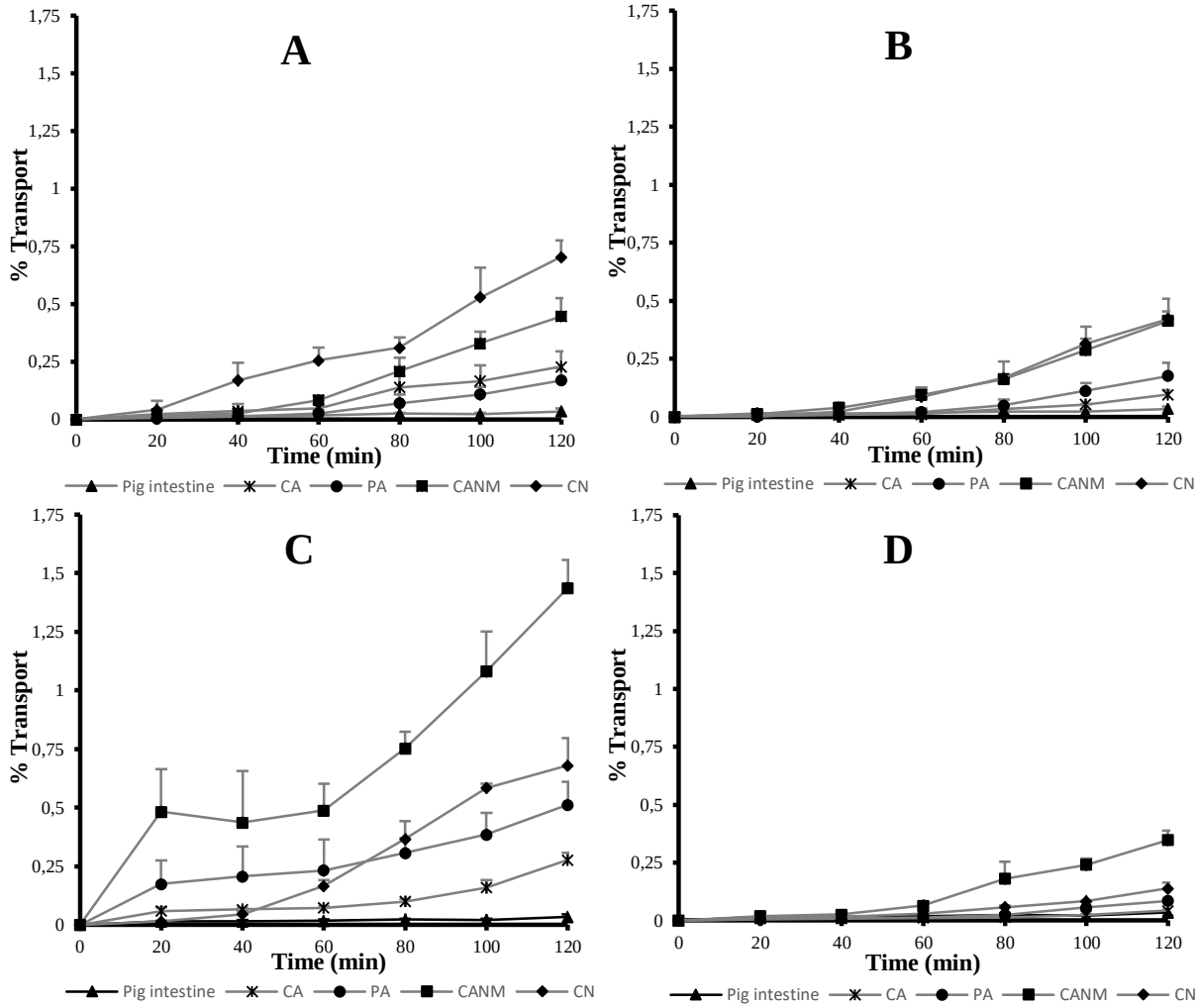


Figure 4. Percentage R6G permeation plotted as a function of time across excised pig intestinal tissue as well as artificial membranes with and without oil impregnation in 0.1 N HCl. A) R6G permeation across membranes without oil impregnation, B) R6G permeation across membranes with olive oil impregnation, (C) R6G permeation across membranes with cognac oil impregnation and D) R6G permeation across membranes with emu oil impregnation.

Table 5. $P_{app}$ values calculated from R6G permeation across the selected artificial membranes with and without oil impregnation in KRB. [*] indicates statistically significant differences from the $P_{app}$ value of the excised pig intestinal tissue, $p < 0.05$.

| Membrane | Medium | Oil impregnation | $P_{app}$ (x $10^{-7}$ cm/s) ± SD |
|---|---|---|---|
| Excised pig intestinal tissue | KRB | N/A | 0.210 ± 0.080 |
| CA | KRB | None | 0.274 ± 0.032 |
| PA | KRB | None | 0.398 ± 0.006 |
| CANM | KRB | None | 0.571 ± 0.111 |
| CN | KRB | None | 0.197 ± 0.069 |
| CA | 0.1 N HCl | None | 1.798 ± 0.576 |
| PA | 0.1 N HCl | None | 1.286 ± 0.396 |
| CANM | 0.1 N HCl | None | 3.599 ± 0.669 [*] |
| CN | 0.1 N HCl | None | 5.399 ± 1.058 [*] |
| CA | KRB | Olive oil | 0.693 ± 0.250 [*] |
| PA | KRB | Olive oil | 0.414 ± 0.007 |
| CANM | KRB | Olive oil | 0.229 ± 0.028 |
| CN | KRB | Olive oil | 0.175 ± 0.008 |
| CA | 0.1 N HCl | Olive oil | 0.681 ± 0.097 |
| PA | 0.1 N HCl | Olive oil | 1.314 ± 0.417 |
| CANM | 0.1 N HCl | Olive oil | 3.205 ± 0.327 [*] |
| CN | 0.1 N HCl | Olive oil | 3.413 ± 0.746 [*] |
| CA | KRB | Cognac oil | 0.502 ± 0.027 |
| PA | KRB | Cognac oil | 0.845 ± 0.088 [*] |
| CANM | KRB | Cognac oil | 1.145 ± 0.153 [*] |
| CN | KRB | Cognac oil | 0.878 ± 0.229 [*] |
| CA | 0.1 N HCl | Cognac oil | 1.784 ± 0.298 |
| PA | 0.1 N HCl | Cognac oil | 3.449 ± 0.469 [*] |
| CANM | 0.1 N HCl | Cognac oil | 9.739 ± 0.934 [*] |
| CN | 0.1 N HCl | Cognac oil | 5.855 ± 0.521 [*] |
| CA | KRB | Emu oil | 0.412 ± 0.031 |
| PA | KRB | Emu oil | 0.156 ± 0.009 |
| CANM | KRB | Emu oil | 0.191 ± 0.010 |
| CN | KRB | Emu oil | 0.151 ± 0.016 |
| CA | 0.1 N HCl | Emu oil | 0.269 ± 0.008 |
| PA | 0.1 N HCl | Emu oil | 0.620 ± 0.040 |
| CANM | 0.1 N HCl | Emu oil | 2.743 ± 0.421 [*] |
| CN | 0.1 N HCl | Emu oil | 0.991 ± 0.107 |

From Table 5, it is clear that the $P_{app}$ value ($0.197 \pm 0.069 \times 10^{-7}$) of R6G across the CN membrane was the closest to the $P_{app}$ value ($0.210 \pm 0.080 \times 10^{-7}$ cm/s) of R6G across excised pig intestinal tissue. The CN membrane was therefore selected for the permeation tests with the gastro-retentive matrix tablet as described below.

### *3.5 Permeation studies across the selected artificial membrane from the gastro-retentive dosage form*

The results obtained from the R6G permeation in HCl across the selected artificial membrane with and without oil impregnation from the gastro-retentive tablets are shown in Figure 5. A lag time in R6G permeation can be observed after which the permeation curves approach straight lines, which is in accordance with the zero-order release pattern exhibited by the gastro-retentive dosage form (Figure 2). Furthermore, impregnation of the membranes with the selected oils changed the permeation of R6G. Oil impregnation of the CN membrane led to a higher rate and extent of R6G permeation than that across the CN membrane alone (without oil impregnation). The $P_{app}$ values for R6G calculated from the permeation curves for KRB and HCl are shown in Table 6.

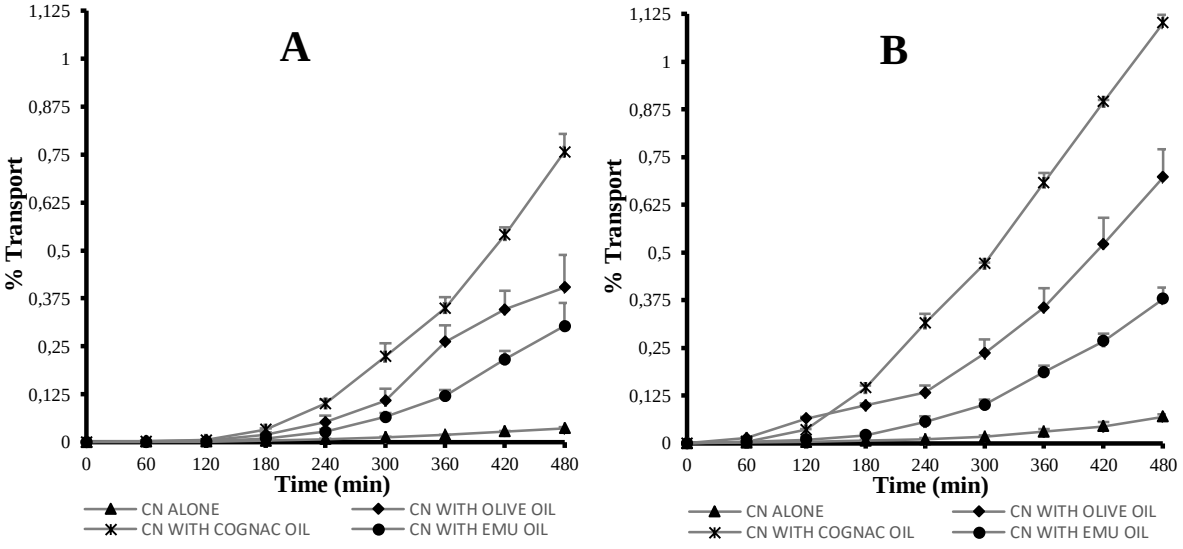


Figure 5**.** Percentage R6G permeation from the gastro-retentive dosage form plotted as a function of time across cellulose nitrate membranes with and without oil impregnation. A) R6G permeation in KRB and B) R6G permeation in HCl.

Table 6. $P_{app}$ values calculated for R6G permeation from gastro-retentive dosage forms, across CN membrane with and without oil impregnation in KRB and HCl. [*] indicates statistically significant differences from the CN without support impregnation in KRB and 0.1 N HCl ($P_{app}$ values) as reported in Table 5, $p < 0.05$.

| Membrane | Medium | Support impregnation | $P_{app}$ (x $10^{-7}$ cm/s) ± SD |
|---|---|---|---|
| CN | KRB | None | 0.070 ± 0.005 |
| CN | KRB | Olive oil | 0.766 ± 0.153 |
| CN | KRB | Cognac oil | 1.437 ± 0.009 |
| CN | KRB | Emu oil | 0.559 ± 0.090 |
| CN | 0.1 N HCl | None | 0.122 ± 0.018 [*] |
| CN | 0.1 N HCl | Olive oil | 1.308 ± 0.166 |
| CN | 0.1 N HCl | Cognac oil | 2.264 ± 0.034 |
| CN | 0.1 N HCl | Emu oil | 0.712 ± 0.049 |

In accordance with previous R6G permeation from solutions (Table 5), the $P_{app}$ values obtained from R6G permeation from the gastro-retentive dosage forms were higher in HCl than in KRB. The standard deviations of these permeation results were relatively small, indicating high reproducibility of results obtained. Furthermore, each oil used for membrane impregnation produced higher $P_{app}$ values in both media compared to that across the membrane without oil impregnation, with the highest increases observed with cognac oil.

## 4. Conclusions

Many *in vitro* models for drug permeation screening exist, each with certain advantages and disadvantages. Measurement of drug delivery across membranes from modified release dosage forms over extended periods of time can contribute to advancement in the development of these *in vitro* models. From the results of this study, it can be deduced that the membrane composed of cellulose nitrate with 0.1 µm pores has an apparent permeability coefficient ($P_{app}$) relatively close to that of excised pig intestinal tissue for the lipophilic model compound (R6G). The artificial membranes impregnated with oils showed in general higher permeability coefficient values than that of excised pig intestinal tissues.

The membrane composed of cellulose acetate-nitrate mixture impregnated with emu oil also showed $P_{app}$ values relatively close to that of excised pig intestinal tissues. The cellulose nitrate membrane showed R6G permeation from the gastro-retentive drug delivery system, which was in accordance with the release profiles.

**Acknowledgments**

This work was supported by the National Research Foundation of South-Africa under Grant number [103479].

**Disclosure of interest**

No potential conflict of interest was reported by the authors.

**References**

Ashford M, 2018. Assessment of biopharmaceutical properties. In: Aulton ME, Taylor KMG, editors. Aulton's pharmaceutics: the Design and Manufacture of Medicines. 5th ed. London(UK): Elsevier Health Sciences; p. 339-363.

Basak S, Rahman J, Ramalingam M. 2007. Design and in vitro testing of a floatable gastroretentive tablet of metformin hydrochloride. Die Pharmazie Int J Pharm Sci. 62(2):145-148.

Baumgartner J, Smuts CM, Malan L, Kvalsvig J, van Stuijvenberg, ME, Hurrell RF, Zimmermann MB. 2012. Effects of iron and n-3 fatty acid supplementation, alone and in combination, on cognition in school children: a randomized, double-blind, placebo-controlled intervention in South Africa. Am J Clin Nutr. 96(6):1327-1338.

Benam KH, Dauth S, Hassell B, Herland A, Jain A, Jang KJ, Karalis K, Kim HJ, MacQueen L, Mahmoodian R. 2015. Engineered in vitro disease models. Annu Rev Pathol. 10:195-262.

Berben P, Brouwers J, Augustijns P. 2018. The artificial membrane inert system as predictive tool for formulation performance evaluation. Int J Pharm. 537(1):22-29.

[BP] British Pharmacopoeia. 2019. [accessed 2019 Mar 29]. https://www-pharmacopoeia-com.nwulib.nwu.ac.za/bp-2019?date=2019-04-01

Buckley ST, Fischer SM, Fricker G, Brandl M. 2012. In vitro models to evaluate the permeability of poorly soluble drug entities: challenges and perspectives. Eur J Pharm Sci. 45(3):235-250.

Corti G, Maestrelli F, Cirri M, Furlanetto S, Mura P. 2006. Development and evaluation of an in vitro method for prediction of human drug absorption I. Assessment of artificial membrane composition. Eur J Pharm. Sci. 27(4):346-353.

CHEMBL Database. 2018– . Release 25. Cambridge (UK): European Bioinformatics Institute. [update 2018 Dec 10; accessed 2019 Jan 24]. https://www.ebi.ac.uk/chembl/beta/compound_report_card/CHEMBL1185241/

Dash S, Murthy PN, Nath L, Chowdhury P. 2010. Kinetic modeling on drug release from controlled drug delivery systems. Acta Pol Pharm. 67(3):217-223.

Deferme S, Annaert P, Augustijns P. 2008. In vitro screening Models to assess intestinal drug absorption and metabolism. In: Ehrhardt C, Kim KJ, editors. Drug absorption studies: In Situ, In Vitro and In Silico Models. Boston(US); Springer p. 182-215.

Garavaglia J, Markoski MM, Oliveira A, Marcadenti A. 2016. Grape Seed Oil Compounds: Biological and Chemical Actions for Health. Nutr Metab Insights. 9:59-64.

Gouda R, Baishya H, Qing Z. 2017. Application of mathematical models in drug release kinetics of Carbidopa and Levodopa ER tablets. J Dev Drugs. 6(02).

Hadi MA, Srinivasa Rao A, Martha S, Sirisha Y, Udaya Chandrika P. 2013. Development of a floating multiple unit controlled-release beads of zidovudine for the treatment of AIDS. J Pharm Res. 6(1):78-83.

Harloff-Helleberg S, Nielsen LH, Nielsen HM. 2017. Animal models for evaluation of oral delivery of biopharmaceuticals. J Control Release. 268:57-71.

Joubert R, Steyn JD, Heystek HJ, Steenekamp JH, Du Preez JL, Hamman JH. 2017. In vitro oral drug permeation models: the importance of taking physiological and physico-chemical factors into consideration. Expert Opin Drug Deliv. 14(2):179-187.

Lopes CM, Bettencourt C, Rossi A, Buttini F, Barata P. 2016. Overview on gastroretentive drug delivery systems for improving drug bioavailability. Int J Pharm. 510(1):144-158.

Lopez S, Bermudez B, Montserrat-de la Paz S, Jaramillo S. Varela LM, Ortega-Gomez A, Abia R, Muriana FJG. 2014. Membrane composition and dynamics: A target of bioactive virgin olive oil constituents. Biochim Biophys Acta. 1838(6):1638-1656.

Luo Z, Liu Y, Zhao B, Tang M, Dong H, Zhang L, Lv B, Wei, L. 2013. Ex vivo and in situ approaches used to study intestinal absorption. J Pharmacol Toxicol. Methods. 68(2):208-216.

McConnell EL, Basit AW. 2018. Modified-release oral dosage forms. In: Aulton ME, Taylor KMG, editors. Aulton's Pharmaceutics: the Design and Manufacture of Medicines. 5th ed. London(UK): Elsevier Health Sciences; p. 518–563.

Miyashita T, Minami K, Ito M, Koizumi R, Sagane Y, Watanabe T, Niwa K. 2018. Emu Oil Reduces LPS-Induced Production of Nitric Oxide and TNF-α but not Phagocytosis in RAW 264 Macrophages. J Oleo Sci. 67(4):471-477.

Nair CM, Sabna C, Murty K, Ramanan S. 2005. Permeability of R6G across Cx43 hemichannels through a novel combination of patch clamp and surface enhanced Raman spectroscopy. Pramana J Phys. 65(4):653.

Papadopoulou V, Kosmidis K, Vlachou M, Macheras P. 2006. On the use of the Weibull function for the discernment of drug release mechanisms. Int. J. Pharm. 309(1-2):44-50.

Pereira C, Costa J, Sarmento B, Araújo F. 2016. Cell-based in vitro models for intestinal permeability studies. In: Sarmento B, editor. Concepts and Models for Drug Permeability Studies: Cell and Tissue Based In Vitro Culture Models. Cambridge(UK): Woodhead Publishing; p. 57-81.

Petit C, Bujard A, Skalicka-Woźniak K, Cretton S, Houriet J, Christen P, Carrupt PA, Wolfender JL. 2016. Prediction of the passive intestinal absorption of medicinal plant extract constituents with the parallel artificial membrane permeability assay (PAMPA). Planta Med. 82(05):424-431.

Ramadan NK, Osman A, Fooad R, Moustafa AA. 2012. Development and validation of spectrophotometric and spectrofluorimetric methods for simultaneous determination of tofisopam. J Appl Pharm Sci. 2(3):112.

Ramteke K, Dighe P, Kharat A, Patil S. 2014. Mathematical models of drug dissolution: a review. Sch Acad J Pharm. 3(5):388-396.

Shabir GA. 2003. Validation of high-performance liquid chromatography methods for pharmaceutical analysis: Understanding the differences and similarities between validation requirements of the US Food and Drug Administration, the US Pharmacopeia and the International Conference on Harmonization. J Chromatogr A. 987(1-2):57-66.

Shekhawat P, Pokharkar, V. 2017. Understanding peroral absorption: regulatory aspects and contemporary approaches to tackling solubility and permeability hurdles. Acta Pharm Sin B 7(3):260-280.

Shoaib MH, Tazeen J, Merchant HA, Yousuf RI. 2006. Evaluation of drug release kinetics from ibuprofen matrix tablets using HPMC. Pak J Pharm Sci. 19(2):119-124.

Sigma-Aldrich. 2019. Rhodamine 6G. [accessed 2019 Jan 24] https://www.sigmaaldrich.com/catalog/product/sigma/83697?lang=en&region=ZA

Singh R. 2013. HPLC method development and validation-an overview. J Pharm Educ Res. 4(1):26.

Streubel A, Siepmann J, Bodmeier R. 2006. Drug delivery to the upper small intestine window using gastroretentive technologies. Curr Opin Pharmacol. 6(5):501-508.

[USP] United States Pharmacopoeia. 2017. Fluorescence Spectroscopy. [accessed 2019 Mar 18] https://hmc.usp.org/sites/default/files/documents/HMC/GCs-Pdfs/c853.pdf

Vo AQ, Feng X, Pimparade M, Ye X, Kim DW, Martin ST, Repka MA. 2017. Dual-mechanism gastroretentive drug delivery system loaded with an amorphous solid dispersion prepared by hot-melt extrusion. Eur J Pharm Sci. 102:71-84.

Volpe DA. 2010. Application of method suitability for drug permeability classification. AAPS J. 12(4):670-678.

Westerhout J, van de Steeg E, Grossouw D, Zeijdner EE, Krul CA, Verwei M, Wortelboer HM. 2014. A new approach to predict human intestinal absorption using porcine intestinal tissue and biorelevant matrices. Eur J Pharm Sci. 63:167-177.

Zhao W, Uehera S, Tanaka K, Tadokoro S, Kusamori K, Katsumi H, Sakane T, Yamamoto A. 2016. Effects of polyoxyethylene alkyl ethers on the intestinal transport and absorption of rhodamine 123: a P-glycoprotein substrate by in vitro and in vivo studies. J Pharm Sci 105(4):1526-1534.

Word count: 7990

# CHAPTER 4: FINAL CONCLUSIONS AND FUTURE RECOMMENDATIONS

## 4.1 Final conclusions

This study examined the usefulness of artificial membranes alone and in combination with selected oils for compound permeation by comparing it to the permeation of a model compound (R6G) across excised pig intestinal tissues. The membranes consisting of CA and PA failed to produce $P_{app}$ values for R6G close to that obtained across the pig intestinal tissues. However, the membrane consisting of CN showed potential to mimic R6G permeation across excised tissues. R6G permeation data indicated that the artificial membranes soaked with oil yielded, in general, higher $P_{app}$ values than that of excised pig intestinal tissues, which can probably be explained by the lipophilic nature of R6G. Furthermore, R6G permeation across the membranes was in general higher in the HCI medium compared to the permeation in KRB medium, which indicates that the environmental pH affected R6G permeability.

From the results in Chapter 3, it is clear that the CN membrane produced a $P_{app}$ value (i.e. 0.197 x $10^{-7}$ cm/s) closest to that of excised pig intestinal tissue (i.e. 0.210 x $10^{-7}$ cm/s) of all the membranes investigated for the model compound R6G. The CANM membrane soaked with emu oil also showed a $P_{app}$ value (i.e. 0.191 x $10^{-7}$ cm/s) that was fairly close to that of excised pig intestinal tissue. Furthermore, membrane impregnation with emu oil yielded overall closer R6G permeation for all the membranes investigated when compared to that across excised pig intestinal tissues. This indicated that emu oil mimicked the inherent permeation characteristics of the biological membrane (i.e. pig intestinal epithelium) the best of all the oils examined in this study. These findings may be attributed to the origins of the oil i.e. sourced from the retroperitoneal and subcutaneous tissue of the emu bird (*Dromaius novaehallandiae*). It can be concluded that the fatty acid composition of each oil, characteristics of each artificial membrane and transport media used exhibited significant effects on the apparent permeability of R6G.

Floatable gastro-retentive dosage forms were successfully prepared and characterised in terms of physical and dissolution behaviour properties. From the dissolution data that was applied to various mathematical models (i.e. first-order, zero-order, Hixson-Crowell, Higuchi, Weibull and Korsmeyer-Peppas), it is clear that the R6G release from the gastro-retentive dosage forms approached zero-order kinetics. The data indicated that the process of R6G release from the gastro-retentive dosage forms was governed by a combination of mechanisms including diffusion, erosion and swelling. The gastro-retentive dosage forms also proved to remain buoyant for ≥ 12 hours (See Figure D.1 of Addendum D for a graphical illustration). As such, the low-density Styrene-divinylbenzene copolymer, proved to be capable in providing the gastro-retentive dosage forms with adequate floating properties.

The CN membrane was successfully used in the application for measurement of R6G delivery from gastro-retentive matrix tablets. In accordance with the solutions, the R6G permeability across the CN membrane from the gastro-retentive tablets also produced higher $P_{app}$ values when soaked with each oil. Being a dosage form designed to provide continuous drug release over extended periods of time (up to 8 h), the drug delivery potential of the gastro-retentive system could not be tested across excised pig intestinal tissues due to the limited viability of the tissues mounted in the diffusion apparatus. As such, the R6G permeation results with the application of the gastro-retentive dosage form across the CN membrane were in line with the zero order release profiles. It is clear that the use of artificial membranes for evaluating drug membrane permeability can circumvent an important limitation (i.e. limited tissue viability), that is associated with techniques that utilise excised tissues sourced from animals. Therefore, the artificial membrane consisting of CN provides a means of assessing drug permeability of sustained-release dosage forms over extended periods of time. Additionally, the cost of biological waste removal and the ethical considerations associated with the use of animal tissues can be overcome by using artificial membranes as an alternative.

The fluorometric analytical method utilised for R6G quantification was validated and complied with each specification as stated in the literature in terms of linearity, accuracy, precision, limit of detection, limit of quantification and specificity. As such, the obtained results were deemed to be reproducible and accurate.

The current study has made an important contribution towards the development of a swift, highly reproducible *in vitro* method based on the use of non-biological artificial membranes as an alternative method for the evaluation of passive drug permeability.

Considering all of the aforementioned findings and facts, it seems that this study should be followed by additional research, as the current study serves as a pilot for the optimisation of the proposed methods applicability in assessing *in vitro* drug permeability. Within this context, the aims of future research should include those mentioned below.

## 4.2 Future recommendations

As identified from this study, there is a need for further investigating the following aspects:

- Transport studies across excised pig intestinal tissue and artificial membranes should be conducted by means of testing on a large set of drugs with varying solubility and permeability properties, to further evaluate the general applicability of the proposed method for assessing passive drug permeability.
- To investigate the effects of drug accumulation within the artificial membranes on the transport behaviour of the compound being tested.

- If the natural oils used in the current study were to be used to conduct further research, they must be acquired from the same source to ensure that the chemical compositions are similar.
- The correlation found between the cellulose nitrate and cellulose acetate nitrate mixture membranes to that of excised pig intestinal tissues can further be investigated, by testing on other well established *in vitro* models (e.g. Caco-2 cell monolayer) and tissues from more than one species of animal.
- More studies can be conducted utilising different natural oils for membrane support impregnation to identify if other oils are capable of mimicking the inherent properties of the biological membrane.

# REFERENCES


Abimosleh, S.M., Tran, C.D. & Howarth, G.S. 2012. Emu oil: a novel therapeutic for disorders of the gastrointestinal tract? *Journal of Gastroenterology and Hepatology*, 27(5):857-861.

Alderborn, G. 2013. Tablets and compaction. (*In* Aulton, ME., *ed.* Aulton's pharmaceutics. the design and manufacture of medicines. 4th ed. New York: Churchill Livingstone, p. 504-549).

Alter, M. & Gutfinger, T. 1982. Phospholipids in several vegetable oils [olive, avocado, cotton, maize, rape]. *Rivista Italiana delle Sostanze Grasse (Italy)*.

Amerongen, H.M. 2018. Anatomy and histology of the digestive tract. (*In* McQueen, C., *ed.* Comprehensive toxicology. 3rd ed. Oxford: Elsevier. p. 3-15).

Amidon, G.L., Lennernäs, H., Shah, V.P. & Crison, J.R. 1995. A theoretical basis for a biopharmaceutic drug classification: the correlation of in vitro drug product dissolution and in vivo bioavailability. *Pharmaceutical Research*, 12(3):413-420.

Ashford, M. 2013a. Assessment of biopharmaceutical properties. (*In* Aulton, ME., *ed.* Aulton's pharmaceutics. the design and manufacture of medicines. 4th ed. New York: Churchill Livingstone, p. 334-354).

Ashford, M. 2013b. Bioavailability—physicochemical and dosage form factors. *(In* Aulton, ME., *ed.* Aulton's pharmaceutics. the design and manufacture of medicines. 4th ed. New York: Churchill Livingstone, p. 314-333).

Ashford, M. 2013c. Gastrointestinal tract–physiology and drug absorption. *(In* Aulton, ME., *ed.* Aulton's pharmaceutics. the design and manufacture of medicines. 4th ed. New York: Churchill Livingstone, p. 296-313).

Aulton, M.E. 2013. Dissolution and solubility. (*In* Aulton, ME., *ed.* Aulton's pharmaceutics. the design and manufacture of medicines. 4th ed. New York: Churchill Livingstone, p. 20-37).

Ayre, A., Dand, N. & Lalitha, K. 2016. Gastroretentive floating and mucoadhesive drug delivery systems-Insights and current applications. *Journal of Pharmacy and Biological Sciences*, 11(3):89-96.

Bánfalvi, G. 2016. Permeability of biological membranes. Switzerland: Springer. p. 2-3.

Beckerbauer, L., Thiel-Cooper, R., Ahn, D., Sell, J., Parrish Jr, F. & Beitz, D. 2001. Influence of Two Dietary Fats on the Composition of Emu Oil and Meat. *Journal of Poultry Science*, 80:187-194.

Benam, K.H., Dauth, S., Hassell, B., Herland, A., Jain, A., Jang, K.-J., Karalis, K., Kim, H.J., MacQueen, L. & Mahmoodian, R. 2015. Engineered in vitro disease models. *Annual Review of Pathology: Mechanisms of Disease*, 10:195-262.

Berben, P., Brouwers, J. & Augustijns, P. 2018. The artificial membrane inert system as predictive tool for formulation performance evaluation. *International Journal of Pharmaceutics*, 537(1):22-29.

Billat, P.-A., Roger, E., Faure, S. & Lagarce, F. 2017. Models for drug absorption from the small intestine: where are we and where are we going? *Drug Discovery Today*, 22(5):761-775.

Boskou, D., Blekas, G. & Tsimidou, M. 2006. Olive oil. 2nd ed. Illinois: AOCS press. p. 41-72.

Boukhchina, S., Sebai, K., Cherif, A., Kallel, H. & Mayer, P.M. 2004. Identification of glycerophospholipids in rapeseed, olive, almond, and sunflower oils by LC-MS and LC-MS-MS. *Canadian Journal of Chemistry*, 82(7):1210-1215.

Buckley, S.T., Fischer, S.M., Fricker, G. & Brandl, M. 2012. In vitro models to evaluate the permeability of poorly soluble drug entities: challenges and perspectives. *European Journal of Pharmaceutical Sciences*, 45(3):235-250.

Chen, Y.-C., Ho, H.-O., Lee, T.-Y. & Sheu, M.-T. 2013. Physical characterizations and sustained release profiling of gastroretentive drug delivery systems with improved floating and swelling capabilities. *International Journal of Pharmaceutics*, 441(1):162-169.

Chillistone, S. & Hardman, J.G. 2017. Factors affecting drug absorption and distribution. *Anaesthesia & intensive Care Medicine*, 18(7):335-339.

Cicero, N., Albergamo, A., Salvo, A., Bua, G.D., Bartolomeo, G., Mangano, V., Rotondo, A., Di Stefano, V., Di Bella, G. & Dugo, G. 2018. Chemical characterization of a variety of cold-pressed gourmet oils available on the Brazilian market. *Food Research International*, 109:517-525.

Clarke, G.M., Newton, J.M. & Short, M.B. 1995. Comparative gastrointestinal transit of pellet systems of varying density. *International Journal of Pharmaceutics*, 114(1):1-11.

Corti, G., Maestrelli, F., Cirri, M., Furlanetto, S. & Mura, P. 2006. Development and evaluation of an in vitro method for prediction of human drug absorption I. Assessment of artificial membrane composition. *European Journal of Pharmaceutical Sciences*, 27(4):346-353.

Daousani, C. & Macheras, P. 2016. Biopharmaceutic classification of drugs revisited. *European Journal of Pharmaceutical Sciences*, 95:82-87.

Dash, S., Murthy, P.N., Nath, L. & Chowdhury, P. 2010. Kinetic modeling on drug release from controlled drug delivery systems. *Actata Poloniae Pharmaceutica*, 67(3):217-223.

Dash, T.R. & Verma, P. 2013. Matrix tablets: an approach towards oral extended release drug delivery. *International Journal of Pharmaceutical Sciences Review*, 2:12-24.

Davis, S.S. 2005. Formulation strategies for absorption windows. *Drug Discovery Today*, 10(4):249-257.

Deferme, S., Annaert, P. & Augustijns, P. 2008. In vitro screening Models to assess intestinal drug absorption and metabolism *(In* Ehrhardt, C. & Kim, K.-J., *eds*. Drug absorption studies: In situ, In vitro and In silico models. Boston, MA: Springer US. p. 182-215).

DeSesso, J.M. & Jacobson, C.F. 2001. Anatomical and physiological parameters affecting gastrointestinal absorption in humans and rats. *Food and Chemical Toxicology*, 39(3):209-228.

Dokala, G.K. & Pallavi, C. 2013. Direct compression-an overview. *International Journal of Research in Pharmaceutical and Biomedical Sciences*, 4(1):155-158.

Dokoumetzidis, A. & Macheras, P. 2006. A century of dissolution research: From Noyes and Whitney to the Biopharmaceutics Classification System. *International Journal of Pharmaceutics*, 321(1-2):1-11.

El Asbahani, A., Miladi, K., Badri, W., Sala, M., Addi, E.A., Casabianca, H., El Mousadik, A., Hartmann, D., Jilale, A. & Renaud, F. 2015. Essential oils: from extraction to encapsulation. *International Journal of Pharmaceutics*, 483(1-2):220-243.

Franco, N.H. 2013. Animal Experiments in Biomedical Research: A Historical Perspective. *Animals*, 3(1):238-273.

Garavaglia, J., Markoski, M.M., Oliveira, A. & Marcadenti, A. 2016. Grape Seed Oil Compounds: Biological and Chemical Actions for Health. *Nutrition and Metabolic Insights*, 9:59-64.

Garg, R. & Gupta, G. 2008. Progress in controlled gastroretentive delivery systems. *Tropical Journal of Pharmaceutical Research*, 7(3):1055-1066.

Giorno, L., Mazzei, R. & Drioli, E. 2010. Comprehensive membrane science and engineering. Oxford: Elsevier. p. 1-12.

Gouda, R., Baishya, H. & Qing, Z. 2017. Application of mathematical models in drug release kinetics of Carbidopa and Levodopa ER tablets. *Journal of Developing Drugs*, 6(171):2.

Hajar, R. 2011. Animal Testing and Medicine. *Journal of the Gulf Heart Association*, 12(1):42-42.

Hanganu, A., Todaşcă, M.-C., Chira, N.-A., Maganu, M. & Roşca, S. 2012. The compositional characterisation of Romanian grape seed oils using spectroscopic methods. *Food Chemistry*, 134(4):2453-2458.

Harloff-Helleberg, S., Nielsen, L.H. & Nielsen, H.M. 2017. Animal models for evaluation of oral delivery of biopharmaceuticals. *Journal of Controlled Release*, 268:57-71.

Holford, N.H.G. 2010. Pharmacokinetics & Pharmacodynamics: rational dosing & the time course of drug action (*In* Katzung, B.G., Masters, S.B. & Trevor, A.J. Basic & Clinical Pharmacology. 12th ed. New York: McGraw-Hill. p. 37-51).

Hosey, C.M. & Benet, L.Z. 2017. Drug classification and drug disposition prediction *(In* Chackalamannil, S., Rotella, D. & Ward, S.E., *eds*. Comprehensive medicinal chemistry. 3rd ed. Oxford: Elsevier. p. 102-129).

Jaimini, M. & Kothari, A.H. 2012. Sustained release matrix type drug deliery system: a review. *Journal of Drug Delivery and Therapeutics*, 2(6).

Jeengar, M.K., Kumar, P.S., Thummuri, D., Shrivastava, S., Guntuku, L., Sistla, R. & Naidu, V.G.M. 2015. Review on emu products for use as complementary and alternative medicine. *The International Journal of Applied and Basic Nutritional Sciences*, 31(1):21-27.

Joubert, R., Steyn, J.D., Heystek, H.J., Steenekamp, J.H., Du Preez, J.L. & Hamman, J.H. 2017. In vitro oral drug permeation models: the importance of taking physiological and physico-chemical factors into consideration. *Expert Opinion on Drug Delivery*, 14(2):179-187.

Kansy, M., Senner, F. & Gubernator, K. 1998. Physicochemical high throughput screening: parallel artificial membrane permeation assay in the description of passive absorption processes. *Journal of Medicinal Chemistry*, 41(7):1007-1010.

Kapoor, A., Sharma, R., Sharma, P. & Gupta, P. 2014. BCS classification system: benchmark for solubility and permeability. *American Journal of Pharmaceutical Research*, 4:2233-2238.

Khan, A.B., Mahamana, R. & Pal, E. 2014. Review on mucoadhesive drug delivery system: Novel approaches in modern era. *Journal of Pharmaceutical Science*, 4(4):128-141.

Lachman, J., Hejtmánková, A., Táborský, J., Kotíková, Z., Pivec, V., Střalková, R., Vollmannová, A., Bojňanská, T. & Dědina, M. 2015. Evaluation of oil content and fatty acid

composition in the seed of grapevine varieties. *LWT - Food Science and Technology*, 63(1):620-625.

Le Ferrec, E., Christophe, C., Artussen, P., Brayden, D., Fabre, G., Gires, P., Grillon, F., Reuset, M., Rubas, W. & Scarino, M.L. 2001. In vitro models of the intestinal barrier. Vol. 29.

Lopes, C.M., Bettencourt, C., Rossi, A., Buttini, F. & Barata, P. 2016. Overview on gastroretentive drug delivery systems for improving drug bioavailability. *International Journal of Pharmaceutics*, 510(1):144-158.

Lopez, S., Bermudez, B., Montserrat-de la Paz, S., Jaramillo, S., Varela, L.M., Ortega-Gomez, A., Abia, R. & Muriana, F.J.G. 2014. Membrane composition and dynamics: A target of bioactive virgin olive oil constituents. *Biochimica et Biophysica Acta (BBA) - Biomembranes*, 1838(6):1638-1656.

Lozoya-Agullo, I., González-Álvarez, I., González-Álvarez, M., Merino-Sanjuán, M. & Bermejo, M. 2015. In Situ Perfusion Model in Rat Colon for Drug Absorption Studies: Comparison with Small Intestine and Caco-2 Cell Model. *Journal of Pharmaceutical Sciences*, 104(9):3136-3145.

Luminescents. 2019. White cognac essential oil. https://www.luminescents.net/shop/oils/essential-oils/white-cognac-vitis-vinifera-100-pure-essential-oil/ Date of access: 26 February 2019.

Luo, Z., Liu, Y., Zhao, B., Tang, M., Dong, H., Zhang, L., Lv, B. & Wei, L. 2013. Ex vivo and in situ approaches used to study intestinal absorption. *Journal of Pharmacological and Toxicological Methods*, 68(2):208-216.

Martinello, M., Hecker, G. & del Carmen Pramparo, M. 2007. Grape seed oil deacidification by molecular distillation: Analysis of operative variables influence using the response surface methodology. *Journal of Food Engineering*, 81(1):60-64.

Martini, F., Nath, J.L. & Bartholomew, E.F. 2014. Fundamentals of anatomy & physiology. 9th ed. United Kingdom: Harlow Pearson. p. 91-123).

Mayavanshi, A. & Gajjar, S. 2008. Floating drug delivery systems to increase gastric retention of drugs: A Review. *Research Journal of Pharmacy and Technology*, 1(4):345-348.

McConnell, EL & Basit, AW. 2013. Modified-release oral drug delivery. (*In* Aulton, ME., *ed.* Aulton's pharmaceutics. the design and manufacture of medicines. 4th ed. New York: Churchill Livingstone, p. 550-565).

Merriam-Webster's medical dictionary. 2018. In vitro. https://merriam-webster.com/dictionary/in%20vitro#medicalDictionary Date of access: 5 March 2018.

Merriam-Webster's medical dictionary. 2018. In vivo. https://merriam-webster.com/dictionary/in%20vivo#medicalDictionary Date of access: 14 May 2018.

Mistry, B.D. & Yadav, J.S. 2016. Time and site specific gastro-retentive floating pulsatile drug delivery system: a review. *International Journal of Pharmaceutical Sciences*, 7(2):74.

Miyashita, T., Minami, K., Ito, M., Koizumi, R., Sagane, Y., Watanabe, T. & Niwa, K. 2018. Emu Oil Reduces LPS-Induced Production of Nitric Oxide and TNF-α but not Phagocytosis in RAW 264 Macrophages. *Journal of Oleo Science*, 67(4):471-477.

Moes, A. 2003. Gastric retention systems for oral drug delivery. *Business Briefing: Pharmatech*:157-159.

Musther, H., Olivares-Morales, A., Hatley, O.J.D., Liu, B. & Rostami Hodjegan, A. 2014. Animal versus human oral drug bioavailability: Do they correlate? *European Journal of Pharmaceutical Sciences*, 57:280-291.

Nef, P. 2001. Key animal models for the identification and validation of drug targets. *Drug Discovery Today*, 6:91-96.

Neumann, M., Schneider, F., Koziolek, M., Garbacz, G. & Weitschies, W. 2017. A novel mechanical antrum model for the prediction of the gastroretentive potential of dosage forms. *International Journal of Pharmaceutics*, 530(1):63-70.

Nokhodchi, A., Raja, S., Patel, P. & Asare-Addo, K. 2012. The Role of Oral Controlled Release Matrix Tablets in Drug Delivery Systems. *BioImpacts : BI*, 2(4):175-187.

Norris, D.A., Leesman, G.D., Sinko, P.J. & Grass, G.M. 2000. Development of predictive pharmacokinetic simulation models for drug discovery. *Journal of Controlled Release*, 65(1):55-62.

Passos, C.P., Silva, R.M., Da Silva, F.A., Coimbra, M.A. & Silva, C.M. 2010. Supercritical fluid extraction of grape seed (Vitis vinifera L.) oil. Effect of the operating conditions upon oil composition and antioxidant capacity. *Chemical Engineering Journal*, 160(2):634-640.

Patil, L., Kulkarni, K., Khanvilkar, V. & Kadam, D.V. 2014. In vitro evaluation of herb-drug interactions: a review. *In vivo*, 10:11.

Pereira, C., Costa, J., Sarmento, B. & Araújo, F. 2016. Cell-based in vitro models for intestinal permeability studies. (*In* Sarmento, B., *ed.* Concepts and Models for Drug Permeability Studies. Cambridge: Woodhead Publishing. p. 57-81).

Petit, C., Bujard, A., Skalicka-Woźniak, K., Cretton, S., Houriet, J., Christen, P., Carrupt, P.-A. & Wolfender, J.-L. 2016. Prediction of the passive intestinal absorption of medicinal plant extract constituents with the parallel artificial membrane permeability assay (PAMPA). *Planta Medica*, 82(05):424-431.

Piacentini, E., Mazzei, R., Drioli, E. & Giorno, L. 2017. Comprehensive membrane science and engineering. 2nd ed. Oxford: Elsevier. p. 1-16.

Pundir, S., Badola, A. & Sharma, D. 2013. Sustained release matrix technology and recent advance in matrix drug delivery system: a review. *International Journal of Drug Research and Technology*, 3(1):8.

Ramteke, K., Dighe, P., Kharat, A. & Patil, S. 2014. Mathematical models of drug dissolution: a review. *Scholars Academic Journal of Pharmacy*, 3(5):388-396.

Rao, C.V., Newmark, H.L. & Reddy, B.S. 1998. Chemopreventive effect of squalene on colon cancer. *Journal of Carcinogenesis*, 19(2):287-290.

Sabir, A., Unver, A. & Kara, Z. 2012. The fatty acid and tocopherol constituents of the seed oil extracted from 21 grape varieties (Vitis spp.). *Journal of the Science of Food and Agriculture*, 92(9):1982-1987.

Shahid, K., Mayank, V., Geeta, A. & Hari, K.S. 2016. Mucoadhesive drug delivery system: a review. *World Journal of Pharmacy and Pharmaceutical Science*, 5(5):362-405.

Shekhawat, P. & Pokharkar, V. 2017. Understanding peroral absorption: regulatory aspects and contemporary approaches to tackling solubility and permeability hurdles. *Acta Pharmaceutica Sinica B*, 7(3):260-280.

Singer, S.J. & Nicolson, G.L. 1972. The fluid mosaic model of the structure of cell membranes. *Science*, 175(4023):720-731.

Singh, R., Sharma, D. & Garg, R. 2017. Review on mucoadhesive drug delivery system with special emphasis on buccal route: an important tool in designing of novel controlled drug delivery system for the effective delivery of pharmaceuticals. *Journal of Developing Drugs*, 6(1):1-12.

Smith, T.J., Yang, G.Y., Seril, D.N., Liao, J. & Kim, S. 1998. Inhibition of 4-(methylnitrosamino)-1-(3-pyridyl)-1-butanone-induced lung tumorigenesis by dietary olive oil and squalene. *Journal of Carcinogenesis*, 19(4):703-706.

Ussing, H.H. & Zerahn, K. 1951. Active transport of sodium as the source of electric current in the short-circuited isolated frog skin. *Acta physiologica*, 23(2-3):110-127.

Vo, A.Q., Feng, X., Pimparade, M., Ye, X., Kim, D.W., Martin, S.T. & Repka, M.A. 2017. Dual-mechanism gastroretentive drug delivery system loaded with an amorphous solid dispersion prepared by hot-melt extrusion. *European Journal of Pharmaceutical Sciences*, 102:71-84.

Volpe, D.A. 2010. Application of method suitability for drug permeability classification. *The American Association of Pharmaceutical Scientists Journal*, 12(4):670-678.

Walter, E. & Kissel, T. 1995. Heterogeneity in the human intestinal cell line Caco-2 leads to differences in transepithelial transport. *European Journal of Pharmaceutical Sciences*, 3(4):215-230.

Watson, H. 2015. Biological membranes. *Essays in Biochemistry*, 59:43-69.

Welling, S.H., Clemmensen, L.K., Buckley, S.T., Hovgaard, L., Brockhoff, P.B. & Refsgaard, H.H. 2015. In silico modelling of permeation enhancement potency in Caco-2 monolayers based on molecular descriptors and random forest. *European Journal of Pharmaceutics and Biopharmaceutics*, 94:152-159.

Yalcin, H., Kavuncuoglu, H., Ekici, L. & Sagdic, O. 2017. Determination of Fatty Acid Composition, Volatile Components, Physico-Chemical and Bioactive Properties of Grape (Vitis vinifera) Seed and Seed Oil. *Journal of Food Processing and Preservation*, 41(2).

Yang, Y. & Yu, L.X. 2009. Oral Drug Absorption, Evaluation, and Prediction. (*In* Chen, Y., Zhang, G.G.Z., Liu, L. & Porter, W.R., *eds*. Developing solid oral dosage forms. San Diego: Academic Press. p. 289-308).

York, P. 2013. Design of dosage forms. (*In* Aulton, ME., ed. Aulton's pharmaceutics. the design and manufacture of medicines. 4th ed. New York: Churchill Livingstone. p. 7-19).

Zhang, C., Tang, J., Liu, D., Li, X., Cheng, L. & Tang, X. 2016. Design and evaluation of an innovative floating and bioadhesive multiparticulate drug delivery system based on hollow structure. *International Journal of Pharmaceutics*, 503(1):41-55.

Zhang, D., Luo, G., Ding, X. & Lu, C. 2012. Preclinical experimental models of drug metabolism and disposition in drug discovery and development. *Acta Pharmaceutica Sinica B*, 2(6):549-561.

# ADDENDUM A: ETHICAL APPROVAL

NORTH-WEST UNIVERSITY
YUNIBESITI YA BOKONE-BOPHIRIMA
NOORDWES-UNIVERSITEIT

Private Bag X6001, Potchefstroom
South Africa 2520

Tel: (018) 299-4900
Faks: (018) 299-4910
Web: http://www.nwu.ac.za

**Ethics Committee**
Tel +27 18 299 4849
Email Ethics@nwu.ac.za

**ETHICS APPROVAL OF PROJECT**

The North-West University Research Ethics Regulatory Committee (NWU-RERC) hereby approves your project as indicated below. This implies that the NWU-RERC grants its permission that provided the special conditions specified below are met and pending any other authorisation that may be necessary, the project may be initiated, using the ethics number below.

**Project title: Excised pig buccal and intestinal tissues as in vitro models for pharmacokinetic studies**

**Project Leader: Prof Sias Hamman**

**Ethics number**:

| N | W | U | - | 0 | 0 | 0 | 2 | 5 | - | 1 | 5 | - | A | 5 |
|---|---|---|---|---|---|---|---|---|---|---|---|---|---|---|
| Institution | | | | Project Number | | | | | | Year | | | Status | |

Status: S = Submission; R = Re-Submission; P = Provisional Authorisation; A = Authorisation

**Approval date**: 2015-04-16 **Expiry date**: 2020-04-15

Special conditions of the approval (if any): None

General conditions:

*While this ethics approval is subject to all declarations, undertakings and agreements incorporated and signed in the application form, please note the following:*

- *The project leader (principle investigator) must report in the prescribed format to the NWU-RERC:*
  - *annually (or as otherwise requested) on the progress of the project,*
  - *without any delay in case of any adverse event (or any matter that interrupts sound ethical principles) during the course of the project.*
- *The approval applies strictly to the protocol as stipulated in the application form. Would any changes to the protocol be deemed necessary during the course of the project, the project leader must apply for approval of these changes at the NWU-RERC. Would there be deviated from the project protocol without the necessary approval of such changes, the ethics approval is immediately and automatically forfeited.*
- *The date of approval indicates the first date that the project may be started. Would the project have to continue after the expiry date, a new application must be made to the NWU-RERC and new approval received before or on the expiry date.*
- *In the interest of ethical responsibility the NWU-RERC retains the right to:*
  - *request access to any information or data at any time during the course or after completion of the project;*
  - *withdraw or postpone approval if:*
    - *any unethical principles or practices of the project are revealed or suspected,*
    - *it becomes apparent that any relevant information was withheld from the NWU-RERC or that information has been false or misrepresented,*
    - *the required annual report and reporting of adverse events was not done timely and accurately,*
    - *new institutional rules, national legislation or international conventions deem it necessary.*

The Ethics Committee would like to remain at your service as scientist and researcher, and wishes you well with your project. Please do not hesitate to contact the Ethics Committee for any further enquiries or requests for assistance.

Yours sincerely

Linda du Plessis

Digitally signed by Linda du Plessis
DN: cn=Linda du Plessis, o=NWU, Vaal Triangle Campus, ou=Vice-Rector: Academic, email=linda.duplessis@nwu.ac.za, c=US
Date: 2015.04.20 20:35:13 +02'00'

**Prof Linda du Plessis**
*Chair NWU Research Ethics Regulatory Committee (RERC)*

# ADDENDUM B: FLUORESCENCE SPECTROPHOTOMETRIC ANALYTICAL METHOD VALIDATION DATA

**Table B.1:** Mean fluorescent value of Rhodamine 6G in specific concentrations used to calculate the correlation coefficient value

| Concentration (µg/ml) | Mean fluorescence | Slope | $R^2$ |
|---|---|---|---|
| 5 | 2983126331 | 589683477,7 | 0,999 |
| 2,5 | 1425051067 | | |
| 0,625 | 327938181,8 | | |
| 0,3125 | 130509379,1 | | |
| 0,15625 | 49216413,8 | | |
| 0,078125 | 29192829,8 | | |
| 0,0390625 | 14123552,13 | | |
| 0,01953125 | 8011540,792 | | |
| 0,009765625 | 3373743,125 | | |

**Table B.2:** Data obtained from Rhodamine 6G sample analysis to determine the accuracy across the concentration range

| **Theoretical concentration (µg/ml)** | | |
|---|---|---|
| 1,5 | 3,0 | 5,0 |
| **Fluorescent values** | | |
| 865940107 | 1777961739 | 2897994251 |
| 862333003 | 1733755275 | 2975799051 |
| 927949771 | 1771488011 | 2986814475 |
| 861247627 | 1772366219 | 2889946379 |
| 861827851 | 1743308427 | 2938023435 |
| 866618251 | 1776447243 | 2913935371 |
| 856309387 | 1795953547 | 2876314635 |
| 861578571 | 1742717707 | 2920966667 |
| 861996939 | 1740584843 | 2957974539 |
| 902567307 | 1771823499 | 2964711691 |
| **Mean fluorescent value** | | |
| 872836881 | 1762640651 | 2932248049 |
| **Actual concentration (µg/ml)** | | |
| 1,480 | 2,989 | 4,972 |
| **Accuracy (% recovery)** | | |
| 98,678 | 99,637 | 99,076 |

**Table B.3:** Data obtained for intra- and inter-day precision of Rhodamine 6G

| **Intra-day precision** | | | | |
|---|---|---|---|---|
| **Concentration (µg/ml)** | **Repeat** | **Mean fluorescent values** | **SD** | **% RSD** |
| 1,5 | 1 | 851354736 | 15285057,53 | 1,79 |
| | 2 | | | |
| | 3 | | | |
| 3,0 | 1 | 1740100995 | 18744224,55 | 1,07 |
| | 2 | | | |
| | 3 | | | |
| 5,0 | 1 | 2847136263 | 35897491,63 | 1,26 |
| | 2 | | | |
| | 3 | | | |
| **Inter-day precision** | | | | |
| **Concentration (µg/ml)** | **Day** | **Mean fluorescent values** | **SD** | **% RSD** |
| 1,5 | 1 | 841360130 | 14549822,71 | 1,72 |
| | 2 | | | |
| | 3 | | | |
| 3,0 | 1 | 1746051361 | 20068051,41 | 1,14 |
| | 2 | | | |
| | 3 | | | |
| 5,0 | 1 | 2835488117 | 40140529,6 | 1,41 |
| | 2 | | | |
| | 3 | | | |

**Table B.4:** Data obtained from Rhodamine 6G sample analysis to determine specificity in combination with all excipients

| **Rhodamine 6G including all excipients** | |
|---|---|
| **Theoretical concentration (µg/ml)** | 5 |
| **Fluorescent values** | 2933884782 |
| | 2826774638 |
| | 2830028654 |
| | 2851487342 |
| | 2813061998 |
| | 2963007086 |
| | 2964866670 |
| | 2836245358 |
| | 2769379438 |
| | 2810061678 |
| **Mean fluorescence** | 2859879764 |
| **Actual concentration (µg/ml)** | 4,923 |
| **Accuracy (% recovery)** | 98,460 |

**Table B.5:** Fluorescent values of the blanks (background noise) used to calculate the limit of detection and limit of quantification

| Blank fluorescent values | Mean | SD | LOD (µg/ml) | LOQ (µg/ml) |
|---|---|---|---|---|
| 44539 | 45508,875 | 2119,275 | 0.0000118153 | 0.0000358038 |
| 44532 | | | | |
| 43228 | | | | |
| 45290 | | | | |
| 49717 | | | | |
| 44878 | | | | |
| 48213 | | | | |
| 43674 | | | | |
| 44539 | | | | |

# ADDENDUM C: *EX VIVO* AND *IN VITRO* TRANSPORT DATA

**Table C.1:** Cumulative percentage transport of Rhodamine 6G across excised pig intestinal tissues.

| Time (min) | % Transport | | | | |
|---|---|---|---|---|---|
| | **Chamber 1** | **Chamber 2** | **Chamber 3** | **SD** | **Mean** |
| **0** | 0,000 | 0,000 | 0,000 | 0,000 | 0,000 |
| **20** | 0,015 | 0,016 | 0,015 | 0,000 | 0,015 |
| **40** | 0,012 | 0,023 | 0,011 | 0,006 | 0,015 |
| **60** | 0,012 | 0,025 | 0,016 | 0,005 | 0,018 |
| **80** | 0,030 | 0,021 | 0,022 | 0,004 | 0,024 |
| **100** | 0,030 | 0,018 | 0,018 | 0,006 | 0,022 |
| **120** | 0,048 | 0,035 | 0,020 | 0,011 | 0,034 |

**Table C.2:** Cumulative percentage transport of Rhodamine 6G across cellulose acetate membranes without oil impregnation in KRB.

| Time (min) | % Transport | | | | |
|---|---|---|---|---|---|
| | **Chamber 1** | **Chamber 2** | **Chamber 3** | **SD** | **Mean** |
| **0** | 0,000 | 0,000 | 0,000 | 0,000 | 0,000 |
| **20** | 0,001 | 0,008 | 0,010 | 0,004 | 0,007 |
| **40** | 0,004 | 0,004 | 0,009 | 0,002 | 0,005 |
| **60** | 0,008 | 0,013 | 0,009 | 0,002 | 0,010 |
| **80** | 0,020 | 0,020 | 0,018 | 0,001 | 0,019 |
| **100** | 0,020 | 0,025 | 0,029 | 0,004 | 0,025 |
| **120** | 0,032 | 0,034 | 0,048 | 0,007 | 0,038 |

**Table C.3:** Cumulative percentage transport of Rhodamine 6G across polyamide membranes without oil impregnation in KRB.

| Time (min) | % Transport | | | | |
|---|---|---|---|---|---|
| | **Chamber 1** | **Chamber 2** | **Chamber 3** | **SD** | **Mean** |
| **0** | 0,000 | 0,000 | 0,000 | 0,000 | 0,000 |
| **20** | 0,002 | 0,003 | 0,012 | 0,005 | 0,005 |
| **40** | 0,006 | 0,006 | 0,022 | 0,008 | 0,011 |
| **60** | 0,011 | 0,015 | 0,021 | 0,004 | 0,016 |
| **80** | 0,016 | 0,023 | 0,030 | 0,006 | 0,023 |
| **100** | 0,029 | 0,036 | 0,048 | 0,008 | 0,038 |
| **120** | 0,057 | 0,051 | 0,055 | 0,003 | 0,054 |

**Table C.4:** Cumulative percentage transport of Rhodamine 6G across cellulose acetate nitrate mixture membranes without oil impregnation in KRB.

| Time (min) | % Transport | | | | |
|---|---|---|---|---|---|
| | Chamber 1 | Chamber 2 | Chamber 3 | SD | Mean |
| **0** | 0,000 | 0,000 | 0,000 | 0,000 | 0,000 |
| **20** | 0,006 | 0,014 | 0,006 | 0,004 | 0,009 |
| **40** | 0,013 | 0,015 | 0,007 | 0,003 | 0,012 |
| **60** | 0,017 | 0,030 | 0,020 | 0,006 | 0,022 |
| **80** | 0,038 | 0,055 | 0,032 | 0,010 | 0,042 |
| **100** | 0,043 | 0,068 | 0,055 | 0,010 | 0,055 |
| **120** | 0,058 | 0,095 | 0,066 | 0,016 | 0,073 |

**Table C.5:** Cumulative percentage transport of Rhodamine 6G across cellulose nitrate membranes without oil impregnation in KRB.

| Time (min) | % Transport | | | | |
|---|---|---|---|---|---|
| | Chamber 1 | Chamber 2 | Chamber 3 | SD | Mean |
| **0** | 0,000 | 0,000 | 0,000 | 0,000 | 0,000 |
| **20** | 0,004 | 0,004 | 0,003 | 0,001 | 0,004 |
| **40** | 0,001 | 0,003 | 0,001 | 0,001 | 0,002 |
| **60** | 0,005 | 0,005 | 0,004 | 0,001 | 0,005 |
| **80** | 0,012 | 0,012 | 0,007 | 0,002 | 0,010 |
| **100** | 0,025 | 0,016 | 0,010 | 0,006 | 0,017 |
| **120** | 0,040 | 0,025 | 0,018 | 0,009 | 0,028 |

**Table C.6:** Cumulative percentage transport of Rhodamine 6G across cellulose acetate membranes without oil impregnation in 0.1 N HCI.

| Time (min) | % Transport | | | | |
|---|---|---|---|---|---|
| | Chamber 1 | Chamber 2 | Chamber 3 | SD | Mean |
| **0** | 0,000 | 0,000 | 0,000 | 0,000 | 0,000 |
| **20** | 0,048 | 0,005 | 0,016 | 0,018 | 0,023 |
| **40** | 0,078 | 0,005 | 0,022 | 0,031 | 0,035 |
| **60** | 0,096 | 0,017 | 0,030 | 0,034 | 0,047 |
| **80** | 0,240 | 0,037 | 0,138 | 0,083 | 0,139 |
| **100** | 0,253 | 0,086 | 0,160 | 0,068 | 0,166 |
| **120** | 0,317 | 0,163 | 0,205 | 0,065 | 0,228 |

**Table C.7:** Cumulative percentage transport of Rhodamine 6G across polyamide membranes without oil impregnation in 0.1 N HCI.

| Time (min) | % Transport | | | | |
|---|---|---|---|---|---|
| | Chamber 1 | Chamber 2 | Chamber 3 | SD | Mean |
| **0** | 0,000 | 0,000 | 0,000 | 0,000 | 0,000 |
| **20** | 0,001 | 0,010 | 0,006 | 0,004 | 0,006 |
| **40** | 0,006 | 0,017 | 0,015 | 0,005 | 0,013 |
| **60** | 0,009 | 0,042 | 0,025 | 0,013 | 0,025 |
| **80** | 0,018 | 0,103 | 0,086 | 0,037 | 0,069 |
| **100** | 0,063 | 0,124 | 0,138 | 0,032 | 0,108 |
| **120** | 0,104 | 0,180 | 0,224 | 0,050 | 0,169 |

**Table C.8:** Cumulative percentage transport of Rhodamine 6G across cellulose acetate nitrate mixture membranes without oil impregnation in 0.1 N HCI.

| Time (min) | % Transport | | | | |
|---|---|---|---|---|---|
| | Chamber 1 | Chamber 2 | Chamber 3 | SD | Mean |
| **0** | 0,000 | 0,000 | 0,000 | 0,000 | 0,000 |
| **20** | 0,004 | 0,012 | 0,027 | 0,009 | 0,014 |
| **40** | 0,022 | 0,029 | 0,027 | 0,003 | 0,026 |
| **60** | 0,065 | 0,105 | 0,080 | 0,017 | 0,083 |
| **80** | 0,166 | 0,290 | 0,170 | 0,058 | 0,208 |
| **100** | 0,314 | 0,398 | 0,276 | 0,051 | 0,329 |
| **120** | 0,410 | 0,556 | 0,373 | 0,079 | 0,446 |

**Table C.9:** Cumulative percentage transport of Rhodamine 6G across cellulose nitrate membranes without oil impregnation in 0.1 N HCI.

| Time (min) | % Transport | | | | |
|---|---|---|---|---|---|
| | Chamber 1 | Chamber 2 | Chamber 3 | SD | Mean |
| **0** | 0,000 | 0,000 | 0,000 | 0,000 | 0,000 |
| **20** | 0,015 | 0,097 | 0,011 | 0,040 | 0,041 |
| **40** | 0,205 | 0,238 | 0,063 | 0,075 | 0,169 |
| **60** | 0,325 | 0,249 | 0,192 | 0,055 | 0,255 |
| **80** | 0,361 | 0,250 | 0,320 | 0,046 | 0,310 |
| **100** | 0,532 | 0,372 | 0,684 | 0,128 | 0,529 |
| **120** | 0,755 | 0,602 | 0,754 | 0,072 | 0,704 |

**Table C.10:** Cumulative percentage transport of Rhodamine 6G across cellulose acetate membranes with olive oil impregnation in KRB.

| Time (min) | % Transport | | | | |
|---|---|---|---|---|---|
| | Chamber 1 | Chamber 2 | Chamber 3 | SD | Mean |
| **0** | 0,000 | 0,000 | 0,000 | 0,000 | 0,000 |
| **20** | 0,030 | 0,006 | 0,002 | 0,013 | 0,013 |
| **40** | 0,034 | 0,007 | 0,001 | 0,014 | 0,014 |
| **60** | 0,060 | 0,020 | 0,008 | 0,022 | 0,029 |
| **80** | 0,079 | 0,032 | 0,017 | 0,026 | 0,042 |
| **100** | 0,099 | 0,056 | 0,031 | 0,028 | 0,062 |
| **120** | 0,144 | 0,084 | 0,060 | 0,035 | 0,096 |

**Table C.11:** Cumulative percentage transport of Rhodamine 6G across polyamide membranes with olive oil impregnation in KRB.

| Time (min) | % Transport | | | | |
|---|---|---|---|---|---|
| | Chamber 1 | Chamber 2 | Chamber 3 | SD | Mean |
| **0** | 0,000 | 0,000 | 0,000 | 0,000 | 0,000 |
| **20** | 0,001 | 0,008 | 0,026 | 0,010 | 0,012 |
| **40** | 0,008 | 0,006 | 0,028 | 0,010 | 0,014 |
| **60** | 0,015 | 0,011 | 0,031 | 0,009 | 0,019 |
| **80** | 0,022 | 0,028 | 0,037 | 0,006 | 0,029 |
| **100** | 0,047 | 0,036 | 0,051 | 0,007 | 0,045 |
| **120** | 0,049 | 0,055 | 0,063 | 0,006 | 0,056 |

**Table C.12:** Cumulative percentage transport of Rhodamine 6G across cellulose acetate nitrate mixture membranes with olive oil impregnation in KRB.

| Time (min) | % Transport | | | | |
|---|---|---|---|---|---|
| | Chamber 1 | Chamber 2 | Chamber 3 | SD | Mean |
| **0** | 0,000 | 0,000 | 0,000 | 0,000 | 0,000 |
| **20** | 0,006 | 0,007 | 0,008 | 0,001 | 0,007 |
| **40** | 0,000 | 0,001 | 0,001 | 0,001 | 0,001 |
| **60** | 0,002 | 0,007 | 0,005 | 0,002 | 0,004 |
| **80** | 0,008 | 0,013 | 0,015 | 0,003 | 0,012 |
| **100** | 0,013 | 0,026 | 0,023 | 0,006 | 0,021 |
| **120** | 0,038 | 0,036 | 0,024 | 0,006 | 0,033 |

**Table C.13:** Cumulative percentage transport of Rhodamine 6G across cellulose nitrate membranes with olive oil impregnation in KRB.

| Time (min) | % Transport | | | | |
|---|---|---|---|---|---|
| | Chamber 1 | Chamber 2 | Chamber 3 | SD | Mean |
| **0** | 0,000 | 0,000 | 0,000 | 0,000 | 0,000 |
| **20** | 0,008 | 0,010 | 0,011 | 0,001 | 0,010 |
| **40** | 0,006 | 0,007 | 0,012 | 0,003 | 0,009 |
| **60** | 0,009 | 0,011 | 0,013 | 0,002 | 0,011 |
| **80** | 0,012 | 0,011 | 0,015 | 0,002 | 0,013 |
| **100** | 0,015 | 0,015 | 0,020 | 0,002 | 0,017 |
| **120** | 0,030 | 0,028 | 0,028 | 0,001 | 0,029 |

**Table C.14:** Cumulative percentage transport of Rhodamine 6G across cellulose acetate membranes with olive oil impregnation in 0.1 N HCI.

| Time (min) | % Transport | | | | |
|---|---|---|---|---|---|
| | Chamber 1 | Chamber 2 | Chamber 3 | SD | Mean |
| **0** | 0,000 | 0,000 | 0,000 | 0,000 | 0,000 |
| **20** | 0,004 | 0,011 | 0,006 | 0,003 | 0,007 |
| **40** | 0,006 | 0,010 | 0,010 | 0,002 | 0,009 |
| **60** | 0,004 | 0,020 | 0,012 | 0,007 | 0,012 |
| **80** | 0,034 | 0,038 | 0,027 | 0,005 | 0,033 |
| **100** | 0,052 | 0,056 | 0,055 | 0,002 | 0,054 |
| **120** | 0,078 | 0,124 | 0,086 | 0,020 | 0,096 |

**Table C.15:** Cumulative percentage transport of Rhodamine 6G across polyamide membranes with olive oil impregnation in 0.1 N HCI.

| Time (min) | % Transport | | | | |
|---|---|---|---|---|---|
| | Chamber 1 | Chamber 2 | Chamber 3 | SD | Mean |
| **0** | 0,000 | 0,000 | 0,000 | 0,000 | 0,000 |
| **20** | 0,002 | 0,008 | 0,001 | 0,003 | 0,004 |
| **40** | 0,000 | 0,023 | 0,003 | 0,010 | 0,009 |
| **60** | 0,008 | 0,044 | 0,013 | 0,016 | 0,021 |
| **80** | 0,028 | 0,086 | 0,034 | 0,026 | 0,050 |
| **100** | 0,107 | 0,157 | 0,072 | 0,035 | 0,112 |
| **120** | 0,133 | 0,259 | 0,137 | 0,059 | 0,176 |

**Table C.16:** Cumulative percentage transport of Rhodamine 6G across cellulose acetate nitrate mixture membranes with olive oil impregnation in 0.1 N HCl.

| Time (min) | % Transport | | | | |
|---|---|---|---|---|---|
| | Chamber 1 | Chamber 2 | Chamber 3 | SD | Mean |
| **0** | 0,000 | 0,000 | 0,000 | 0,000 | 0,000 |
| **20** | 0,010 | 0,007 | 0,023 | 0,007 | 0,013 |
| **40** | 0,054 | 0,020 | 0,048 | 0,015 | 0,041 |
| **60** | 0,125 | 0,061 | 0,098 | 0,026 | 0,095 |
| **80** | 0,177 | 0,156 | 0,157 | 0,009 | 0,163 |
| **100** | 0,357 | 0,250 | 0,258 | 0,049 | 0,288 |
| **120** | 0,453 | 0,362 | 0,429 | 0,039 | 0,415 |

**Table C.17:** Cumulative percentage transport of Rhodamine 6G across cellulose nitrate membranes with olive oil impregnation in 0.1 N HCl.

| Time (min) | % Transport | | | | |
|---|---|---|---|---|---|
| | Chamber 1 | Chamber 2 | Chamber 3 | SD | Mean |
| **0** | 0,000 | 0,000 | 0,000 | 0,000 | 0,000 |
| **20** | 0,011 | 0,000 | 0,000 | 0,005 | 0,004 |
| **40** | 0,052 | 0,008 | 0,008 | 0,021 | 0,023 |
| **60** | 0,142 | 0,070 | 0,049 | 0,040 | 0,087 |
| **80** | 0,267 | 0,120 | 0,114 | 0,071 | 0,167 |
| **100** | 0,416 | 0,291 | 0,240 | 0,074 | 0,315 |
| **120** | 0,540 | 0,400 | 0,330 | 0,087 | 0,423 |

**Table C.18:** Cumulative percentage transport of Rhodamine 6G across cellulose acetate membranes with cognac oil impregnation in KRB.

| Time (min) | % Transport | | | | |
|---|---|---|---|---|---|
| | Chamber 1 | Chamber 2 | Chamber 3 | SD | Mean |
| **0** | 0,000 | 0,000 | 0,000 | 0,000 | 0,000 |
| **20** | 0,015 | 0,003 | 0,004 | 0,006 | 0,008 |
| **40** | 0,019 | 0,009 | 0,007 | 0,005 | 0,012 |
| **60** | 0,030 | 0,020 | 0,014 | 0,006 | 0,021 |
| **80** | 0,039 | 0,031 | 0,028 | 0,005 | 0,033 |
| **100** | 0,057 | 0,044 | 0,047 | 0,005 | 0,049 |
| **120** | 0,072 | 0,066 | 0,058 | 0,006 | 0,065 |

**Table C.19:** Cumulative percentage transport of Rhodamine 6G across polyamide membranes with cognac oil impregnation in KRB.

| Time (min) | % Transport | | | | |
|---|---|---|---|---|---|
| | Chamber 1 | Chamber 2 | Chamber 3 | SD | Mean |
| **0** | 0,000 | 0,000 | 0,000 | 0,000 | 0,000 |
| **20** | 0,010 | 0,010 | 0,010 | 0,000 | 0,010 |
| **40** | 0,013 | 0,018 | 0,020 | 0,003 | 0,017 |
| **60** | 0,024 | 0,034 | 0,040 | 0,006 | 0,033 |
| **80** | 0,049 | 0,070 | 0,053 | 0,009 | 0,057 |
| **100** | 0,076 | 0,094 | 0,087 | 0,008 | 0,086 |
| **120** | 0,093 | 0,118 | 0,102 | 0,010 | 0,104 |

**Table C.20:** Cumulative percentage transport of Rhodamine 6G across cellulose acetate nitrate mixture membranes with cognac oil impregnation in KRB.

| Time (min) | % Transport | | | | |
|---|---|---|---|---|---|
| | Chamber 1 | Chamber 2 | Chamber 3 | SD | Mean |
| **0** | 0,000 | 0,000 | 0,000 | 0,000 | 0,000 |
| **20** | 0,016 | 0,024 | 0,009 | 0,006 | 0,016 |
| **40** | 0,016 | 0,015 | 0,009 | 0,003 | 0,013 |
| **60** | 0,040 | 0,032 | 0,027 | 0,005 | 0,033 |
| **80** | 0,072 | 0,063 | 0,047 | 0,010 | 0,060 |
| **100** | 0,124 | 0,106 | 0,095 | 0,012 | 0,108 |
| **120** | 0,179 | 0,148 | 0,127 | 0,021 | 0,151 |

**Table C.21:** Cumulative percentage transport of Rhodamine 6G across cellulose nitrate membranes with cognac oil impregnation in KRB.

| Time (min) | % Transport | | | | |
|---|---|---|---|---|---|
| | Chamber 1 | Chamber 2 | Chamber 3 | SD | Mean |
| **0** | 0,000 | 0,000 | 0,000 | 0,000 | 0,000 |
| **20** | 0,024 | 0,025 | 0,043 | 0,009 | 0,031 |
| **40** | 0,032 | 0,019 | 0,037 | 0,008 | 0,029 |
| **60** | 0,043 | 0,023 | 0,061 | 0,015 | 0,042 |
| **80** | 0,063 | 0,036 | 0,069 | 0,014 | 0,056 |
| **100** | 0,089 | 0,052 | 0,102 | 0,021 | 0,081 |
| **120** | 0,144 | 0,087 | 0,166 | 0,033 | 0,132 |

**Table C.22:** Cumulative percentage transport of Rhodamine 6G across cellulose acetate membranes with cognac oil impregnation in 0.1 N HCI.

| Time (min) | % Transport | | | | |
|---|---|---|---|---|---|
| | Chamber 1 | Chamber 2 | Chamber 3 | SD | Mean |
| **0** | 0,000 | 0,000 | 0,000 | 0,000 | 0,000 |
| **20** | 0,080 | 0,046 | 0,052 | 0,015 | 0,059 |
| **40** | 0,062 | 0,066 | 0,073 | 0,005 | 0,067 |
| **60** | 0,067 | 0,083 | 0,070 | 0,007 | 0,073 |
| **80** | 0,091 | 0,115 | 0,097 | 0,010 | 0,101 |
| **100** | 0,155 | 0,201 | 0,123 | 0,032 | 0,160 |
| **120** | 0,253 | 0,320 | 0,259 | 0,030 | 0,277 |

**Table C.23:** Cumulative percentage transport of Rhodamine 6G across polyamide membranes with cognac oil impregnation in 0.1 N HCI.

| Time (min) | % Transport | | | | |
|---|---|---|---|---|---|
| | Chamber 1 | Chamber 2 | Chamber 3 | SD | Mean |
| **0** | 0,000 | 0,000 | 0,000 | 0,000 | 0,000 |
| **20** | 0,315 | 0,122 | 0,087 | 0,100 | 0,174 |
| **40** | 0,386 | 0,124 | 0,110 | 0,127 | 0,207 |
| **60** | 0,418 | 0,145 | 0,137 | 0,131 | 0,233 |
| **80** | 0,496 | 0,192 | 0,234 | 0,135 | 0,307 |
| **100** | 0,515 | 0,339 | 0,305 | 0,092 | 0,386 |
| **120** | 0,644 | 0,489 | 0,405 | 0,099 | 0,513 |

**Table C.24:** Cumulative percentage transport of Rhodamine 6G across cellulose acetate nitrate mixture membranes with cognac oil impregnation in 0.1 N HCI.

| Time (min) | % Transport | | | | |
|---|---|---|---|---|---|
| | Chamber 1 | Chamber 2 | Chamber 3 | SD | Mean |
| **0** | 0,000 | 0,000 | 0,000 | 0,000 | 0,000 |
| **20** | 0,738 | 0,376 | 0,334 | 0,181 | 0,483 |
| **40** | 0,477 | 0,684 | 0,151 | 0,219 | 0,438 |
| **60** | 0,556 | 0,582 | 0,329 | 0,113 | 0,489 |
| **80** | 0,748 | 0,841 | 0,670 | 0,070 | 0,753 |
| **100** | 1,052 | 1,302 | 0,892 | 0,168 | 1,082 |
| **120** | 1,506 | 1,536 | 1,270 | 0,119 | 1,437 |

**Table C.25:** Cumulative percentage transport of Rhodamine 6G across cellulose nitrate membranes with cognac oil impregnation in 0.1 N HCI.

| Time (min) | % Transport | | | | |
|---|---|---|---|---|---|
| | Chamber 1 | Chamber 2 | Chamber 3 | SD | Mean |
| **0** | 0,000 | 0,000 | 0,000 | 0,000 | 0,000 |
| **20** | 0,013 | 0,021 | 0,014 | 0,003 | 0,016 |
| **40** | 0,066 | 0,034 | 0,038 | 0,014 | 0,046 |
| **60** | 0,201 | 0,159 | 0,139 | 0,026 | 0,166 |
| **80** | 0,367 | 0,362 | 0,371 | 0,004 | 0,367 |
| **100** | 0,565 | 0,608 | 0,582 | 0,018 | 0,585 |
| **120** | 0,844 | 0,575 | 0,624 | 0,117 | 0,681 |

**Table C.26:** Cumulative percentage transport of Rhodamine 6G across cellulose acetate membranes with emu oil impregnation in KRB.

| Time (min) | % Transport | | | | |
|---|---|---|---|---|---|
| | Chamber 1 | Chamber 2 | Chamber 3 | SD | Mean |
| **0** | 0,000 | 0,000 | 0,000 | 0,000 | 0,000 |
| **20** | 0,007 | 0,003 | 0,008 | 0,002 | 0,006 |
| **40** | 0,004 | 0,006 | 0,006 | 0,001 | 0,005 |
| **60** | 0,012 | 0,014 | 0,011 | 0,001 | 0,012 |
| **80** | 0,022 | 0,025 | 0,028 | 0,002 | 0,025 |
| **100** | 0,031 | 0,042 | 0,036 | 0,004 | 0,036 |
| **120** | 0,054 | 0,058 | 0,055 | 0,002 | 0,055 |

**Table C.27:** Cumulative percentage transport of Rhodamine 6G across polyamide membranes with emu oil impregnation in KRB.

| Time (min) | % Transport | | | | |
|---|---|---|---|---|---|
| | Chamber 1 | Chamber 2 | Chamber 3 | SD | Mean |
| **0** | 0,000 | 0,000 | 0,000 | 0,000 | 0,000 |
| **20** | 0,006 | 0,005 | 0,004 | 0,001 | 0,005 |
| **40** | 0,003 | 0,002 | 0,004 | 0,001 | 0,003 |
| **60** | 0,006 | 0,007 | 0,010 | 0,001 | 0,008 |
| **80** | 0,012 | 0,013 | 0,012 | 0,001 | 0,012 |
| **100** | 0,015 | 0,013 | 0,017 | 0,002 | 0,015 |
| **120** | 0,021 | 0,021 | 0,022 | 0,001 | 0,021 |

**Table C.28:** Cumulative percentage transport of Rhodamine 6G across cellulose acetate nitrate mixture membranes with emu oil impregnation in KRB.

| Time (min) | % Transport | | | | |
|---|---|---|---|---|---|
| | Chamber 1 | Chamber 2 | Chamber 3 | SD | Mean |
| **0** | 0,000 | 0,000 | 0,000 | 0,000 | 0,000 |
| **20** | 0,000 | 0,000 | 0,000 | 0,000 | 0,000 |
| **40** | 0,000 | 0,000 | 0,000 | 0,000 | 0,000 |
| **60** | 0,002 | 0,001 | 0,002 | 0,000 | 0,002 |
| **80** | 0,010 | 0,007 | 0,007 | 0,002 | 0,008 |
| **100** | 0,017 | 0,014 | 0,015 | 0,002 | 0,015 |
| **120** | 0,025 | 0,024 | 0,024 | 0,001 | 0,024 |

**Table C.29:** Cumulative percentage transport of Rhodamine 6G across cellulose nitrate membranes with emu oil impregnation in KRB.

| Time (min) | % Transport | | | | |
|---|---|---|---|---|---|
| | Chamber 1 | Chamber 2 | Chamber 3 | SD | Mean |
| **0** | 0,000 | 0,000 | 0,000 | 0,000 | 0,000 |
| **20** | 0,008 | 0,005 | 0,007 | 0,001 | 0,007 |
| **40** | 0,005 | 0,001 | 0,004 | 0,002 | 0,003 |
| **60** | 0,010 | 0,006 | 0,011 | 0,002 | 0,009 |
| **80** | 0,015 | 0,007 | 0,011 | 0,003 | 0,011 |
| **100** | 0,012 | 0,011 | 0,015 | 0,002 | 0,013 |
| **120** | 0,024 | 0,020 | 0,026 | 0,002 | 0,023 |

**Table C.30:** Cumulative percentage transport of Rhodamine 6G across cellulose acetate membranes with emu oil impregnation in 0.1 N HCl.

| Time (min) | % Transport | | | | |
|---|---|---|---|---|---|
| | Chamber 1 | Chamber 2 | Chamber 3 | SD | Mean |
| **0** | 0,000 | 0,000 | 0,000 | 0,000 | 0,000 |
| **20** | 0,014 | 0,007 | 0,005 | 0,004 | 0,008 |
| **40** | 0,015 | 0,007 | 0,004 | 0,004 | 0,009 |
| **60** | 0,015 | 0,009 | 0,006 | 0,004 | 0,010 |
| **80** | 0,017 | 0,012 | 0,011 | 0,003 | 0,013 |
| **100** | 0,028 | 0,022 | 0,021 | 0,003 | 0,023 |
| **120** | 0,046 | 0,041 | 0,040 | 0,003 | 0,042 |

**Table C.31:** Cumulative percentage transport of Rhodamine 6G across polyamide membranes with emu oil impregnation in 0.1 N HCl.

| Time (min) | % Transport | | | | |
|---|---|---|---|---|---|
| | Chamber 1 | Chamber 2 | Chamber 3 | SD | Mean |
| **0** | 0,000 | 0,000 | 0,000 | 0,000 | 0,000 |
| **20** | 0,003 | 0,007 | 0,008 | 0,002 | 0,006 |
| **40** | 0,013 | 0,004 | 0,007 | 0,004 | 0,008 |
| **60** | 0,018 | 0,009 | 0,015 | 0,004 | 0,014 |
| **80** | 0,028 | 0,018 | 0,027 | 0,004 | 0,025 |
| **100** | 0,056 | 0,056 | 0,057 | 0,001 | 0,056 |
| **120** | 0,090 | 0,076 | 0,088 | 0,006 | 0,085 |

**Table C.32:** Cumulative percentage transport of Rhodamine 6G across cellulose acetate nitrate mixture membranes with emu oil impregnation in 0.1 N HCl.

| Time (min) | % Transport | | | | |
|---|---|---|---|---|---|
| | Chamber 1 | Chamber 2 | Chamber 3 | SD | Mean |
| **0** | 0,000 | 0,000 | 0,000 | 0,000 | 0,000 |
| **20** | 0,031 | 0,012 | 0,013 | 0,009 | 0,019 |
| **40** | 0,035 | 0,024 | 0,018 | 0,007 | 0,025 |
| **60** | 0,068 | 0,079 | 0,047 | 0,013 | 0,065 |
| **80** | 0,154 | 0,280 | 0,107 | 0,073 | 0,180 |
| **100** | 0,232 | 0,277 | 0,211 | 0,027 | 0,240 |
| **120** | 0,349 | 0,398 | 0,296 | 0,041 | 0,348 |

**Table C.33:** Cumulative percentage transport of Rhodamine 6G across cellulose nitrate membranes with emu oil impregnation in 0.1 N HCl.

| Time (min) | % Transport | | | | |
|---|---|---|---|---|---|
| | Chamber 1 | Chamber 2 | Chamber 3 | SD | Mean |
| **0** | 0,000 | 0,000 | 0,000 | 0,000 | 0,000 |
| **20** | 0,008 | 0,021 | 0,016 | 0,005 | 0,015 |
| **40** | 0,007 | 0,021 | 0,019 | 0,006 | 0,016 |
| **60** | 0,018 | 0,035 | 0,031 | 0,007 | 0,028 |
| **80** | 0,052 | 0,066 | 0,054 | 0,006 | 0,057 |
| **100** | 0,082 | 0,086 | 0,081 | 0,002 | 0,083 |
| **120** | 0,103 | 0,155 | 0,156 | 0,025 | 0,138 |

**Table C.34:** Cumulative percentage transport of Rhodamine 6G from gastro-retentive dosage form across cellulose nitrate membranes without oil impregnation in KRB.

| Time (min) | % Transport | | | | |
|---|---|---|---|---|---|
| | Chamber 1 | Chamber 2 | Chamber 3 | SD | Mean |
| **0** | 0,000 | 0,000 | 0,000 | 0,000 | 0,000 |
| **60** | 0,001 | 0,001 | 0,002 | 0,000 | 0,001 |
| **120** | 0,001 | 0,001 | 0,001 | 0,000 | 0,001 |
| **180** | 0,003 | 0,004 | 0,003 | 0,000 | 0,003 |
| **240** | 0,007 | 0,009 | 0,007 | 0,001 | 0,008 |
| **300** | 0,012 | 0,014 | 0,012 | 0,001 | 0,013 |
| **360** | 0,018 | 0,020 | 0,018 | 0,001 | 0,019 |
| **420** | 0,027 | 0,030 | 0,027 | 0,002 | 0,028 |
| **480** | 0.033 | 0,039 | 0,035 | 0,002 | 0,036 |

**Table C.35:** Cumulative percentage transport of Rhodamine 6G from gastro-retentive dosage form across cellulose nitrate membranes without oil impregnation in 0.1 N HCI.

| Time (min) | % Transport | | | | |
|---|---|---|---|---|---|
| | Chamber 1 | Chamber 2 | Chamber 3 | SD | Mean |
| **0** | 0,000 | 0,000 | 0,000 | 0,000 | 0,000 |
| **60** | 0,001 | 0,001 | 0,001 | 0,000 | 0,001 |
| **120** | 0,001 | 0,005 | 0,003 | 0,001 | 0,003 |
| **180** | 0,003 | 0,010 | 0,006 | 0,003 | 0,006 |
| **240** | 0,006 | 0,014 | 0,008 | 0,004 | 0,009 |
| **300** | 0,011 | 0,022 | 0,016 | 0,004 | 0,016 |
| **360** | 0,029 | 0,039 | 0,022 | 0,007 | 0,030 |
| **420** | 0,040 | 0,059 | 0,033 | 0,011 | 0,044 |
| **480** | 0,067 | 0,077 | 0,063 | 0,006 | 0,069 |

**Table C.36:** Cumulative percentage transport of Rhodamine 6G from gastro-retentive dosage form across cellulose nitrate membranes with olive oil impregnation in KRB.

| Time (min) | % Transport | | | | |
|---|---|---|---|---|---|
| | Chamber 1 | Chamber 2 | Chamber 3 | SD | Mean |
| **0** | 0,000 | 0,000 | 0,000 | 0,000 | 0,000 |
| **60** | 0,005 | 0,001 | 0,001 | 0,002 | 0,002 |
| **120** | 0,009 | 0,003 | 0,002 | 0,003 | 0,005 |
| **180** | 0,029 | 0,013 | 0,015 | 0,007 | 0,019 |
| **240** | 0,075 | 0,034 | 0,048 | 0,017 | 0,052 |
| **300** | 0,144 | 0,068 | 0,111 | 0,031 | 0,108 |
| **360** | 0,227 | 0,124 | 0,178 | 0,042 | 0,262 |
| **420** | 0,354 | 0,235 | 0,318 | 0,050 | 0,346 |
| **480** | 0,485 | 0,286 | 0,439 | 0,085 | 0,403 |

**Table C.37:** Cumulative percentage transport of Rhodamine 6G from gastro-retentive dosage form across cellulose nitrate membranes with olive oil impregnation in 0.1 N HCl.

| Time (min) | % Transport | | | | |
|---|---|---|---|---|---|
| | Chamber 1 | Chamber 2 | Chamber 3 | SD | Mean |
| **0** | 0,000 | 0,000 | 0,000 | 0,000 | 0,000 |
| **60** | 0,014 | 0,014 | 0,011 | 0,002 | 0,013 |
| **120** | 0,064 | 0,059 | 0,070 | 0,005 | 0,065 |
| **180** | 0,101 | 0,104 | 0,093 | 0,005 | 0,099 |
| **240** | 0,140 | 0,150 | 0,108 | 0,018 | 0,133 |
| **300** | 0,258 | 0,264 | 0,182 | 0,037 | 0,235 |
| **360** | 0,391 | 0,391 | 0,283 | 0,051 | 0,355 |
| **420** | 0,557 | 0,583 | 0,426 | 0,069 | 0,522 |
| **480** | 0,719 | 0,774 | 0,597 | 0,074 | 0,697 |

**Table C.38:** Cumulative percentage transport of Rhodamine 6G from gastro-retentive dosage form across cellulose nitrate membranes with cognac oil impregnation in KRB.

| Time (min) | % Transport | | | | |
|---|---|---|---|---|---|
| | Chamber 1 | Chamber 2 | Chamber 3 | SD | Mean |
| **0** | 0,000 | 0,000 | 0,000 | 0,000 | 0,000 |
| **60** | 0,001 | 0,002 | 0,003 | 0,001 | 0,002 |
| **120** | 0,006 | 0,004 | 0,006 | 0,001 | 0,005 |
| **180** | 0,030 | 0,031 | 0,037 | 0,003 | 0,033 |
| **240** | 0,087 | 0,105 | 0,110 | 0,010 | 0,101 |
| **300** | 0,175 | 0,250 | 0,246 | 0,035 | 0,223 |
| **360** | 0,310 | 0,376 | 0,362 | 0,028 | 0,350 |
| **420** | 0,514 | 0,555 | 0,553 | 0,019 | 0,541 |
| **480** | 0,691 | 0,786 | 0,796 | 0,047 | 0,757 |

**Table C.39:** Cumulative percentage transport of Rhodamine 6G from gastro-retentive dosage form across cellulose nitrate membranes with cognac oil impregnation in 0.1 N HCl.

| Time (min) | % Transport | | | | |
|---|---|---|---|---|---|
| | Chamber 1 | Chamber 2 | Chamber 3 | SD | Mean |
| **0** | 0,000 | 0,000 | 0,000 | 0,000 | 0,000 |
| **60** | 0,005 | 0,004 | 0,002 | 0,001 | 0,004 |
| **120** | 0,036 | 0,037 | 0,031 | 0,002 | 0,034 |
| **180** | 0,142 | 0,153 | 0,139 | 0,006 | 0,145 |
| **240** | 0,324 | 0,338 | 0,279 | 0,025 | 0,314 |
| **300** | 0,474 | 0,469 | 0,468 | 0,003 | 0,470 |
| **360** | 0,655 | 0,719 | 0,673 | 0,027 | 0,682 |
| **420** | 0,897 | 0,899 | 0,890 | 0,004 | 0,895 |
| **480** | 1,094 | 1,131 | 1,080 | 0,021 | 1,102 |

**Table C.40:** Cumulative percentage transport of Rhodamine 6G from gastro-retentive dosage form across cellulose nitrate membranes with emu oil impregnation in KRB.

| Time (min) | % Transport | | | | |
|---|---|---|---|---|---|
| | Chamber 1 | Chamber 2 | Chamber 3 | SD | Mean |
| **0** | 0,000 | 0,000 | 0,000 | 0,000 | 0,000 |
| **60** | 0,000 | 0,000 | 0,001 | 0,000 | 0,000 |
| **120** | 0,002 | 0,001 | 0,003 | 0,001 | 0,002 |
| **180** | 0,008 | 0,006 | 0,014 | 0,003 | 0,009 |
| **240** | 0,023 | 0,021 | 0,037 | 0,007 | 0,027 |
| **300** | 0,068 | 0,051 | 0,077 | 0,011 | 0,066 |
| **360** | 0,137 | 0,099 | 0,125 | 0,016 | 0,121 |
| **420** | 0,241 | 0,188 | 0,218 | 0,021 | 0,216 |
| **480** | 0,380 | 0,230 | 0,298 | 0,061 | 0,302 |

**Table C.41:** Cumulative percentage transport of Rhodamine 6G from gastro-retentive dosage form across cellulose nitrate membranes with emu oil impregnation in 0.1 N HCI.

| Time (min) | % Transport | | | | |
|---|---|---|---|---|---|
| | Chamber 1 | Chamber 2 | Chamber 3 | SD | Mean |
| **0** | 0,000 | 0,000 | 0,000 | 0,000 | 0,000 |
| **60** | 0,007 | 0,001 | 0,002 | 0,003 | 0,003 |
| **120** | 0,019 | 0,004 | 0,002 | 0,007 | 0,009 |
| **180** | 0,029 | 0,016 | 0,016 | 0,006 | 0,020 |
| **240** | 0,077 | 0,047 | 0,044 | 0,015 | 0,056 |
| **300** | 0,119 | 0,097 | 0,087 | 0,013 | 0,101 |
| **360** | 0,198 | 0,200 | 0,160 | 0,018 | 0,186 |
| **420** | 0,294 | 0,262 | 0,246 | 0,020 | 0,267 |
| **480** | 0,420 | 0,362 | 0,353 | 0,030 | 0,378 |

# ADDENDUM D: *IN VITRO* BUOYANCY AND DISSOLUTION DATA

**Table D.1:** Cumulative percentage Rhodamine 6G released from the uncompressed powder.

| Time (min) | % Dissolution | | | | |
|---|---|---|---|---|---|
| | **Vessel 1** | **Vessel 2** | **Vessel 3** | **SD** | **Mean** |
| **0** | 0,000 | 0,000 | 0,000 | 0,000 | 0,000 |
| **15** | 60,508 | 67,469 | 66,833 | 3,142 | 64,937 |
| **30** | 77,442 | 84,548 | 84,191 | 3,269 | 82,060 |
| **60** | 89,294 | 93,386 | 95,577 | 2,604 | 92,752 |
| **90** | 94,765 | 95,438 | 96,483 | 0,707 | 95,562 |
| **120** | 97,230 | 96,842 | 97,073 | 0,159 | 97,048 |

**Table D.2:** Cumulative percentage Rhodamine 6G released from the gastro-retentive dosage form.

| Time (min) | % Dissolution | | | | |
|---|---|---|---|---|---|
| | **Vessel 1** | **Vessel 2** | **Vessel 3** | **SD** | **Mean** |
| **0** | 0,000 | 0,000 | 0,000 | 0,000 | 0,000 |
| **15** | 3,238 | 3,644 | 3,536 | 0,172 | 3,472 |
| **30** | 5,441 | 5,778 | 5,889 | 0,191 | 5,702 |
| **60** | 13,502 | 11,785 | 11,597 | 0,857 | 12,295 |
| **120** | 25,000 | 24,813 | 23,323 | 0,751 | 24,379 |
| **180** | 36,328 | 36,985 | 33,329 | 1,592 | 35,547 |
| **300** | 57,340 | 59,026 | 57,270 | 0,812 | 57,879 |
| **480** | 88,075 | 87,439 | 91,227 | 1,656 | 88,914 |

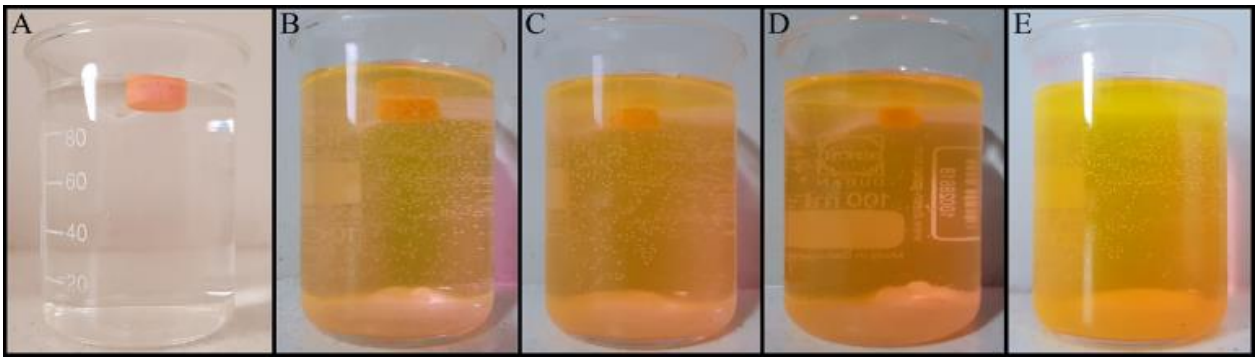


**Figure D.1:** Graphical presentation of *in vitro* buoyancy study of the gastro-retentive formulation. (A) Initial (B) 4 h. (C) 8 h. (D) 12 h. (E) 24 h.